

Astrobiology: Exploring Life on Earth and Beyond Habitability of the Universe before Earth

Series Editors

Pabulo Rampelotto

Federal University of Rio Grande do Sul, Porto Alegre, Brazil

Richard Gordon

Gulf Specimen Marine Laboratory, Panacea, FL, United States

Wayne State University, Detroit, MI, United States

Joseph Seckbach

The Hebrew University of Jerusalem, Jerusalem, Israel

Volume Editors

Richard Gordon

Gulf Specimen Marine Laboratory, Panacea, FL, United States

Wayne State University, Detroit, MI, United States

Alexei A. Sharov

National Institute on Aging, NIH, Baltimore, MD, United States



ACADEMIC PRESS

An imprint of Elsevier

EMERGENCE OF POLYGONAL SHAPES IN OIL DROPLETS AND LIVING CELLS: THE POTENTIAL ROLE OF TENSEGRITY IN THE ORIGIN OF LIFE

Richard Gordon^{*,†}, Martin M. Hanczyc[‡], Nikolai D. Denkov[§], Mary A. Tiffany[¶], Stoyan K. Smoukov^{||}

^{*}*Gulf Specimen Marine Laboratories, Panacea, FL, United States*

[†]*Wayne State University, Detroit, MI, United States*

[‡]*Università degli Studi di Trento, Povo, Italy*

[§]*Sofia University, Sofia, Bulgaria*

[¶]*Bainbridge Island, WA, United States*

^{||}*Queen Mary University of London, London, United Kingdom*

University of Cambridge, Cambridge, United Kingdom

University of Sofia, Sofia, Bulgaria

CHAPTER OUTLINE

1 Introduction.....	428
2 Shaped Droplets.....	428
3 Oil-Based Protocells.....	434
4 Polygonal Prokaryotes.....	438
5 Mechanisms Controlling the Shapes of Prokaryote Cells.....	443
6 Possible Functions of a Polygonal Shape of Cells	454
7 Polygonal Diatoms	457
8 Conclusion	459
Acknowledgments	460
Appendix. Overview of Tensegrity Structures	461
A Toy Model for the Polygonal Shape of Shaped Droplets	469
References	474
Further Reading	489

An organism with such a square shape is without precedent and it is not surprising, therefore, that the original report of the square bacterium was received with some skepticism (Parkes & Walsby, 1981).

1 INTRODUCTION

A full model of the origin of life must be multifaceted to explain all features of life (e.g., self-reproduction, heredity, metabolism, sensing and response, capturing resources, and evolutionary mechanisms). Diversity in shape is a central property that influences a number of these features and is observed in all organisms, including bacteria and Archaea. Small changes in shape in prokaryotes can be associated with profound advantages in motility and nutrient uptake, avoiding predation and biofilm structure, which are top on the list of evolutionary pressures (Smith et al., 2017; Young, 2006, 2007, 2010). In this chapter, instead of relying on cellular cytoskeleton mechanisms or information-rich genetics to form or program such shapes, we hypothesize that shapes in protocells may have emerged simply as tensegrity structures in liquid droplets driven by phase-change mechanisms. Recent experiments show that regular geometric shapes with liquid cores may emerge simply in oil droplets from phase transitions upon cooling (Cholakova et al., 2016; Denkov et al., 2015; Haas et al., 2017). Our proposal is consistent with the hypothesis of a lipid world (Bar-Even et al., 2004; Segré et al., 2001) and an oil-droplet-based origin of life (Hanczyc, 2014; Sharov, 2016; Sharov & Gordon, 2017). We build on:

1. Shaped droplets: a new discovery, that cooled oil droplets with surfactants acquire flat, polygonal shapes (Denkova et al., 2015) (Fig. 1);
2. Oil-based protocells: models for the origin of life from oil droplets (Hanczyc, 2014; Sharov, 2016; Sharov & Gordon, 2017), preceding membrane-bound vesicles (Fiore & Strazewski, 2016), with genomic evidence that life started from an “oily” state (Mannige et al., 2012);

And we show how these shaped droplets and their potential role as protocells may have given rise to present-day organisms and their structures, including:

3. Polygonal prokaryotes: the fact that many halophilic Archaea (thought on discovery to have been bacteria) have flat, polygonal shapes (Walsby, 1980) (Fig. 1);
4. Molecular dating indicating the ancient origin of cytoskeleton, and recent evidence of its central role in cell functioning (Gordon & Gordon, 2016a);
5. Polygonal diatoms: we suggest that the valve silicalemma of polygonal diatoms has a flat, polygonal shape, resulting in precipitation of the silica within as a polygon (Fig. 1).

This adventure is new, and thus our sketch will leave many gaps in our understanding, some of which, however, are approachable experimentally. What we are interjecting into the dialogue on the origin of life is that the shape of protocells may have been adaptive, and that structure has evolutionary consequences. We have called cooled oil droplets with flat, polygonal shapes “shaped droplets.” We do not discuss traditional topics related to the origin of life, such as the emergence of proto-heredity and proto-metabolism, though we suggest that the structure of shaped droplets may have provided new evolutionary opportunities for improving various cell functions, including heredity and metabolism.

2 SHAPED DROPLETS

It may seem strange that a three-dimensional spherical liquid drop of oil can take on a nearly two-dimensional, polygonal shape when cooled slowly, forming what we have called “shaped droplets” (Fig. 1). We are just beginning to understand the mechanism by which this happens (Azadi &

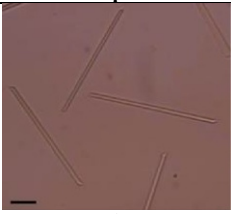
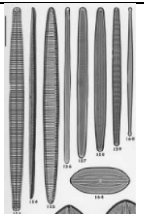
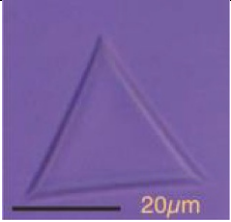
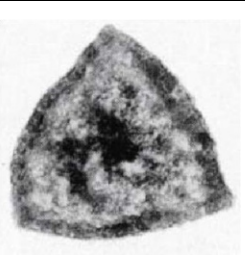

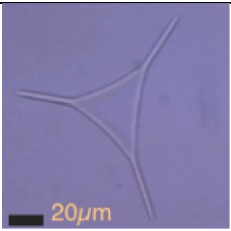
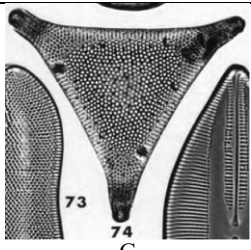
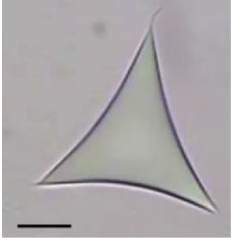
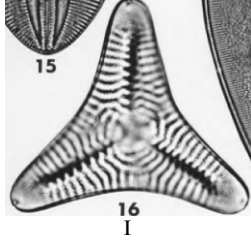

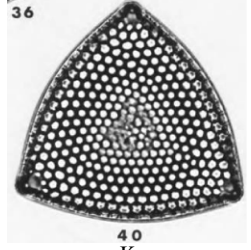
# sides	Droplets	Archaea	Diatoms
2	 A		 B
3 equilateral	 C	 D	 E
3 pointed	 F		 G
3 concave	 H		 I
3 spiked	 J		 K

FIG. 1—Cont'd

See figure legend on next page.

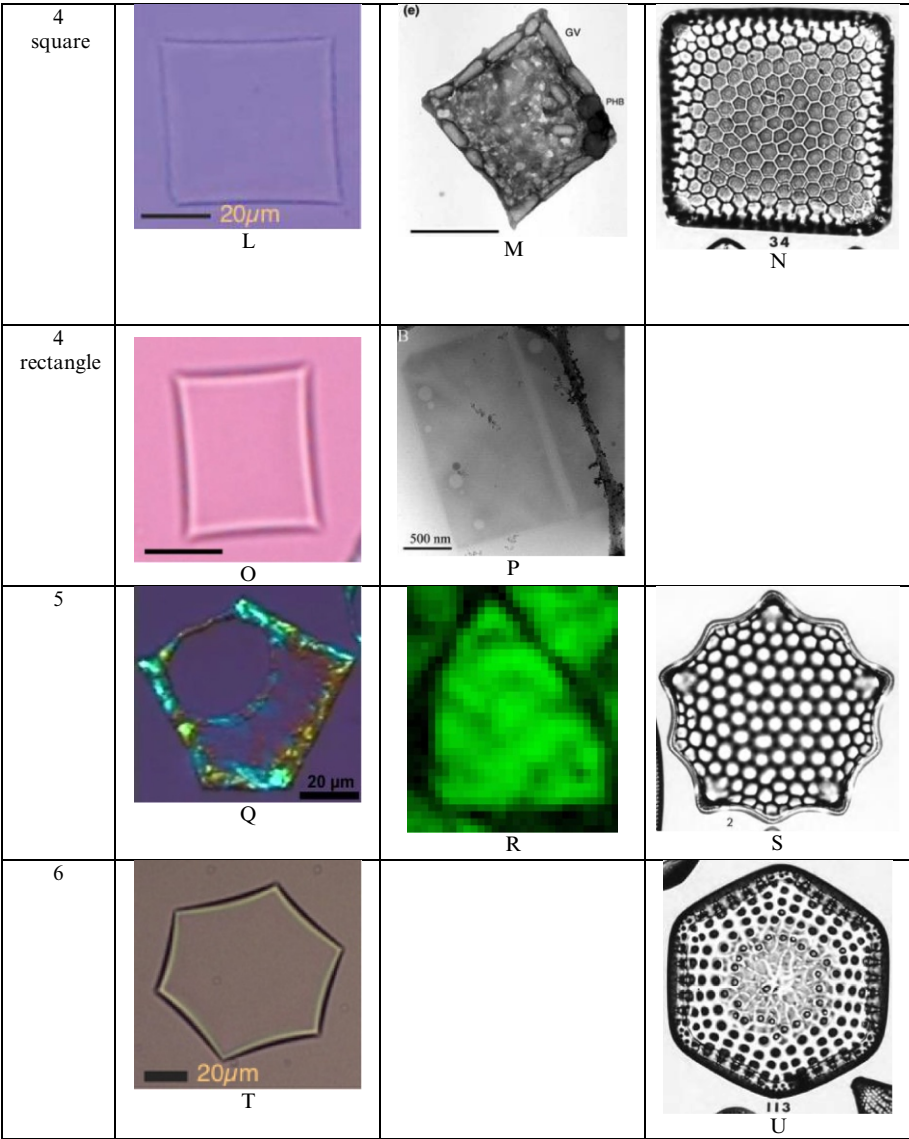


FIG. 1—Cont'd

See figure legend on opposite page.

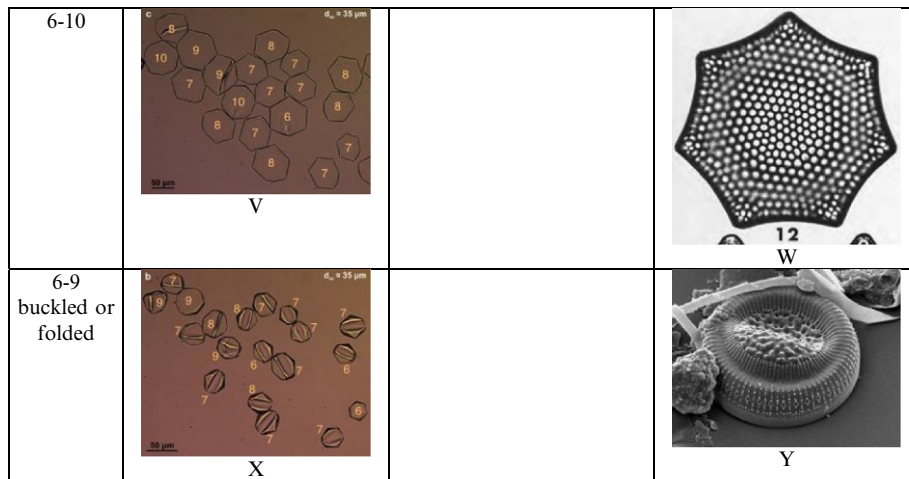


FIG. 1—Cont'd

Shaped droplets vs. Archaea and diatoms. *Left column*: samples of abiotic drops, matched with comparable prokaryotic Archaea (*middle column*) and eukaryotic diatom valves (*right column*). Archaea: D: *Haloarcula japonica* (Takao, 2006). M, P: *Haloquadratum walsbyi*. Diatoms: B: 153 *Tabularia gaillonii*, 154 *Nitzschia macilenta*, 155 *Alveus marinus*, 156 *Synedra fulgens*, 157 *Synedra baculus*, 158 *Synedra formosa*, 159 *Synedra superba*, and 160 *Hyalosynedra* (?) sp. indet. E: *Triceratium morlandii* var. *morlandii*. G: *Biddulphia spinosa*. I: *Schuetzia annulata*. K: *Triceratium broeckii*. N: *Triceratium favus* fo. *quadrata*. S: *Triceratium campechianum*. U: *Stictodiscus parallelus* fo. *hexagona*. W: *Triceratium septangulatum*. Y: *Cyclotella litoralis*.

(A, C, F, H, J, L, Q, T, V, X) From Denkov, N., Tcholakova, S., Lesov, I., Cholakova, D., Smoukov, S.K., 2015. Self-shaping of oil droplets via the formation of intermediate rotator phases upon cooling. *Nature* 528(7582), 392–395, with permission of Nature Publishing Group. (B, G, I, K, N, S, U, W) From Stidolph, S.R., Sterrenburg, F.A.S., Smith, K.E.L., Kraberg, A., 2012. Stuart R. Stidolph Diatom Atlas: U.S. Geological Survey Open-File Report 2012–1163. <http://pubs.usgs.gov/of/2012/1163/>, in public domain. (E) From Mikhaltsov, A., 2014. File:Triceratium morlandii var. morlandii.jpg. https://commons.wikimedia.org/wiki/File:Triceratium_morlandii_var._morlandii.jpg with permission under the Creative Commons Attribution-Share Alike 4.0 International license. (M) From Burns, D.G., Camakaris, H.M., Janssen, P.H., Dyll-Smith, M.L., 2004. Cultivation of Walsby's square haloarchaeon. *FEMS Microbiology Letters* 238(2), 469–473, with permission of Oxford University Press. (P) From Comolli, L.R., Duarte, R., Baum, D., Luef, B., Downing, K.H., Larson, D.M., Csencsits, R., Banfield, J.F., 2012. A portable cryo-plunger for on-site intact cryogenic microscopy sample preparation in natural environments. *Microscopy Research and Technique* 75(6), 829–836, with permission of John Wiley and Sons. (Y) From Gordon, R., Tiffany, M.A., 2011. Possible buckling phenomena in diatom morphogenesis, in: Seckbach, J., Kocielek, J.P. (Eds.), *The Diatom World*. Springer, Dordrecht, The Netherlands, pp. 245–272, with permission of Springer. (R) is an enlargement of one cell in Fig. 4E.

Grason, 2016; Cholakova et al., 2016; Denkov et al., 2015, 2016; Grason, 2016; Guttman et al., 2016a,b; Haas et al., 2017), and much experimental, theoretical, and computer simulation (molecular dynamics) work lies ahead. Shape is a global property of a cell ((Boulbitch, 2000), as discussed in (Gordon & Gordon, 2016a)), presumed, but rarely demonstrated, to be the result of a balance of forces (Pomp et al., 2016; Sain et al., 2015; Sims et al., 1992). The same notion applies to the spherical liquid drop of oil and thus presumably to its shaped droplet state. A general framework in which to consider such problems is that of tensegrity structures, which have been applied at many hierarchical levels, from

molecules to the human body (Levin, 2006a,b; Scarr, 2014), on up to human edifices. We have made a preliminary suggestion that shaped droplets are tensegrity structures (Cholakova et al., 2016), promising a full manuscript, which is this chapter. We provide an Appendix overviewing tensegrity structures and giving a toy model for flat, polygonal tensegrity structures.

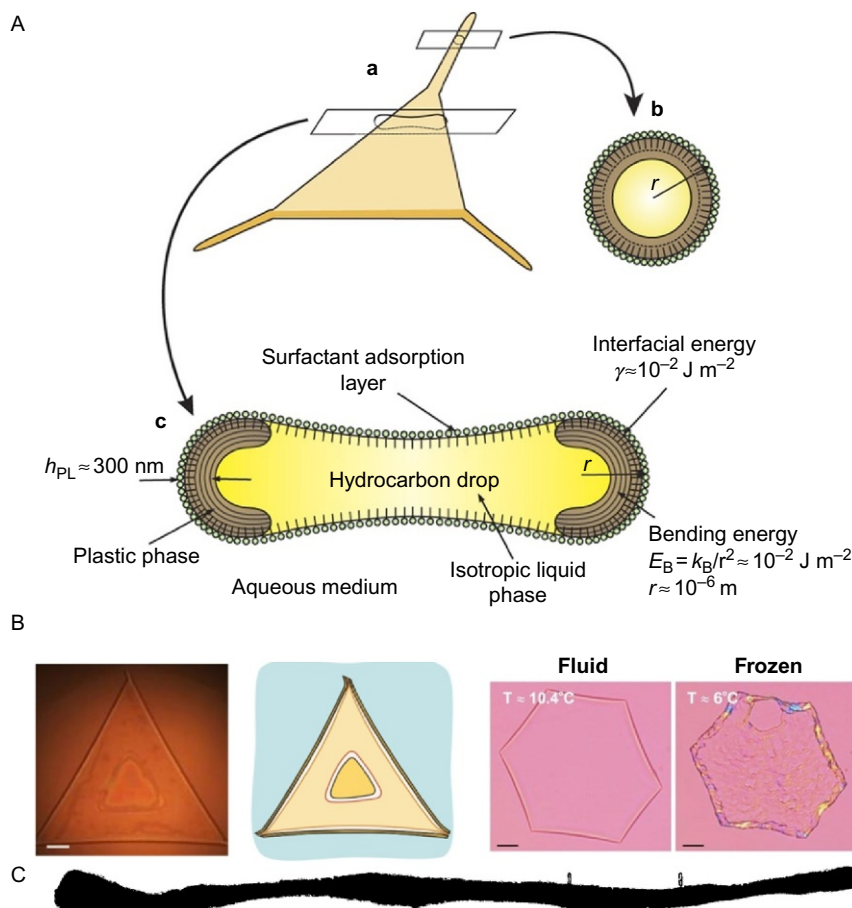
Contrary to our former intuition of spherical shapes determined by minimization of interfacial energy, shaped droplets can be thin, flat, and have straight edges and sharp corners. Shaped droplets have been successfully obtained over the size range of 1–50 μm diameter (Denkov et al., 2015), about the same size range as most cells:

Recently, we reported (Denkov et al., 2015) a novel bottom-up mechanism for morphogenesis within droplets of linear alkanes, which leads to the formation of micrometer sized particles with different shapes. This phenomenon is driven by the formation of a “skin” of intermediate rotator phases in cooled alkane droplets—a process which was triggered by freezing adsorption layers of long-chain surfactants. These rotator phases (called also “plastic crystals” or “highly ordered smectics”) are characterized with a long-range translational order of the molecules, yet with some rotational freedom around the long molecular axis in the case of linear alkanes (Sirota et al., 1993). We showed (Denkov et al., 2015) how the formation of anisotropic rotator phases, within the confines of the micro-scale fluid droplets, results in a surprisingly wide array of regular geometric shapes, including regular polyhedra; hexagonal, tetragonal and trigonal platelets, with and without fibers protruding from their corners. Furthermore, we found that frozen solid particles with the respective shapes can be produced by selecting appropriate cooling rates. In this way, we succeeded in making a non-trivial link between a novel process for making complex shapes in materials science and the fundamental discovery that phase transitions confined inside a drop could be a driving force for morphogenesis (Denkov et al., 2015). The process opens new opportunities for both scalable particle synthesis and studying the structure/shape formation processes in amazingly simple chemical systems

(Cholakova et al., 2016).

Similar “faceted liquid droplets” were soon after independently discovered by Guttman et al. (2016a,b), though rather than formation of a tensegrity structure to counteract a measurable surface tension in order to create the shapes, they ascribed the process to an ultra-low surface tension. Subsequent reports have shown that the surface tension in these systems is not ultra-low (Denkov et al., 2016), confirming the plastic crystal tensegrity structure argument.

Using the general tensegrity background knowledge (see Appendix), we can now consider the balance of forces in a shaped droplet. At the smallest scale, the individual atoms are stiff. Surfactant at the surface of an oil droplet in water consists of linear molecules that align perpendicularly to the surface and from the liquid oil template the interfacial freezing of a 2D plastic crystal solid, at temperatures slightly below, at, or even above the bulk freezing point of the oil. The formation of such a stiff plastic crystal layer may counteract the surface tension of the whole droplet and form shapes far from the area-minimizing sphere. Let us examine how a droplet of oil capable of forming plastic crystal phases with amphiphilic molecules (amphiphiles or surfactants) at the surface can be a tensegrity structure. The overall surface tension is the tension component, while the thin layers of plastic crystal forming edges at some parts of the droplet interface provide the stiff elements, acting as struts (Fig. 2A). These struts, however, are not fixed, but can grow as their formation can be favorable under conditions of supercooling.

**FIG. 2**

(A) Schematic of alkane packing in the plastic crystal phase resulting in a cylindrical morphology. We don't yet know the reason the molecules pack in this fashion—with cylindrical packing—no curvature in one direction, a certain curvature in the other. In our case, the curvature is much lower than that of the nanotube on the right, so the diameter is microns instead of nanometers. The plastic phase of the alkane molecules results in a stiff element along each straight edge that balances the surface tension of the surfactant-coated oil droplet (the compressive element), making this a tensegrity structure (see [Appendix](#)). Inside the alkane (hydrocarbon), molecules are in a liquid phase. (B) Light micrographs showing the thicker border, and the thin film in the middle, of shaped droplets. In the triangle, a sizeable thin patch has formed inside, whereas in the hexagon it has stretched all the way. Sometimes in these shapes, because the middle film is so thin, they puncture before they can stretch all the way, creating holes. The second triangle is a sketch of the first. Scale bars = $20 \mu\text{m}$. (C) A binary mask of an electron micrograph cross section of a square Archaea made by hand using ImageJ from Fig. 6B in ([Stoeckenius, 1981](#)). The distance between the vertical tic marks is $1 \mu\text{m}$. Mean thickness is $T = 0.204 \mu\text{m}$ and length of the cross section is $L = 7.36 \mu\text{m}$.

(A) From Denkov, N., Tcholakova, S., Lesov, I., Cholakova, D., Smoukov, S.K., 2015. Self-shaping of oil droplets via the formation of intermediate rotator phases upon cooling. *Nature* 528(7582), 392–395, with permission of Nature Publishing Group.

In addition to the energetics of strut formation, there are discontinuities at the corners, with their own energies that are not fully clear. The persistence of common angles (60, 120 degrees) in these structures suggests that these defect energies are far higher than any local deformation energies during shape changes, so they are not usually influenced/changed. In the Appendix, we present a simple physical toy model that shows the tensegrity analogy with modular sidewalls built from magnetic discs, where the magnetic attraction is the analogy of the surface tension in the drops. In addition, it can illustrate the observed disproportionation of sides even in the absence of growth of the plastic crystal, as magnetic discs can flip from one edge to another due to defects between them. The dynamics at the corners of shaped droplets deserve detailed modeling.

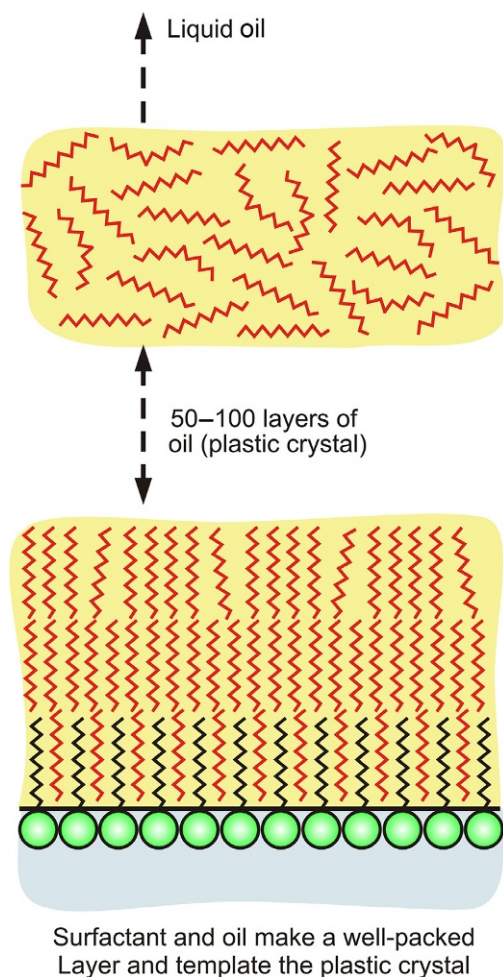
In a more detailed model (Haas et al., 2017), we also consider the preference of certain angles in the observed structure and connect the balance of the surface tension with the stiffness of the rods of plastic crystal forming edges and the ability for material transfer from one edge to another. We also associated the overall growth rate of the edges with the thermodynamic driving force for formation of the plastic crystal. The model is able to predict the exact sequence of polygonal shape transformations, as well as the stable puncture that occurs in some of them, resulting in a shaped, topologically toroidal oil droplet (triangle in Fig. 2B). There are a number of unknowns still in this fascinating phenomenon, including the detailed origin of the preference for some angles and the exact packing of the molecules resulting in the observed curvature of the plastic crystal edges that are a matter of active investigation.

Usually, the stiffness of a frozen surfactant layer is orders of magnitude lower than the surface tension. However, when oil droplets are cooled slowly, a number of layers of straight-chain alkanes near the interface can form a plastic state in which they are free to rotate around their long axes but not translate (“rotator phase”). Though more flexible than other crystals, the stiffness of these regions is enough to counteract the surface tension of the droplet and impart a nonspherical shape to it (Figs. 2 and 3). Shaped droplets provide anisotropic flat surfaces which could have provided metabolic, mobility, and other advantages to oil-based protocells, as we’ll see in the next section. Such shapes may have been stabilized further by reactions at the surface, such as mineralization by inorganic precipitation and adsorption of polymers (Simon et al., 1995), either hydrophobic polymers on the inside or hydrophilic polymers on the outside. Polymers with stretches of both could weave in and out of the surface like extant membrane proteins.

3 OIL-BASED PROTOCELLS

Our interest in the shape of oil droplets stems from increasing support for the hypothesis that life may have started from oil or lipid droplets in water (Sharov, 2016; Segré et al., 2001; Segré & Lancet, 2000). An oil droplet that absorbs a tar-like complex mixture of abiotic compounds has no membrane, yet is capable of movement in various ways (Hanczyc & Ikegami, 2010; Horibe et al., 2011) via internal oil flow (Hanczyc, 2011). Such oil droplets can hydrodynamically split themselves, imitating cell division without specific polymers being involved (Caschera et al., 2013; Tcholakova et al., 2017). See also (Banno et al., 2015; Turk-MacLeod et al., 2015).

We have demonstrated the interplay between stability and dynamics in a recursive spherical oil droplet division and fusion cycle (Caschera et al., 2013). In this system, starting far from equilibrium due to the solvation of a cationic surfactant in the organic phase and anionic surfactant in the aqueous phase, we observe a temporal window on the way to equilibrium due to surfactant diffusion at the

**FIG. 3**

Model of the plastic phase at the edges of shaped droplets. Tens of layers of molecules must order in these plastic crystal layers to overcome the interfacial tension keeping droplets otherwise circular. The molecules close the surface interdigitate with the surfactant tails, making a well-packed monolayer. That monolayer anchors the formation of the rotator (plastic crystal) phase, which progressively gets more and more disordered and eventually transitions to the liquid which is contained inside all these deformed droplets.

interface where the interfacial tension is minimized. During this time period, the droplet is easily affected by force, whether externally applied or internally generated. Often the droplet will spontaneously divide into daughter droplets due to internal fluid dynamic instability, which then round up as the system approaches a thermodynamic equilibrium.

Self-shaping droplets are nonlinear systems which convert the thermal fluctuations of the environment into phase-transition energy which, in its own turn, is used for droplet shape transformations and

for drop division into smaller “daughter” droplets (Cholakova et al., 2016, 2017; Denkov et al., 2015; Tcholakova et al., 2017). The “feeding” of the daughter drops via coalescence with other drops or via capturing dissolved organic molecules transferred via the aqueous medium from smaller to larger droplets (in a process equivalent to the “Ostwald ripening” of crystals (Taylor, 1998; Tcholakova et al., 2011)) could lead to prebiotic increase of the drop size via basic physicochemical mechanisms. The freezing of the shaped droplets at low temperatures fixes and preserves their shape until the temperature is raised again, resembling the process of cell hibernation. Therefore, shaped droplets are probably the simplest chemical system, in terms of composition, which could appear naturally in water pools containing organic molecules and which are able to utilize the day/night (and other) natural thermal cycles for realization of basic protocell processes, such as complex shape-transformations, division and growth, and hibernation, thus mimicking some of the fundamental processes of living cells.

It is important to emphasize that droplet self-shaping and self-splitting have been observed with a wide variety of organic molecules (alkanes, alcohols, triglycerides, esters, etc.) and with complex mixtures of such molecules. This is direct evidence that these are general phenomena, not bound to very specific classes of molecules (Cholakova et al., 2016, 2017), and shaped droplets could thus be called a “generic” mechanism for morphogenesis (Newman, 2014). Note that only basic physicochemical processes, such as phase transitions and interfacial phenomena, are involved in the above processes, without the complex molecular machinery used by evolutionary developed living organisms. Furthermore, all these physicochemical processes are highly reproducible and could serve as a basis for development of more subtle and complex processes, such as droplet attachment on specific substrates and accumulation of molecules on specific domains of the drop surface (e.g., on the edges, corners, broad surfaces, or tips of the shaped drops), thus allowing the beginning of a subsequent evolutionary development of more complex molecular machines.

Another remarkable feature of shaped droplets is that they adapt to the variations of the environmental energy and acquire shape and other related properties which correspond to equilibrium at the given temperature. Therefore, they do not need a constant influx of energy from the environment to maintain their “homeostasis,” which is a typical feature of living organisms. From this viewpoint, shaped droplets appear as an intermediate state between natural inorganic matter, which has an entirely passive response to changes in the environment, and living organisms which use complex molecular mechanisms, requiring a regular influx and conversion of energy, to handle their homeostasis and to adapt to the variations in the external conditions.

One of the strongest arguments in favor of the oily origin of life is the relative abundance of oil-like organic molecules. There are potentially three main sources of organic material in places where life could have originated: arrival from space, energy-coupled chemistry in the atmosphere, and ocean floor vent chemistry. Investigations of the interstellar medium have produced evidence of short-chain alcohols, aldehydes, ketones, acids, aliphatic hydrocarbons, amines, amides, esters, ethers, cyanide derivatives of paraffin, as well as aromatic rings (e.g., benzene) and even large and complex carbon structures (e.g., cyanopolynes and polyaromatic hydrocarbons (Henning & Salama, 1998; Kwok, 2007)). In the lab, the UV irradiation of interstellar ice analogs with water, methanol, CO, ammonia, and other components produced not only various organic molecules (Bernstein et al., 1995; Gerakines et al., 2001), but also structures resembling oil droplets and vesicles (Dworkin et al., 2001). Certain carbonaceous chondrite meteorites found on the Earth contain an organic crust with oily substances including aliphatic and aromatic hydrocarbons that may form oil droplets in water (Krishnamurthy

et al., 1992; Yuen et al., 1984). Considering the ocean floor as a source of organic chemistry, two identified chemical processes may be at play: the coupled processes of serpentinization and Fischer-Tropsch Type synthesis. These chemical processes can produce short- and medium-chain alkanes (Holm & Charlou, 2001; Macleod et al., 1994; Schulte et al., 2006; Sherwood Lollar et al., 2002; Simoneit, 1995; Sleep et al., 2004), which could form oil droplets. Finally, the atmosphere of early Earth could have also been a source for organic chemistry and molecules. The spirit of this inquiry was captured in the famous Urey-Miller experiment first published in 1953 (Miller, 1953; Miller & Urey, 1959). Here, a simulated prebiotic Earth atmosphere was constructed in the lab and subjected to repeated electrical sparks to simulate lightening. Using such approaches and varying the initial conditions, studies have produced several different types of molecules such as amino acids and monocarboxylic acids (Miller, 1953; Rode, 1999), along with much more complex molecules including tar and oil phases (Allen & Ponnamperna, 1967; Yuen et al., 1981). It is not clear if complex and relatively unstable organic molecules (e.g., amino acids and sugars) can reach biologically relevant concentrations without life (Sharov & Gordon, 2017). However, hydrocarbons, and especially alkanes, could become abundant on planets and form oil droplets in water. The addition of polar moieties in the synthesis of such organics could have produced a variety of simple surfactants (Hanczyc & Monnard, 2017).

There are some recent arguments emerging that support the idea of an oily origin of life. The reconstructed putative last common ancestral proteome appears to have high degree of hydrophobicity, with evolution following an “oil escape” towards more water-friendly proteins (Mannige, 2013; Mannige et al., 2012). This does not necessarily mean that ancestral proteins were embedded in an oil droplet. It could simply indicate that proper protein folding largely depends on the hydrophobic effects in an aqueous medium. Nevertheless, the functioning of proteins has been demonstrated in nonaqueous solvents (Klibanov, 2001; Zaks & Klibanov, 1985). In some cases, the yield and longevity of an enzymatic reaction is improved when embedded in largely organic media (Stolarow et al., 2015). Further investigation of enzymes in organic solvents revealed that some enzymes acquire new properties including greater stability, altered selectivity, and molecular memory (Klibanov, 2003). Therefore, it is not only possible for some of the basic biochemical functionalities to be hosted in oil droplets, but perhaps advantageous.

Many researchers have contemplated a “lipid world” scenario for the origin of life where the importance of the container for the first protocells is considered (Anella & Danelon, 2014; Bar-Even et al., 2004; Bukhryakov et al., 2015; Cavalier-Smith, 2001; Kauffman, 2013; Lombard et al., 2012; Paleos, 2015; Paleos et al., 2004; Sharov & Gordon, 2017; Szathmáry, 2006; Szathmáry et al., 2005; Wieczorek, 2012). This is based on the spontaneous self-assembly of both primitive and evolved surfactant molecules into higher order structures. Such supramolecular structures include oil droplet emulsions, bilayer lamellar vesicles, micelles, and others. These supramolecular assemblies not only consist of single amphiphiles, but also mixtures that are often notably more stable under varying environmental conditions (Hanczyc & Monnard, 2017). Such mixtures of amphiphilic molecules in supramolecular structures could carry heritable compositional information as an early and primitive form of protocellular information (Gross et al., 2014; Hunding et al., 2006; Markovitch & Lancet, 2014; Naveh et al., 2004; Segré et al., 2001; Segré & Lancet, 2000; Shenhav et al., 2004, 2005; Wu & Higgs, 2008). Additionally, heritable information in such scenarios could have been represented by catalytically active self-reproducing molecules, inside or on the surfaces of oil droplets in water (Sharov, 2016).

One scenario to consider is a transition from an oil droplet-based protocell to a water-centric vesicle that reflects the current biological cell membrane architecture. Perhaps, the oil droplet protocell came first as it was easier to form and more robust. This oil droplet contained some essential biochemical machinery. Persistent shapes, whether repeatedly formed or stabilized, would have given such protocells advantages in hydrodynamic mobility, surface-area-based feeding/metabolism, resistance to being merged/diluted with other droplets, and driven a kind of protocell evolution (Young, 2006, 2007, 2010). This oil-first model was then overtaken by a cell architecture based on a thin lipid membrane with an aqueous interior, which became the obviously dominant form of known life. Such a scenario faces difficult challenges which still must be explored. Here, we simply note the similar lenticular shape of both shaped droplets and polygonal Archaea, including the development of holes or closely apposed membranes where the two surfaces meet (Figs. 2b and 4d). Stabilization of double droplets or “water-in-oil-in-water (W/O/W) emulsions” (Leong et al., 2017) affords a model for the transition from droplets to membrane-bound vesicles (Chong et al., 2015).

4 POLYGONAL PROKARYOTES

Polygonal shapes of cooled oil droplets described above appear surprisingly similar to the polygonal prokaryotes. With the first discovery of a square “bacterium” in a natural pond of evaporating marine water in the Sinai (Walsby, 1980), now recognized as an Archaea (Bolhuis, 2005), a worldwide search for halophilic polygonal prokaryotes began. The following geometrically regular shapes have been reported across taxa (Gupta et al., 2015):

Flat Archaea:

1. Triangles (Andrade et al., 2015; Baxter et al., 2005; Burns et al., 2004; Castillo et al., 2006; Chaban et al., 2006; Emerson et al., 1994; Grant & Larsen, 1989; Hamamoto et al., 1988; Horikoshi et al., 1993; Javor et al., 1982; Lasbury, 2013; Malfatti et al., 2009; Mehrshad et al., 2015, 2016; Miyashita et al., 2015; Mullakhanbhai & Larsen, 1975; Nishiyama et al., 1992; Oren, 1999; Oren et al., 1990, 1999; Otozai et al., 1991; Ozawa et al., 2000, 2005; Sabet et al., 2009; Takashina et al., 1990; Wakai et al., 1997; Walsby, 1980; Yang et al., 2007; Yatsunami et al., 2014)
2. Squares (Andrade et al., 2015; Bardavid & Oren, 2008a; Baxter et al., 2005; Bolhuis et al., 2006; Burns et al., 2004, 2007; Castillo et al., 2006, 2007; Chaban et al., 2006; Dyall-Smith et al., 2011; Fredrickson et al., 1989; Ghai et al., 2011; Grant & Larsen, 1989; Hamamoto et al., 1988; Javor et al., 1982; Kamekura, 1998; Lasbury, 2013; Lobasso et al., 2008; Malfatti et al., 2009; Mullakhanbhai & Larsen, 1975; Oh et al., 2010; Oren, 1994, 1999, 2005; Oren et al., 1990, 1996, 1999; Romanenko, 1981; Santos et al., 2012; Torrella, 1986; Tully et al., 2015; Walsby, 1980, 1994; Yang et al., 2007)
3. Rectangles (Dyall-Smith et al., 2011; Javor et al., 1982; Mullakhanbhai & Larsen, 1975; Oren, 1999, 2005; Oren et al., 1996)
4. Rhombi (Hamamoto et al., 1988; Oren, 1999; Takashina et al., 1990)
5. Trapezoids (Oren, 1999, 2005; Walsby, 1980)
6. Pentagons (Malfatti et al., 2009)
7. Circles, ovals, plates, disks (Duggin et al., 2015; Mehrshad et al., 2016; Mullakhanbhai & Larsen, 1975; Stetter, 1982)

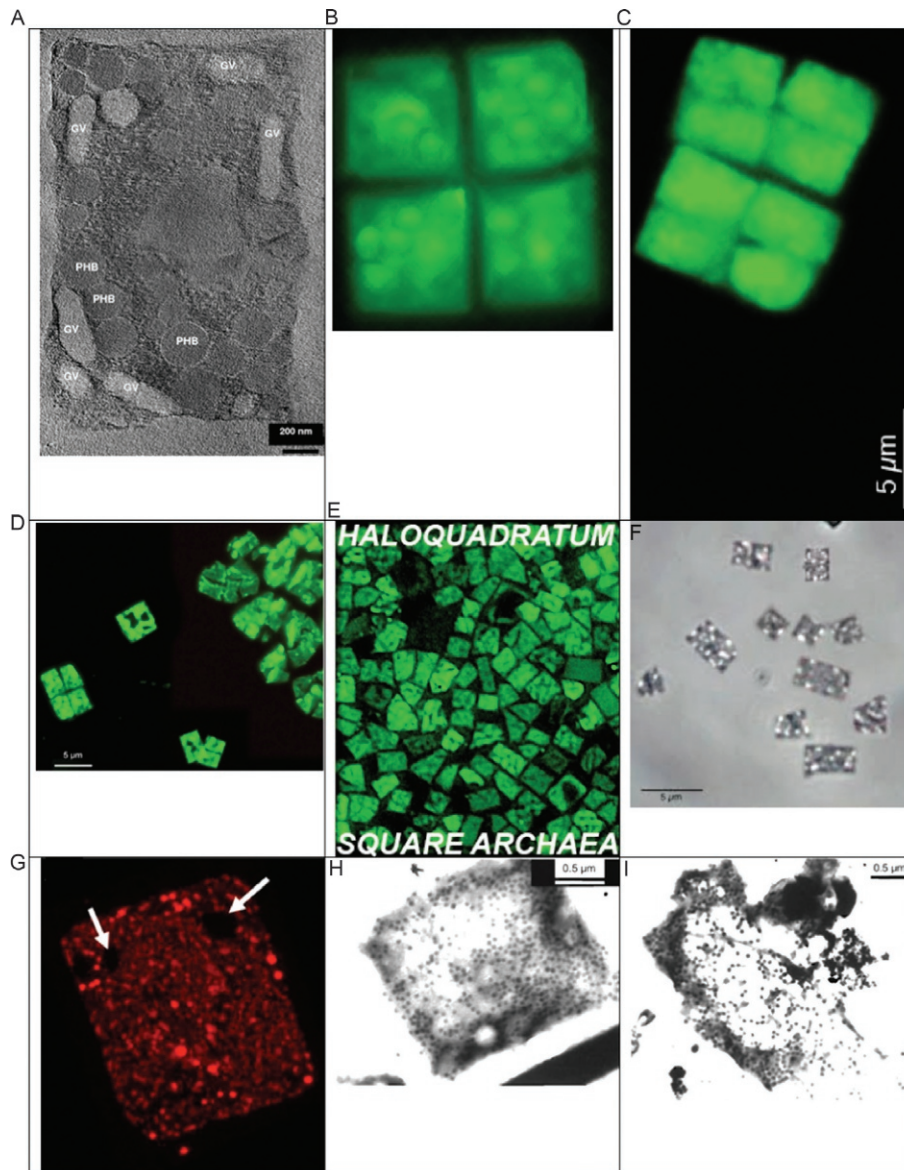


FIG. 4

Square Archaea. (A) Electron tomograph by H. Engelhardt of a “Spanish isolate of the square halophilic archaeon *Haloquadratum walsbyi* strain HBSQ001.” GV=gas vesicle, others “most likely poly-3-hydroxy-butyric acid (PHB) polymers.” (B) Four cells of *Haloquadratum walsbyi* in the “postage stamp” array. (C) 8-cell colony. Note the sharp corners and the parallel third divisions, suggesting cell-cell communication. Green fluorescence image with acridine orange staining per (Burns & Dyll-Smith, 2006; Burns et al., 2004). (D, E) *H. walsbyi*:

(Continued)

Flat Bacteria:

8. Triangles (Awramik & Barghoorn, 1977; Fritz et al., 2004; Lafitskaya & Vasilieva, 1976; Vasilyeva & Semenov, 1984, 1985)
9. Squares (Oren, 1999; Whang & Hattori, 1990)
10. Rectangles (Kuhn, 1981; Whang & Hattori, 1990)
11. Stars (Chernykh et al., 1988; Fritz et al., 2004; Hirsch, 1974; Hirsch et al., 1977; Hirsch & Schlesner, 1981; Reimer & Schlesner, 1989; Rusconi et al., 2013; Semenov & Vasilyeva, 1987; Staley, 1968; Vasilyeva, 1970, 1985; Vasilyeva et al., 1974; Vasilyeva & Semenova, 1986)

Three-dimensional bacteria:

12. Hexagonal columns (Wu et al., 2012)
13. Heptagonal columns (Wu et al., 2012)
14. Corrugated columns (star-shaped in cross section) (Lasbury, 2013; Wanger et al., 2008; Wu et al., 2012)
15. Tetrahedra (Fritz et al., 2004)
16. Pyramids (Baxter et al., 2005)

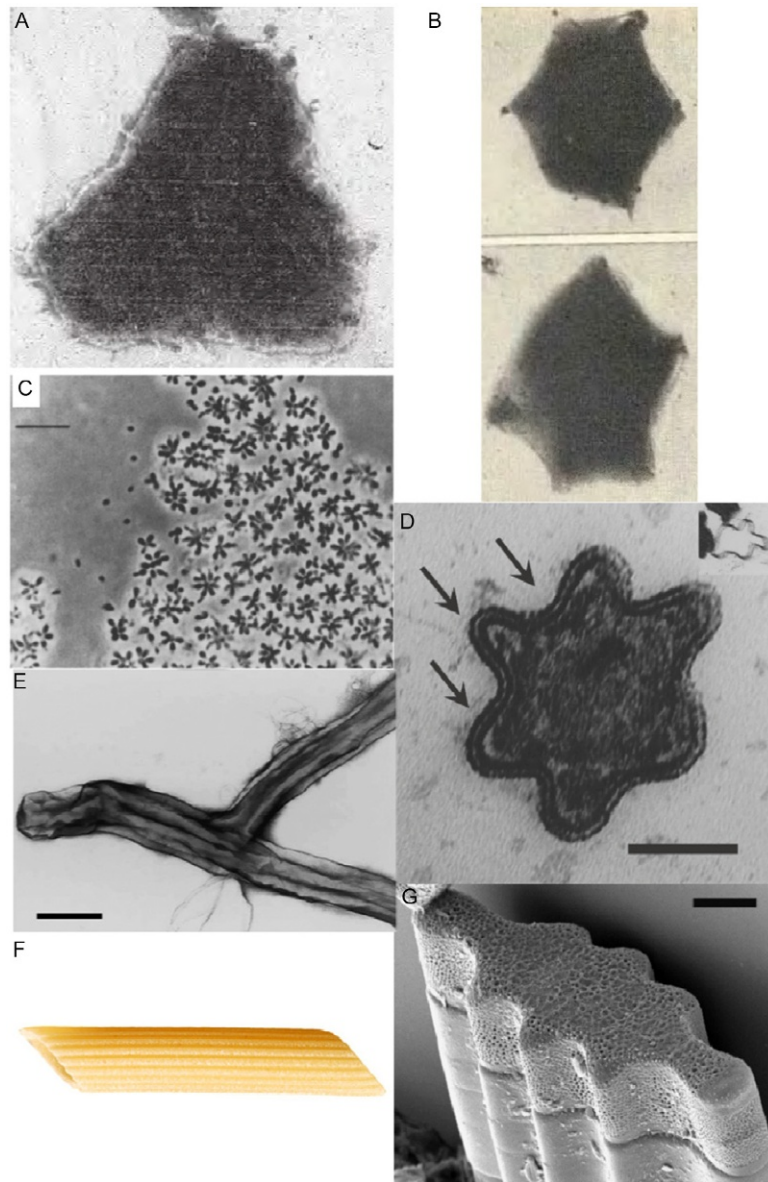
Some halophiles are reported as pleomorphic, yet do not show polygonal geometries (Liao et al., 2016; Mori et al., 2016; Shimane et al., 2015; Wang et al., 2016b; Xu et al., 2016; Yin et al., 2015), while others are rod-shaped (Mou et al., 2012) or sometimes so (Duggin et al., 2015). In Fig. 5, we have catalogued a number of three-dimensional polygonally faceted and corrugated shapes, because their structures may provide hints of mechanisms also applicable to flat cells. The straightness of edges can vary with fixation technique and resolution of microscopy (cf. Rusconi et al., 2013). We include flat, circular Archaea, as equivalent to polygons with an infinite number of edges, per Archimedes (Aktümen & Kaçar, 2007). Most of the bacteria have rounded corners and edges (Fig. 5).

There are now a few different polygonal Archaea species distinguished, including the original (Walsby, 1980) now named *Haloquadratum walsbyi* (Burns et al., 2007; Dyall-Smith et al., 2011), *Haloarcula quadrata* (Burns et al., 2004; Oren et al., 1999; Yang et al., 2007), *Haloarcula argentinensis* (Yang et al., 2007), *Haloarcula japonica* (Takashina et al., 1990; Yang et al., 2007), *Haloarcula*

FIG. 4—Cont'd

Note that in the same culture, triangular, square, rectangular, trapezoidal, quadrilateral, and pentagonal cells may be seen. Note that two cells in each image appear to have holes. (F) The white spots in the image are gas vesicles. (G) Arrows indicate two “holes” in the fluorescence image of an *H. walsbyi* cell stained with Nile Blue for its intracellular polyhydroxybutyrate granules. (H) “Square Archaea with phage particles, head diameter ca 40 nm.” (I) “Square Archaea lysed by phages, head diameter ca 50 nm.” Transmission electron micrographs.

(A) From Bolhuis, H., Palm, P., Wende, A., Falb, M., Rampp, M., Rodriguez-Valera, F., Pfeiffer, F., Oesterhelt, D., 2006. The genome of the square archaeon *Haloquadratum walsbyi*: life at the limits of water activity. *BMC Genomics* 7, #169, with permission from Biomed Central under a Creative Commons Attribution License (CC BY); (B) From Wikipedia, 2008. File: *Haloquadratum walsbyi*00.jpg. https://commons.wikimedia.org/wiki/File:Haloquadratum_walsbyi00.jpg, in public domain; (C, D, E) from Mike L. Dyall-Smith with his kind permission; (G) From Zenke, R., von Gronau, S., Bolhuis, H., Gruska, M., Pfeiffer, F., Oesterhelt, D., 2015. Fluorescence microscopy visualization of halomucin, a secreted 927 kDa protein surrounding *Haloquadratum walsbyi* cells. *Front. Microbiol.* 6, #249, with permission under a Creative Commons Attribution License (CC BY); (H, I) From Guixa-Boixereu, N., Calderón-Paz, J.I., Haldal, M., Bratbak, G., Pedrós-Alíó, C., 1996. Viral lysis and bacterivory as prokaryotic loss factors along a salinity gradient. *Aquat. Microb. Ecol.* 11(3), 215–227, with permission under a Creative Commons by Attribution Licence (CC-BY).

**FIG. 5**

Polygonal bacteria seem not to have straight edges, nor sharp corners. (A) Triangular bacterium, 0.7–0.9 μm in width. (B) *Stella humosa*, star-shaped bacterium. See also *Prosthecomicrobium*: “Each has six appendages extending in one plane” (Staley, 1968). (C) Rosette budding bacteria with “a stable protein envelope.” Scale bar = 10 μm . (D) This is a star-shaped cross section of a bacterium (E) whose corrugated cell wall resembles penne rigate pasta (F). This example has 6 “points.” Cells were reported with 4, 5, 6, 7, and 9 “points.” “The Stars reproduce by forming branching structures. . . . How the Stars manage to hold their shape is a puzzling

(Continued)

marismortui (Oren et al., 1990), *Haloferax* sp. (Emerson et al., 1994), *Halovivax asiaticus* (Castillo et al., 2006), *Halosiccatus urmianus* (Mehrshad et al., 2016), *Halogeometricum borinquense* (Malfatti et al., 2009); most containing gas vesicles (Walsby, 1994), some not (Javor et al., 1982). The star-shaped *Stella vacuolata* and *Stella humosa* are gram-negative bacteria (Vasilyeva, 1985).

Square Archaea represent over 50%–60% of the cells found in crystallizer ponds of salterns worldwide (Antón et al., 1999; Bardavid et al., 2008; Bettarel et al., 2011; Bolhuis, 2005; Mutlu & Guven, 2015), though sampling may have been done at times of blooms (Ram-Mohan et al., 2016). They are present, but not predominant, in the Dead Sea (Bodaker et al., 2010) and the Great Salt Lake (Baxter et al., 2005). The square archaeon has a thickness of as little as 0.1 μm at the edge “or even less in the central regions” (Parkes & Walsby, 1981), “possibly even as thin as 0.07 μm ” (Oren, 1999). Thus, it is lenticular in shape (Fig. 2C), like shaped droplets (Fig. 2A,B), although somewhat irregular in thickness away from the square edges, perhaps due to cell inclusions and/or fixation artifacts (Stoeckenius, 1981). In fact, the thickness seems to go to near zero in some places, “where the opposing cell membranes are in contact,” without affecting the shape of the cell (Zenke et al., 2015), again as observed in shaped droplets (Figs. 2 and 4).

Square Archaea have been reported as 0.25 μm thick for all sizes, with squares of 2 μm and 4 or 5 μm or rectangles of 2 μm by 4 μm , and in electron microscopy cross section, with a lenticular shape (Stoeckenius, 1981). Rectangular cells have been imaged as small as 1.5 μm by 2.1 μm (Fig. 1P), and squares have been reported (Oren, 1999; Romanenko, 1981) as small as 1.4 μm . (A square/rectangular bacterium is reported even smaller as 0.3–2 μm on a side (Whang & Hattori, 1990).) Pure cultures yield square cells of different sizes. The variability in size with congruent shapes suggests that there is no rigid component of a specific length that accounts for the straight edges.

Except for a brief mention of “triangles/pyramids” and the presence of spheres in a collected population containing squares (Baxter et al., 2005), we found no reports that any of the flat Archaea have alternative three-dimensional shapes. While prokaryotes in general can come in many shapes (Gordon & Gordon, 2016a; Huang et al., 2008; Margolin, 2009; Yang et al., 2016; Young, 2007), the flat Archaea have only been observed flat. Star-shaped bacteria change their morphology in some culture conditions (Semenov et al., 1989; Semenov & Vasilyeva, 1985, 1987; Vasilyeva & Semenova, 1986), though the authors did not report that flat cells became three-dimensional.

FIG. 5—Cont'd

question. ... No internal skeleton was observed within the Star. In some plasmolyzed cells. . . , the inner membrane detached from the outer [S-]layer, however, the star-shape was maintained.” Scale bar for cross section = 0.1 μm . Scale bar for side view = 0.2 μm . (G) The columnar, corrugated-centric diatom *Terpsinoë musica*, collected from Whitefield Creek (by the Salton Sea), California. It shows a flat valve face at the top. Scale bar = 20 μm . Cf. (Gordon & Tiffany, 2011).

(A) From Lafitskaya, T.N., Vasilyeva, L.V., 1976. A new triangular bacterium. *Mikrobiologiya* 45(5), 812–816, with kind permission of Lina V. Vasilyeva; (B) From Vasilyeva, L.V., Lafitskaya, T.N., Aleksandrushkina, N.L., Krasilnikova, E.N., 1974. Physiological-biochemical peculiarities of the prosthecobacteria *Stella humosa* and *Prosthecomicrobium* sp. *Izv. Akad. Nauk SSSR Seri. Biol.* 5, 699–714, also with permission of Lina V. Vasilyeva; (C) From König, E., Schlesner, H., Hirsch, P., 1984. Cell wall studies on budding bacteria of the Planctomyces/Pasteuria group and on a Prosthecomicrobium sp. *Arch. Microbiol.* 138(3), 200–205, with permission of Springer; (F) From Wanger, G., Onstott, T.C., Southam, G., 2008. Stars of the terrestrial deep subsurface: a novel ‘star-shaped’ bacterial morphotype from a South African platinum mine (Corrigendum: (6), 421). *Geobiology* 6(3), 325–330, with permission of John Wiley and Sons.

5 MECHANISMS CONTROLLING THE SHAPES OF PROKARYOTE CELLS

Spherical oil droplets become shaped droplets when the temperature is lowered. Polygonal Archaea become rounded when the salinity is lowered. If we look at the plastic phase of shaped droplets and the polygonal shaping of Archaea as phase transitions or precipitations (Kim & Bae, 2003), then they may be examples of a generic process such as is seen in Hofmeister series ranking anions and cations according to their influence on macroscopic properties (Schwierz et al., 2016).

Archaea have a cell wall external to the cell membrane called the S-layer, and some internal cytoskeletal components. There are four general factors that may cause polygonal shapes in Archaea:

1. The S-layer creates the shape of the chamber within which the cell lives.
2. The cell membrane creates the shape.
3. The cytoskeleton creates the shape.
4. Two or three of the above, in concert, create the shape.

Most of these options have been proposed but not rigorously tested, so we are left with evaluating observations that may bear on the question. However, strangely, a nonstructural, physical “mechanism” has been suggested, namely turgor pressure. So we’ll start with that.

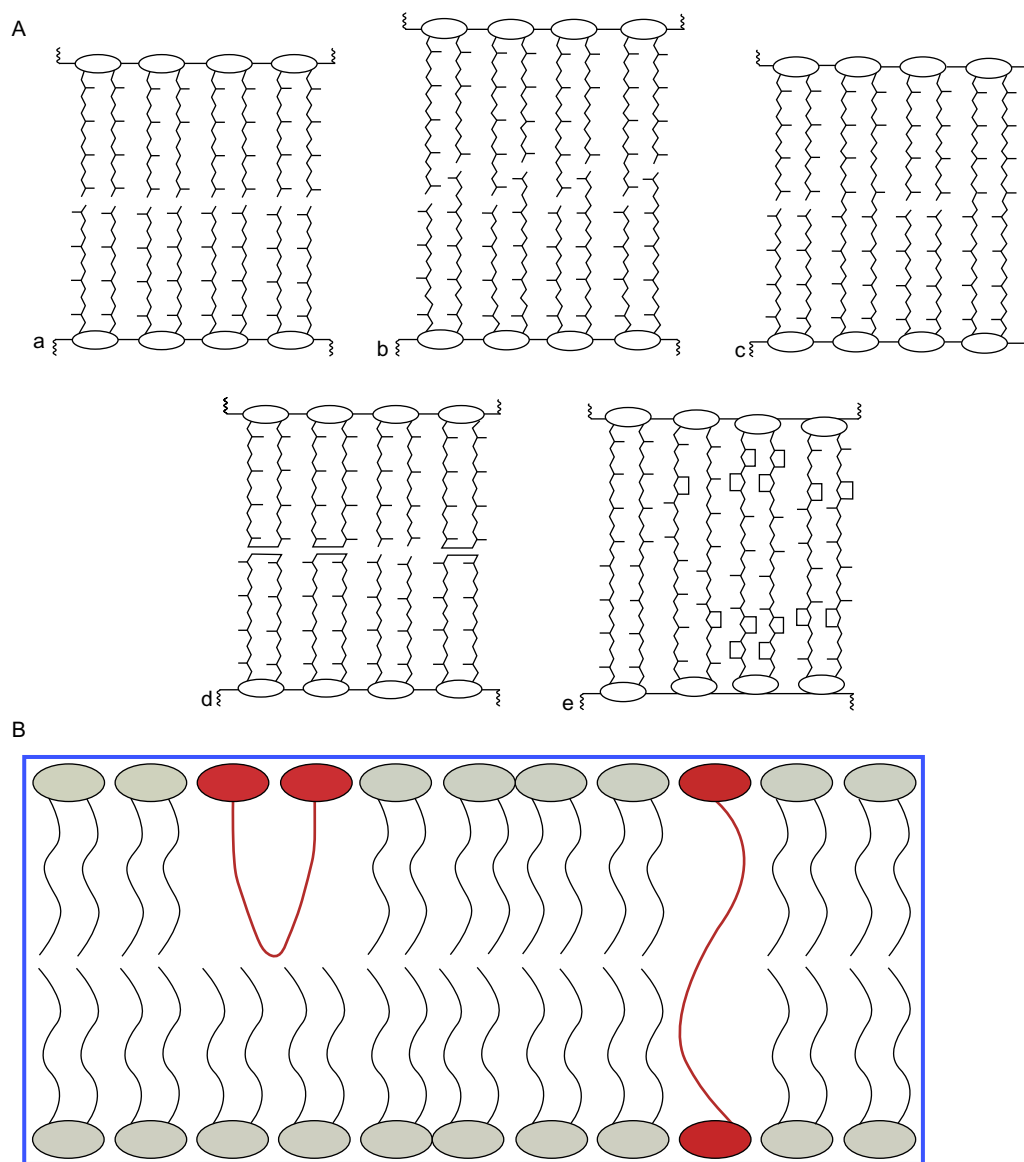
In square Archaea living in saturated salt environments, it has been argued that there is no turgor pressure, and that this somehow “allows” the cells to take on nonspherical shapes (Kessel & Cohen, 1982; Walsby, 1980, 2005). The experiment of osmotically shocking (Berthaud et al., 2016) square cells to watch how they change shape has not yet been done, nor have they been subjected to atomic force microscopy and other physical probes. However, cells lysed by phage (viruses) retain sharp corners (Guixa-Boixereu et al., 1996) (Fig. 4I).

Next, let’s consider the cytoskeleton. A form of actin, crenactin, and an associated protein form a helical microfilament (Braun et al., 2015) that correlates with the rod shape of the archaeon *Pyrobaculum calidifontis* (Ettema et al., 2011). Electron cryotomography shows no internal cytoskeletal structures adjacent to the cell membrane, including at corners in square *Haloquadratum walsbyi*, which have radii of curvature as low as 50 nm (measured from Fig. 1E in (Burns et al., 2007)). Furthermore:

The extreme flatness of the cells may imply the complete absence of cell turgor but the forces that cause cell edges to be as straight as they are observed are currently enigmatic since no genes could be identified in the genome that might express structural proteins involved in maintaining the cell structure

(Zenke et al., 2015).

Next, let’s consider the cell membrane as a possible source of polygonal structure. In general, the membrane lipids of bacteria are unipolar, while those of Archaea are bipolar (Fig. 6). The lipids of square Archaea, in particular, have been elucidated (Lobasso et al., 2008; Oren, 1993; Oren et al., 1996). The membrane lipids of polygonal Archaea could, by themselves, provide geometric structure in a couple of ways. For example, it is possible that specific lipids accumulate at or form membrane regions of high curvature (Boekema et al., 2013; Mukhopadhyay et al., 2008). The bipolar lipids of some Archaea (Figs. 6 and 7) by themselves tend to form flat (Chong, 2010), stiff (Jacquemet et al., 2009; Jain et al., 2014; Kates, 1992) structures, but when mixed with unipolar lipids, the latter can partition more to one side, creating a curved surface (Lelkes et al., 1983). This phase separation of lipid species (Liu et al., 2006) has been used to hypothesize how bacteria and

**FIG. 6**

(A) Various configurations of polar lipids found in Archaea. Those which covalently subtend the whole membrane are called bipolar and represent about 90% of Archaea membranes (Forbes et al., 2006). (B) An additional configuration for bipolar lipids, also called bolaamphiphiles, is the U-shape, where both polar groups are on the same side of the membrane.

(A) From Gambacorta, A., Gliozzi, A., Derosa, M., 1995. *Archaeal lipids and their biotechnological applications*. *World J. Microbiol. Biotechnol.* 11(1), 115–131, with permission; (B) From Forbes, C.C., DiVittorio, K.M., Smith, B.D., 2006. Bolaamphiphiles promote phospholipid translocation across vesicle membranes. *J. Am. Chem. Soc.* 128(28), 9211–9218, with permission of the American Chemical Society.

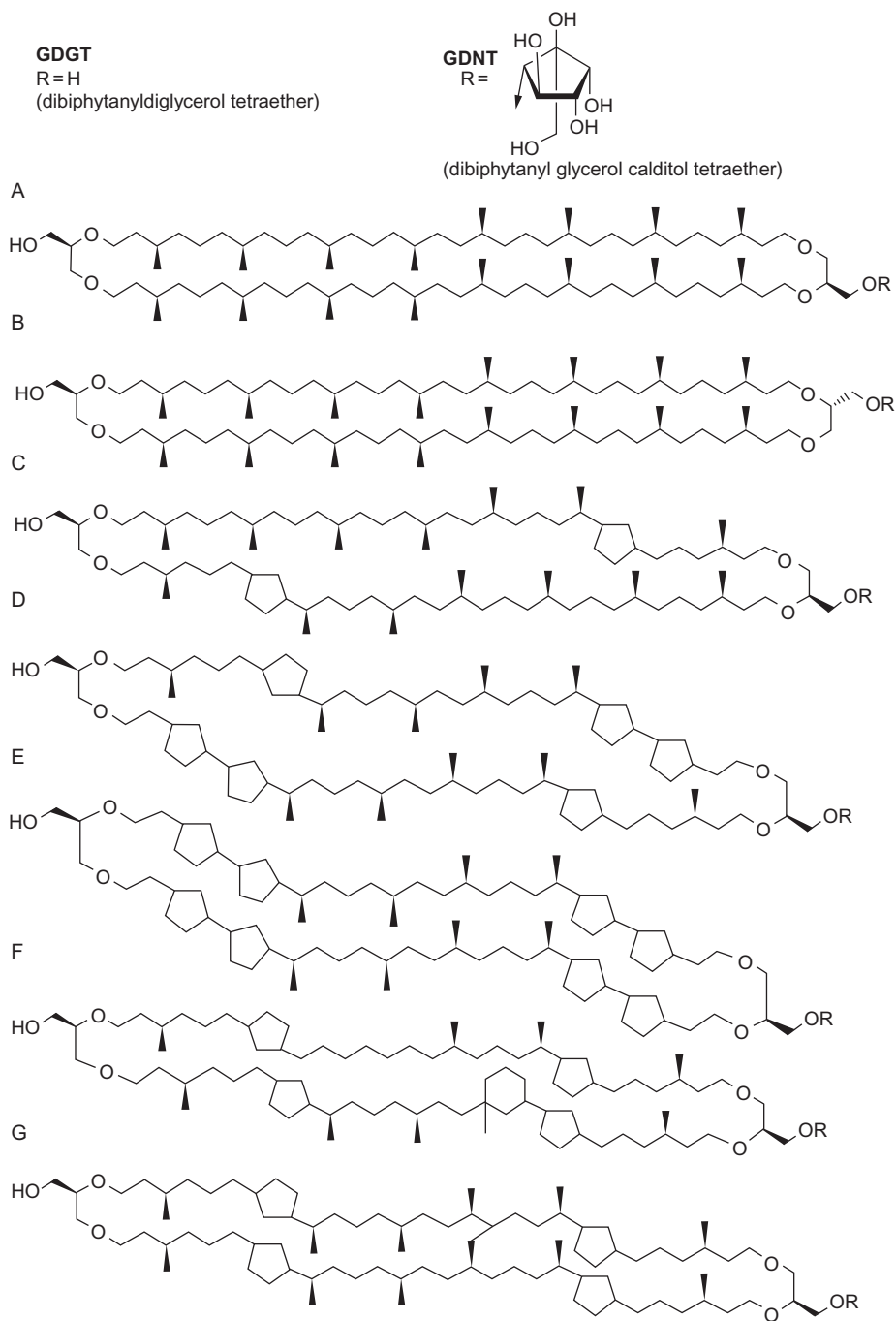


FIG. 7

Examples of tetraether bipolar lipids in Archaea membranes.

From Jacquemet, A., Barbeau, J., Lemiègre, L., Benvegna, T., 2009. Archaeal tetraether bipolar lipids: structures, functions and applications. Biochimie 91(6), 711–717, with permission of Elsevier Paris.

Archaea split apart in early evolution (Wächtershauser, 2003; Yokoi et al., 2012). The degree of fluctuations in shape versus temperature provides a means of analyzing stability of shape (Bivas, 2010; Döbereiner et al., 1997).

However, in at least one case of the bipolar lipid membrane of an Archaea, the membrane makes the transition to a 2D fluid when the minimum temperature for growth is reached (Bartucci et al., 2005). At that point, its fluidity and permeability properties become similar to those of bilayer membranes at lower temperatures. Thus, in its normal temperature range, this archaean's membrane lacks the rigidity it exhibits at lower temperatures:

At the growth temperature of a given organism, the membranes are in a liquid-crystalline state (Melchior, 1982; Melchior & Steim, 1976) which implies substantial dynamics of lipid movement, ensuring optimal functioning of the membrane proteins.... Because of the low melting point of the archaeol and caldarchaeol-based polar lipid membranes of Archaea, these membranes are in a liquid-crystalline phase over a wide temperature range of 0 and 100°C that is physiologically relevant (De Rosa et al., 1986)

(Driessen & Albers, 2007).

A caveat is that the same authors appear to contradict themselves:

...monolayer type of organization gives the membrane a high degree of rigidity (Bartucci et al., 2005; Elferink et al., 1994; Fan et al., 1995; Gliozzi et al., 1983; Mirghani et al., 1990; Thompson et al., 1992)

(Driessen & Albers, 2007).

In any case, the liquidity of the 2D lipid array in polygonal Archaea needs further investigation, especially since it is possible that they may be able to adjust their membrane lipid composition to changing conditions:

Moreover, bacteria can also stabilize their membranes at high temperatures through elongation of membrane lipids (Marr & Ingraham, 1962). ... Surprisingly, little is known about membrane adaptation mechanisms of Archaea to temperature

(Andrade et al., 2015).

If membrane proteins form condensations, i.e., two-dimensional phase transitions, this is the phenomenon of “capping” of membrane proteins that are otherwise mobile in the 2D liquid cell membrane which might provide structure. Capping appears to require attachment to the underlying cytoskeleton (Kindzelskii et al., 1994). Thus, it would seem an unlikely candidate for producing the long range, regular order of polygonal Archaea.

Prokaryotes are often surrounded by 2D crystalline glycoprotein cell walls called S-layers. Square Archaea have a glycoprotein S-layer (König, 1994) that appears to be a hexagonal array with a spacing of 20 nm (Parkes & Walsby, 1981; Stoeckenius, 1981; Sumper, 1993). Electron microscopy shows one S-layer evenly around a corner of *Haloquadratum walsbyi* and two S-layers around a new *Haloquadratum* species (Burns et al., 2007).

The S-layers, if most prokaryotes, are presumed, without proof, to cause and/or maintain the shape of the cell within (Akca et al., 2002; Sleytr et al., 1986). This notion has been contradicted in most cases:

...observations that the loss of S-layers is not accompanied by a morphological change of the progeny cells make it most unlikely that in organisms possessing a rigid cell envelope component, the paracrystalline arrays have an important function in determining cell shape

(Sleytr & Messner, 1983).

An exception is the *Halobacterium salinarum* cell, rod-shaped at high salt concentrations (Sleytr & Messner, 1983), which becomes spherical on proteolysis or alteration of the S-layer (Mescher & Strominger, 1976) or at lower salt (Engelhardt, 2007b).

For polygonal Archaea, the following is the closest we have to a published model, which invokes the cell membrane and the S-layer:

If the cells are not exposed to osmotic imbalance, and the lipids or other cellular factors. . . do not force strong prebending of the membrane, the S-layer-membrane assembly would assume a shape approaching the tension minimum, i.e., a flat, sheet-like arrangement in the ideal case. A model system shown in (Engelhardt, 2007a) illustrates the expected effect. The reconstituted S-layer of *Delftia acidovorans* (p4 symmetry, lattice constant 10.5 nm), interacts with the membrane via bound lipid molecules (Engelhardt et al., 1991) and flattens the symmetrical lipid layer of the vesicles. Interestingly, disk-like species such as *H. volcanii* and *Methanoplanus limicola*, or Archaea forming flat cellular boxes (“Square Bacterium”) do possess S-layers with p6 symmetry and particularly short lattice constants (14.7–16.8 nm. . .). Although other, possibly unknown mechanisms might contribute to the architecture of Archaeal cells, it is conceivable that the biophysical properties of the S-layer-membrane assembly are sufficient to flatten cells (Engelhardt, 2007a)

(Engelhardt, 2007b).

The consensus idea at the moment is that the shape is most likely determined by the rigidity of the S-layer in combination with the absence of turgor pressure. . . Kessel and Cohen (Kessel & Cohen, 1982) noted from their electron microscopic images that the edges are curved or rounded rather than straight, as would be expected for a perfect square or rectangular box with a very narrow width (cf. Fig. 2A). They envisioned the organism as a flattened cylinder, which, to my opinion, is the most likely explanation for the square shape

(Bolhuis, 2005).

The idea then is that the source of flattening of the cell is indeed the S-layer, because it is intrinsically flat and attaches to the cell membrane (Engelhardt, 2007b; Engelhardt & Peters, 1998). One way of investigating this question is to see if there is a fixed or arbitrary angular relationship between the 2D crystal axes of the S-layer and the edges of the square cell. “However, it is generally thought that in halobacteria, the cell wall determines the cell shape, and it is difficult to reconcile the hexagonal lattice with the rectangular shapes of the cells” (Stoeckenius, 1981). A less definitive observation in this regard is that flagella of square cells of *Haloarcula quadrata* (Chaban et al., 2006; Grant & Larsen, 1989; Oren et al., 1999) and the “extracellular fibrils” of *Haloquadratum* sp. (Santos et al., 2012) occur at arbitrary positions along the cell’s perimeter, not preferentially at an edge or corner (Alam et al., 1984). (*Haloquadratum walsbyi* lacks flagella (Bolhuis, 2005)). Damage to “the cell envelope” by the bile salt taurocholate (Bardavid & Oren, 2008b) might, at low doses, prove useful to separating the roles of the S-layer and the cell membrane. Note that “no direct genetic indication was found that can explain how this peculiar organism retains its square shape” (Bolhuis et al., 2006). S-layer self-assembly gives various cylindrical, tubular, and ribbon shapes (Pum & Sleytr, 2014), but nothing resembling a flat polygon. While the tubulin-related CetZ1-GFP “localizations are envelope associated” in *Haloferax volcanii*, this species is disc- or rod-shaped (Duggin et al., 2015), not polygonal.

In regard to membrane/S-layer interaction, we arrive at the conclusion that it is not sufficient to generate polygonal shapes:

The biophysical consequences of synergistic functions between S-layers and the cell membrane in Archaea, and the outer membrane or the peptidoglycan in bacteria are still largely unexplored. ... Experimental data on natural systems are rare. ... The lipid molecules are immobilized indirectly by non-specific association to the S-layer protein whereby the membranes become less fluid, less flexible, more stable and heat-resistant, and presumably more resistant to hydrostatic pressure. ... Natural association of S-layers with the cytoplasmic membrane occur in Archaea only. ... that up to 5% of the lipids may be immobilized by interactions with the S-layer anchor, disregarding other proteins. The important point is that the anchors, unlike common membrane proteins, do not freely float in the lipid phase. ... Taken together, it becomes evident that the inherent properties of S-layers are probably insufficient to constitute a distinct shape-determining function by themselves, beyond that of a passive shape-modifying effect. There is obviously a need for additional structural or functional ingredients. ... The conclusion from these considerations is that S-layers may be shape-maintaining and shape-modifying but they are not shape-determining in a strong (process-related) sense.

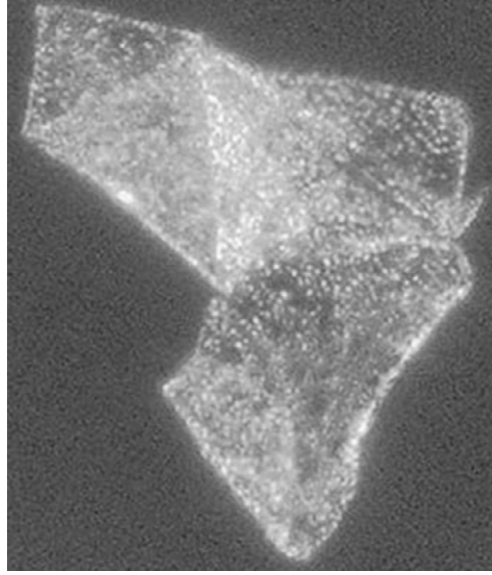
(Engelhardt, 2007a).

There are alternatives to the S-layer that have been considered. It has been suggested that: “A cross-linked matrix of poly-gamma-glutamate may contribute to the cell wall rigidity and maintenance of the unique square morphology” (Lobasso et al., 2008), though there is no proof this matrix exists in *Haloquadratum walsbyi* (Albers & Meyer, 2011; Bolhuis et al., 2006; Wu et al., 2012). Halomucin has been invoked in the “water enriched capsule,” with speculation on its rigidity (Bolhuis et al., 2006). Later work showed halomucin only “loosely attached to cells” (Zenke et al., 2015).

Note that “the sensitivity of the cells to mechanical shearing” and “flexibility of the larger cell structures. ... rarely found in an unfolded state” (Bolhuis et al., 2004), also described as “extremely fragile” (Dyall-Smith et al., 2011), suggests rigidity, because each folded section remains flat (Fig. 8), with some sort of crease at the folding line, perhaps like stiff paper. Flat, disc-shaped Archaea are also fragile (Stetter, 1982). In contrast to square Archaea, bacterial cell walls can be highly elastic and capable of resisting turgor pressures up to 30 atmospheres (Hemmingsen & Hemmingsen, 1980).

Some bacteria are long ribbons that are star-shaped in cross section only (Fig. 5), resembling the presumed buckling patterns of some “corrugated” diatoms (Gordon & Tiffany, 2011). This led us to consider whether most of the patterns of single Archaea and bacteria listed above might be due to variations on a single mechanism, known as wrinkle/ridge (Jin et al., 2015) or buckling/folding (Schmalholz & Podladchikov, 1999) transitions (Fig. 9). Buckling has been invoked for shaping of one Archaea (Pum et al., 1991).

A cell is topologically a sphere. Here we would like to propose that polygonal Archaea may best be modeled as deflated spheres of a material, probably the S-layer, whose equilibrium shape, were it not constrained by a spherical geometry, would be planar. This property is evident in images of folded cells, which are creased rather than undulated (Fig. 8). A deflated soccer ball provides a qualitative model, from which we can see, at least for a material with the constitutive properties of a soccer ball, that various polygonal shapes with reasonably straight edges and sharp corners do develop (Fig. 10). This effect has recently been investigated (Quilliet et al., 2008) and polygons develop on the surfaces of spheres as their volume decreases below critical values (Knoche & Kierfeld, 2011, 2014b,c) (Fig. 11). Unfortunately, none of the simulations or experiments has yet been taken to the extreme found in shaped droplets and flat Archaea, so while cross-sectional sketches of the collapsed shapes are available (Fig. 11), we do not know if the full three-dimensional shapes will reflect those of polygonal Archaea or those of collapsing shaped droplets (Fig. 12).

**FIG. 8**

"Darkfield microscopic image of a large folded sheet of 'Haloquadratum walsbyi,' revealing its sharp edges and straight corners. Size is $\sim 40 \times 40 \mu\text{m}$. White spots are gas vesicles."

From Bolhuis, H., 2005. Walsby's square archaeon—it's hip to be square, but even more hip to be culturable. In: Gunde-Cimerman, N., Oren, A., Plemenitaš, A. (Eds.), *Adaptation to Life at High Salt Concentrations in Archaea, Bacteria, and Eukarya*. Springer, Dordrecht, The Netherlands, pp. 185–199, with permission of Springer.

To check where on the volume reduction scale square Archaea fall, for instance, let's consider one cell for which we have both width (L) and thickness (T) measurements (Fig. 2C), approximating it as a flat, square box with rounded edges. The cell volume is:

$$V = T(L - T)^2 + 2\pi TL \approx TL^2,$$

and the surface area is:

$$A = 2(L - T)^2 + 2\pi TL \approx 2L^2$$

assuming a half cylindrical shape of the edges. Here, we are approximating the cell as a flat, rather than lenticular shape, so that $T = 2r$, where r is the radius of a cross section of an edge (Fig. 2A). A sphere of equivalent area has a radius R calculated from:

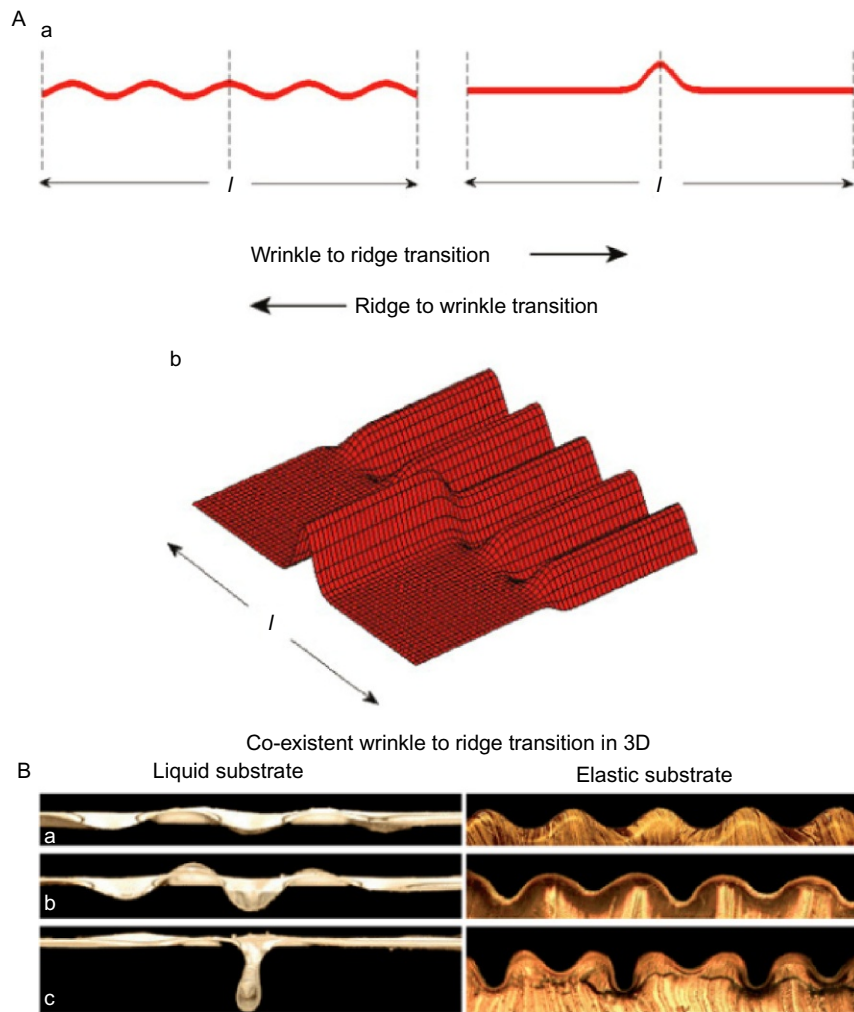
$$A = 4\pi R^2$$

Its volume is:

$$V_0 = (4/3)\pi R^3 = L^3 / (3\sqrt{\pi/2})$$

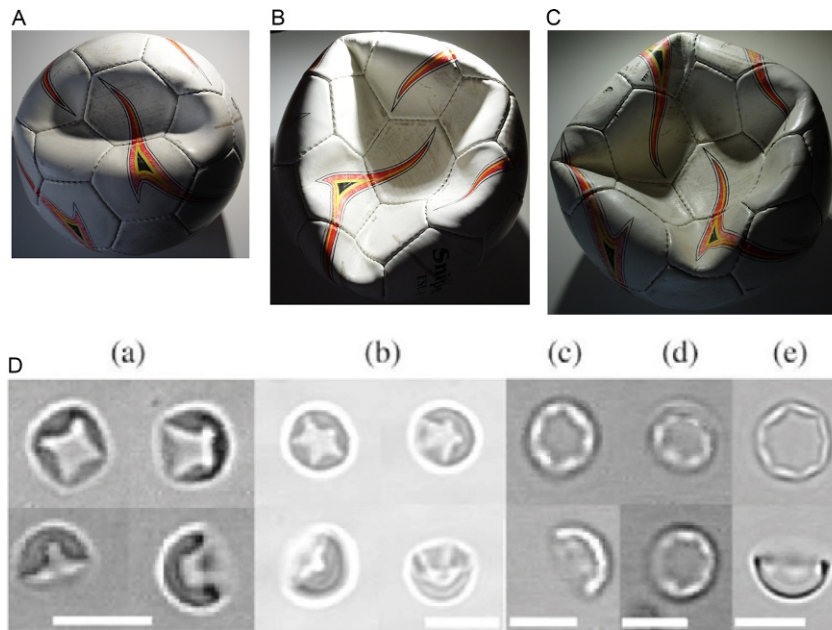
Thus, the abscissa in Fig. 11B is:

$$V/V_0 = (3\sqrt{\pi/2})T/L$$

**FIG. 9**

(A) Whether a surface makes rolling wrinkles or produces sharp folds with nearly straight edges depends on prestress and nonlinear mechanical properties of the substrate under the sheet of buckling material, in the case of prokaryotes, the cell membrane/S-layer, and the cytoplasm mechanical properties. The transition is unstable, i.e., snapping occurs between the two states of a surface (Takei et al., 2014). (B) Folding (left) or buckling (right) depends on the viscosity or elasticity of the substrate, or more generally, on its viscoelasticity.

(A) From Jin, L., Takei, A., Hutchinson, J.W., 2015. Mechanics of wrinkle/ridge transitions in thin film/substrate systems. *J. Mech. Phys. Solids* 81, 22–40, with permission of Elsevier; (B) From Brau, F., Damman, P., Diamant, H., Witten, T.A., 2013. Wrinkle to fold transition: influence of the substrate response. *Soft Matter* 9(34), 8177–8186, with permission of the Royal Society of Chemistry.

**FIG. 10**

Symmetry breaking in deflated balls. (A–C) Buckled soccer ball illustrating 2, 3, and 4 edges, with thanks to Diane Sucharyna. (D) “...colloidal spheres filled with oil, in a mixture of water and ethanol... showing 4–8 wrinkles (a–e). Each subfigure shows different transmission optical microscopy views of the same object. Scale bar 5 μm , except subfigure (c): 2 μm ... The oil consists of low molecular polydimethylsiloxane (PDMS) oligomers. By adding tetraethoxysilane (TEOS), a solid shell forms at the surface of the droplets, consisting mainly of PDMS with average oligomer length 4, cross-linked with hydrolyzed TEOS units.” Computer simulations are reported there and in (Quilliet, 2012; Vliegenthart & Gompfer, 2011), some reaching to a 14-sided polygon: “...the thinner the shell, the larger the number of wrinkles [polygonal edges] are to be expected” (Marmottant et al., 2011). At the lower limit, triangles are observed in stomatocytes (abnormally shaped red blood cell) (Lim et al., 2002), and buckling with 2-, 3-, or 4-sided polygons, the latter often irregular quadrilaterals, occur in some polymer particles (Okubo et al., 2001). For collapsed basketballs showing polygons see: 2-sided (Jicepex, 2015); 3-sided (Logan, 2015); 4-sided (Mitic, 2015; ShopAdvisor, 2015); 5-sided (Garnett, 2015).

From Quilliet, C., Zoldesi, C., Riera, C., van Blaaderen, A., Imhof, A., 2008. Anisotropic colloids through non-trivial buckling [Erratum: 32(4), 419–420]. *Eur. Phys. J. E* 27(1), 13–20, with permission of Springer.

For the square cell in Fig. 2C, we estimate $V/V_0 = 0.10$ (assuming the cross section was parallel to an edge), which coincides with category 4_c in Fig. 11B. Thus, its shape is consistent with the idea that it is due to spherical buckling caused by volume shrinkage with its area retained.

The transition between a spherical shape and a polygonal shape of an Archaea as salt concentration increases (Javor et al., 1982) may indeed involve exit of water from the cell and loss of cell volume, i.e., crenation. The transitions between shapes may be due to the various energy levels of different configurations, some of which are metastable (Knoche & Kierfeld, 2011, 2014a,b,c). The energy differences between states and the heights of their metastabilities may be guides to why certain polygons

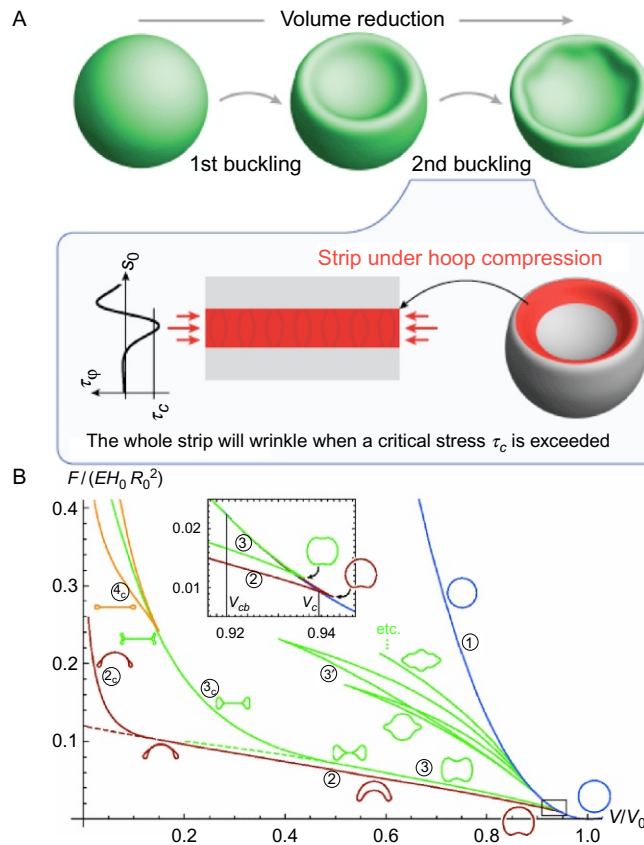


FIG. 11

(A) Buckling of a sphere whose surface area is retained but whose volume is decreased occurs in two stages. The second stage leads to wrinkling under hoop compression that results in a regular polygon around the rim.

The authors estimated polygons of 6, 7, or 8 sides for various values of the parameters. (B) “Bifurcation diagram for given volume of a capsule [collapsed or crenated sphere with a thin, solid shell] with \bar{E}_B [dimensionless bending modulus] = 0.001.” Only midline cross sections are shown. The abscissa is the volume relative to a sphere, and the ordinate is a dimensionless ratio of the stored elastic energy F to the Young modulus E . Note that configurations 3c and 4c resemble the cross sections of shaped droplets and polygonal Archaea.

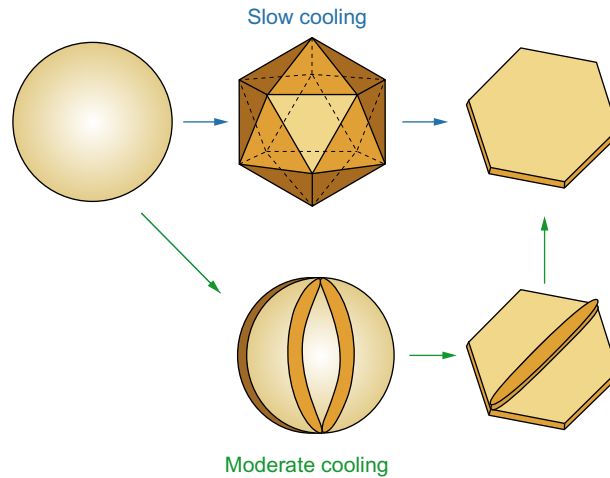
(A) Graphical abstract from Knoche, S., Kierfeld, J., 2014. The secondary buckling transition: wrinkling of buckled spherical shells. *Eur. Phys. J. E* 37(7), #62, with permission of Springer; (B) From Knoche, S., Kierfeld, J., 2011. Buckling of spherical capsules. *Phys. Rev. E* 84(4), #046608, with permission of the American Physical Society.

E 84(4), #046608, with permission of the American Physical Society.

are more frequent in occurrence than others, as we have observed for shaped droplets (Haas et al., 2017).

Our crenated sphere buckling model for polygonal Archaea has a few peculiar characteristics:

1. The polygons formed can have any number of sides, independent of the 2D crystallinity of the S-layer.

**FIG. 12**

Two modes of shape change of a sphere to a shaped droplet at constant volume: polyhedron as an intermediate phase, and folding as an intermediate phase. Cf. (Denkov et al., 2015; Dubois et al., 2001; Guttman et al., 2016a).

2. Nevertheless, when a polygon edge is parallel to a crystallographic direction, as in triangles or hexagons, the crystallinity of the S-layer may contribute to the stability of the polygon.
3. The S-layer is always somewhere in a state of stress, since at least in parts it is bent out of its equilibrium planar configuration.
4. Edges are in effect creases in the structure of the S-layer and may include changes in the basic 2D lattice that accommodate the high local stress via dislocations and other rearrangements of the S-layer proteins.
5. As the cell membrane is attached to the S-layer, it may develop regions of liquid crystal or plastic behavior, especially along the creases.
6. At corners of the polygons, we can anticipate even greater dislocations; in both S-layer and membrane lipids.
7. Thus, the total energy of the system includes the sum of the crease energy, the corner energy, and the deviations from planarity (curvature).

Thus, our 1D model for shaping in the Appendix, based on analogy with the linear arrays of magnets with periodic boundary conditions, may be of relevance in the crenated sphere buckling model, approximating molecular phenomena around the rim of the polygon. This is particularly so, since the sharp creasing of folded square Archaea (Fig. 8) suggests a nonlinear response of the S-layer (and perhaps the cell membrane) versus degree of bending. This nonlinearity may have to be added to the crenated sphere buckling model. In particular, we can anticipate its importance at edges and corners. It is probably a reversible nonlinearity, as suggested by squares changing to triangles in a time-lapse study of *Haloarcula japonica* (Hamamoto et al., 1988). While the cells they observed roughly divided into two daughter cells of equal area, the angle of the plane of division (“cell plate”) seems to have no fixed relationship to the sharp corners (“apices”) at the perimeter, unlike the polar growth of rod-shaped prokaryotes (Kysela et al., 2013). In each case where there is a change in the number of corners, the cell shows a reduction from 4 to 3 corners.

In our model of shaped droplets, the plastic phase is visualized as occurring at the edges (Fig. 2A). The configurations at corners and over the broad, nearly planar top and bottom surfaces, are not considered. There is, however, no reduction in volume. Rather, shape change occurs with an increase in surface area. While this contrasts with the soccer ball model, where surface area is constant, both may be accommodated by adding a third axis to the phase diagram of Fig. 11, namely A/A_0 . Shaped droplets would all be on the plane $V=V_0$.

The basic mechanism of flat polygon formation seems to be hoop compression around the rim of the indentation of a sphere. The formation of a cup shape has been called “first buckling” and the formation of polygonal structure has been called “second buckling” due to hoop compression (Fig. 11). Second buckling occurs over a limited range of mechanical parameters. Hoop compression is found in a number of contexts in biology, including the microfilament ring in eukaryotic cell division, the FtsZ ring in prokaryote cell division, and in the rim of the blastula during animal embryogenesis. It may well be worth looking carefully for polygon formation in these cases. Polygonal arrangements occur in microfilament rings in epithelial cells and at the perimeter of the silicalemma in polygonal diatoms, though in both cases it would seem there is a preexisting polygonal constraint. We can now recognize the formation of problastopores (Gordon & Gordon, 2016a; Gordon, 1999; Gordon et al., 1994) as a case of hoop compression, which ordinarily results in a normal embryo, but may be what sometimes generates a two-, three-, or four-headed embryo (Laale, 1984) (contrary to a priori considerations (Murray, 2012)). Armadillos form 4 to 12 monozygous embryos, which might come from a similar mechanism, followed by separation of the individuals (reviewed in (Gordon, 1999)). So what we may have here in hoop compression is what has been called a “generic” mechanism in development (Newman & Comper, 1990). While this is important and perhaps eye opening to know, it also presents a cautionary tale: things that look alike may not be related by evolutionary descent. This similarity results from so called “convergent evolution” (Powell & Mariscal, 2015).

6 POSSIBLE FUNCTIONS OF A POLYGONAL SHAPE OF CELLS

Small differences in shape have been associated with profound advantages in motility, drag reduction, surface-proportional nutrient uptake, and predator avoidance (here resistance to being merged/diluted with other droplets)—key drivers for evolutionary selection (Young, 2006, 2007, 2010). These differences could play a significant role in selecting and enhancing metabolic difference selection in proto-life entities capable only of some of the functions of life, e.g., metabolism, replication, and heredity. Curiously, in addition to defying spherical form upon cooling, shaped oil droplets have recently been shown to exhibit spontaneous decrease in size, capturing the necessary energy to do so from thermal fluctuations (Tcholakova et al., 2017). The increase in interfacial energy shows that very simple chemical systems may be able to harvest energy from the environment in a fashion similar to life. Breakup of droplets has been seen previously due to various one-time chemical or thermal stimuli via different mechanisms. Yet self-shaping droplets can harness small thermal fluctuations for repeated droplet deformation and corresponding breakup, a likely common and repeated stimulus to have occurred on early Earth and elsewhere.

Additional potentialities for straight edges in shaped primordial oil droplets and polygonal Archaea may be that they can hypothetically accommodate long, straight polymers along their straight edges that may be predecessors of the later development of a cytoskeleton. This may simply be a wall effect (Aliabadi et al., 2015; Robledo & Rowlinson, 1986; van Roij et al., 2000). For example, gas vesicles are often found preferentially along the edges in square Archaea (Figs. 1: 4-sided polygons, 4A, 13).

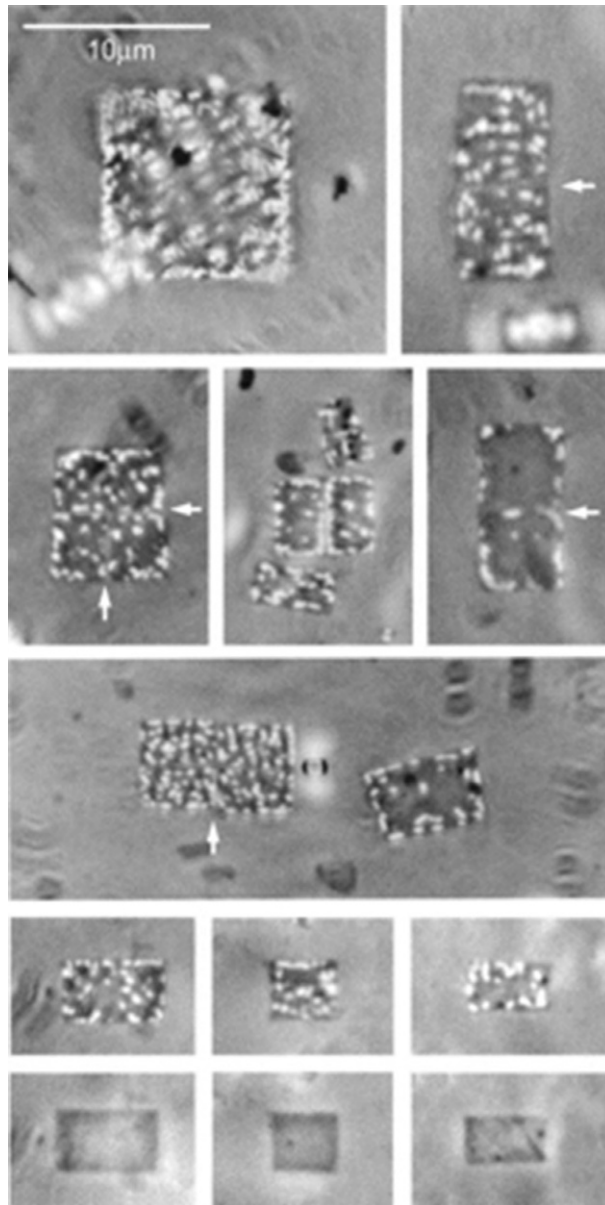


FIG. 13

“The square archeon from the Sinai. Phase contrast light micrographs of the original square haloarcheon discovered in a brine sample from a sabkha near Nabq, Sinai. Division lines (arrows) are visible in some of the cells but not in the largest, top left. Gas vesicles show as bright refractile granules in all cells except those in the last line, which have been exposed to pressure (the same cells as in the line above). Scale bar represents 10 μm .” Note the frequent alignment of gas vesicles with the straight edges of the cell and the “division line.” This figure is rearranged from figures in (Walsby, 1980) and copied in (Walsby, 2005) and here. See also Fig. 1C in (Parkes & Walsby, 1981).

From Walsby, A.E., 2005. *Archaea with square cells*. *Trends Microbiol.* 13(5), 193–195, with permission of Elsevier and Walsby, A.E., 1980. *A square bacterium*. *Nature* 283, 69–71, with permission of Nature Publishing Group.

Note that the cell shape does not change when the gas vesicles are collapsed by centrifugation (Stoeckenius, 1981).

At this juncture, the best we can do is speculate on what polymeric molecules might have been aligned in shaped protocells and review experiments on extant polymeric molecules confined in cells or small droplets or vesicles. A model for protocells has been advanced in which the inner surface of a vesicle is the site for polymer adsorption (Fig. 14). Shaped droplets would give the interface a specific structure onto which they could adsorb.

Oil vesicles enriched with polymer molecules aligned along the surface can be compared with a somewhat analogous system in extant cells: liposomes with cytoskeleton bundles (Fig. 15):

We reconstitute a minimal model system of liposomes containing actin-fascin bundles to elucidate how a lipid membrane and a simplified actin cytoskeleton influence each other's organization through mechanical interactions. When the liposomes are sufficiently deformable, the bundles can deform the membrane into finger-like protrusions, reminiscent of cellular filopodia. The protrusions can reach lengths of up to 60 μm . In contrast, liposomes having a membrane with a large bending rigidity predominantly remain spherical and force the bundles to form cortical rings. . . . Half of the protruded stiff liposomes have bundles with sharp kinks arranged in a planar ring-like structure in the main body. . .

(Tsai & Koenderink, 2015).

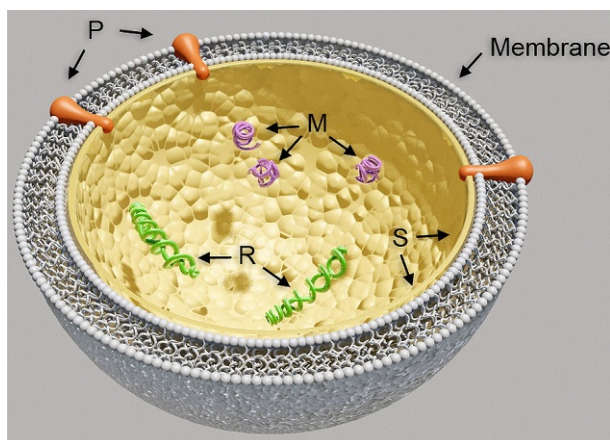


FIG. 14

The SPRM vesicle model for a protocell with adsorbed polymers. “An S-polymer arises by chance that stabilizes protocell membranes allowing them to survive to return their contents to the anhydrous phase. Protocells then evolve the P-polymer, which gives them access to nutrients through transmembrane pores. Access to nutrients supports the emergence of metabolism catalyzed by M-polymers. Metabolism will generate products that support replication (R-polymers)” (Damer & Deamer, 2015). Note that the hypothesized first component, the S-polymer, is in the place of future cortical cytoplasm, suggesting that a cytoskeletal component was the first step after the cell membrane in the origin of life. This model is guiding the search for the simplest molecules that can have the four functions. Note that the hypothesized S-protein is inside the membrane, whereas the Archaea S-layer is outside, so they may not be related.

Reproduced with kind permission of Bruce F. Damer and David W. Deamer.

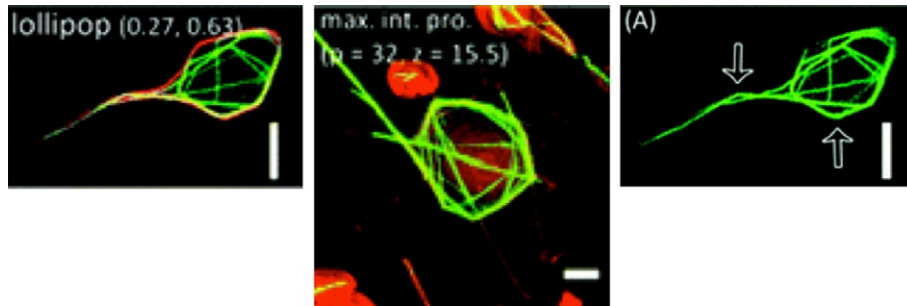


FIG. 15

Microfilaments confined in liposomes. The microfilaments often exhibit kinks, and the liposome bilayer membrane distorts with protrusions, so they are interacting. Sometimes nearly polygonal configurations result. “To address the competition between the deformability of the membrane and the enclosed actin bundles, we tune the [microfilament] bundle stiffness (through the fascin-to-actin molar ratio) and the membrane rigidity (through protein decoration). Scale bars 5 μm .”

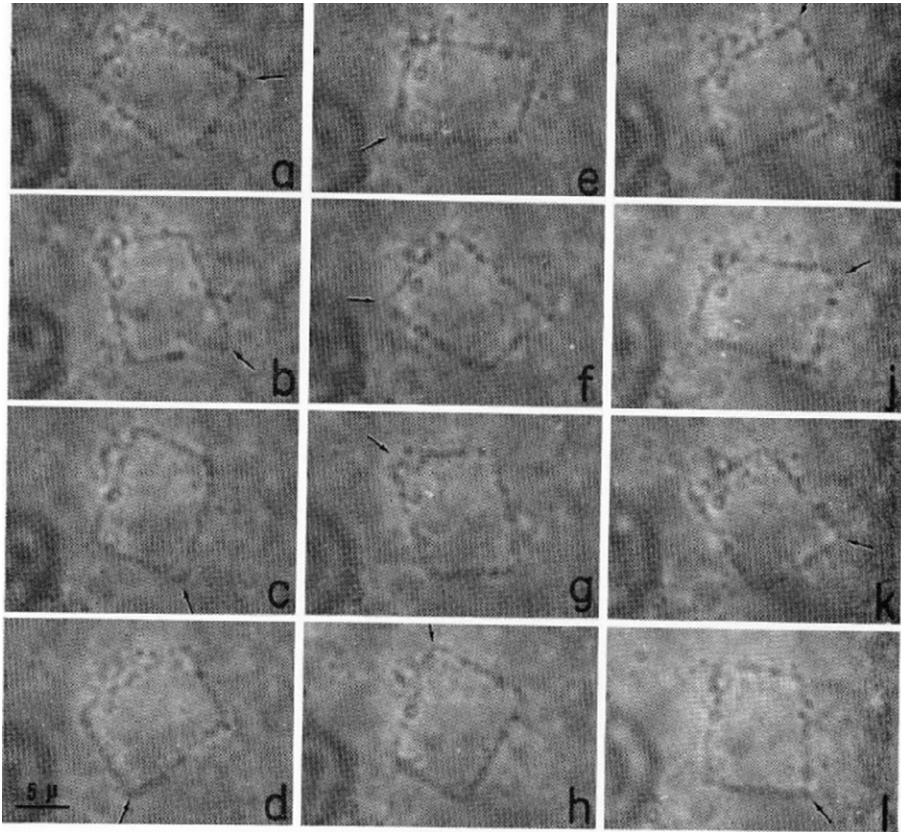
From Tsai, F.-C., Koenderink, G.H., 2015. Shape control of lipid bilayer membranes by confined actin bundles. *Soft Matter* 11(45), 8834–8847, with permission of the Royal Society of Chemistry.

Thus, confined linear polymers produce planar polygons, and we can imagine a positive feedback between shaped droplet protocells and their kinked polymeric contents. Computer simulations (Koudehi et al., 2016) could be extended to include such interactions. Once cytoskeletal molecules became associated with motor molecules, their behavior in a liquid-crystalline environment may have become important, by analogy to that of motile bacteria confined in small volumes of liquid crystals (Mushenheim et al., 2015). Propagating kinks (Fig. 16), if they also occur in confined microfilaments, would provide a further mechanism for polygonal interactions between cell shape and cytoskeletal shape.

7 POLYGONAL DIATOMS

We have demonstrated the uncanny rotational symmetry of some centric diatom valves that have n radially arranged sectors by rotating their scanning electron microscopy (SEM) images by $2\pi/n$ radians and subtracting the rotated image from the original (Sterrenburg et al., 2007). The valves are made of amorphous silica and thus, unlike snowflakes, they in themselves have no crystalline structure, despite their symmetry. Some diatoms, all in the Class Mediophyceae (Medlin & Kaczmarska, 2004), have polygonal shapes similar to shaped droplets (Fig. 1).

The precipitation of a new silica shell (the face of which is called a “valve”) occurs inside flat membrane bags called silicalemmas (Crawford, 1981; Gordon & Drum, 1994). While the microtubule organizing center (MTOC) attached outside the valve silicalemma has been considered as a patterning device for the deposition of silica inside the silicalemma (Parkinson et al., 1999), we had no explanation for the high degree of symmetry of some diatoms. The exploratory behavior of microtubules (Gerhart & Kirschner, 1997, 2007; Kirschner & Gerhart, 1998; Schulze & Kirschner, 1988) seemed to be a

**FIG. 16**

“The propagation of angles of a polygon as waves. Particles attaching to the fibril do not change their positions. (a–l) Intervals of successive pictures: 1/2 s. Arrows show a corner which propagates as a wave. (Observed with an inverted brightfield microscope.)” Here there are 4 waves. Each is a corner that propagates through the fibril in a clockwise fashion. In other words, it is the sharp bend that propagates along the closed loop fibril, i.e., the fibril itself is not rotating.

From Kuroda, K., 1964. *Behavior of naked cytoplasmic drops isolated from plant cells*. In: Allen, R.D., Kamiya, N. (Eds.), *Primitive Motile Systems in Cell Biology*. Academic Press, New York, pp. 31–41, with permission from Elsevier.

possibility, but no mechanism was apparent that would lead to position them in a precise, equal angle arrangement. By analogy with the shaped droplets, we can now come up with a working model:

1. The microtubules in the MTOC attached to the silicalemma and the precipitating silica inside the silicalemma provide the rigid components of a tensegrity apparatus similar to the cell state splitter (Appendix, Fig. 24B) in developing embryos (Gordon & Gordon, 2016a,b; Gordon, 1999; Gordon & Brodland, 1987).

2. The microfilament ring around the outside of the perimeter of the silicalemma (Gordon et al., 2009; Pickett-Heaps & Kowalski, 1981; Pickett-Heaps et al., 1979a,b) and perhaps the silicalemma membrane and/or a radial network of microfilaments (Medlin, 2016) provide compressive elements of this tensegrity apparatus.
3. Under some conditions, the microfilament ring becomes polygonal, as in Figs. 15 and 16.

This then becomes another case of hoop compression (Fig. 11).

This model could be explored by computer simulation as a dynamic tensegrity structure (Caluwaerts et al., 2014; Shen & Wolynes, 2005), via simulations of buckling of the nascent diatom valve (Diaz Moreno et al., 2015; Gutiérrez et al., 2017), and via molecular dynamics (Annenkov & Gordon, 2017). Direct observation of the stages of formation of the valve inside live diatoms is also feasible, using fluorescently labeled microtubules and microfilaments. The nascent valve is formed in under 15 min, as demonstrated by fluorescent silica labeling (Hazelaar et al., 2005). This time is consistent with the dynamic instability of microtubules (Yenjerla et al., 2010). One must look through an older valve to see the newly-forming valve inside the silicalemma, which is inside the cell. The older valve could be cloaked (made “invisible” Koprowski, 2013) by using a nontoxic medium matching its refractive index ($n = 1.43$ (Fuhrmann et al., 2004)), for example, with methyl cellulose ($n = 1.4970$ (Scientific Polymer, 2013)) diluted to an appropriate concentration.

8 CONCLUSION

Our hypothesis is then that tensegrity is a universal mechanism for generating a variety of polygonal cell shapes. The discovery of such structures in self-shaping oil droplets and the potential advantages they can confer to protocell mobility, metabolism, and selection (Sharov, 2017) lends further support for droplets as primordial protocells in the lipid world scenario of the origin of life. Later in evolution, similar tensegrity generation mechanisms seem to have been utilized by Archaea, which individually can undergo a series of shape variations that closely follow the series of shapes in cooled oil droplets. Their structures agree on many points:

1. Sharp corners.
2. Straight edges.
3. No linear molecular structures supporting those edges.
4. Lenticular form, i.e., thinner in the middle.
5. Formation of holes.
6. Comparable size ranges.
7. Ability to change the number of edges.
8. Ability to reversibly adopt a spherical shape with the change of one environmental parameter.

A difference between them is that shaped oil droplets transform under constant volume, whereas polygonal Archaea tend to transform shape under constant area. Conditions that affect shape transformation in droplets and Archaea are temperature and salinity, respectively. The salinity parameter has yet to be explored for shaped droplets. We are at the beginning of understanding the behavior and dynamics of shaped droplets over time and whether these primitive droplet systems might display hysteresis or have mechanisms that confer robustness. At this point, we can say that such primitive-shaped droplets could have existed, but may be too primitive to preserve structure under environmental change

or perturbation. Oil protocells apparently had neither genes nor proteins, but some molecules could have supported compositional and structural heredity by adsorption at edges and/or via the wall effect.

It is meaningless to talk about possibility of a direct descent of prokaryotes from the oil-based primordial self-reproducing systems, because of the enormous difference in their functional complexity. The evolutionary path towards the complexity of prokaryotes included numerous intermediate stages and possibly took several billion years (Sharov & Gordon, 2017). It is unlikely that all these intermediate steps required flat polygonal cells. However, we suggest that polygonal shapes recurrently appeared in evolution, and the physical implementation of these shapes was based on the same generic tensegrity principle with variations in the details.

The role of polygonal shapes in the origin of life is still obscure. Although there is a possibility that primordial polymers could have been constructed more effectively along the edges, we don't know which polymers formed the first adhesions to the edges of shaped protocells, possibly stabilizing their forms and providing a basis for the cytoskeleton and/or nucleic acids. Further, it is not clear how oil droplets had evolved into membrane-bound vesicles. We suggest double water-oil-water droplets as an intermediate step. Is it possible that the emergence of protein synthesis was facilitated by the presence of cell edges? There is a huge literature on the paths towards the origin of life. What we are then suggesting is that the existence of polygonal shapes in oil droplets rescales the possibilities of those scenarios that may permit us to hone in on a working hypothesis for the steps in the origin of life.

As for more recent ancestral organisms, it may be possible to evaluate the possibility whether, for example, LUCA (the Last Universal Common Ancestor) was a flat polygonal cell. Testing for such a possibility may require the analysis of genes that correlate with such shapes. This is a testable prediction, given that 355 protein families in LUCA have been deduced (Weiss et al., 2016) and we now have the complete genome sequences of some polygonal Archaea (Liu et al., 2011; Malfatti et al., 2009; Wikipedia, 2016c). The only halophilic Archaea used in ascertaining LUCA was *Haloferax volcanii* (Weiss et al., 2016), which occasionally has an indistinct triangular shape (Emerson et al., 1994), generally looking like a “potato chip” (Oren, 1999). A greater sampling of the genomes of truly polygonal Archaea might show a closer similarity with LUCA than currently reported (Weiss et al., 2016).

Our finding of polygon-shaped oil droplets opens new logical paths for the analysis of the origin of life. We surmise that some of these paths will eventually bring us closer to the understanding of the fundamental question: how did life come into being in the Universe? As oil droplets can be shaped in any aqueous environment subject to occasional or periodic slow cooling, we can anticipate shaped droplet protocells on many Earth-like exoplanets, including those that formed before the Earth. We extrapolated that the time interval from protocell to LUCA took so long that this process started before the Earth was formed (Sharov & Gordon, 2017). Thus the role of shaped droplets in the origin of life and its evolution may have begun prior to Earth's appearance.

ACKNOWLEDGMENTS

We would like to thank Stephen M. Levin for helpful comments on the overview of tensegrity, Diana Cholakova for providing the images of the shaped drops from the experiments, Jack Rudloe for discussions in the context of embryogenesis and his hosting of RG at Gulf Specimen Marine Laboratory & Aquarium while this was being written, and Alexei Sharov for his fine editorial job on our manuscript.

APPENDIX OVERVIEW OF TENSEGRITY STRUCTURES

Tensegrity structures were originally conceived as manmade systems of isolated components of two kinds: stiff parts (bars) that could bear compression with little distortion, and taut or prestressed parts (cables) attached to them that either hold the stiff elements from moving or additionally compress them to some extent (usually not to the point of buckling). Such simplest tensegrity structure is shown in Fig. 17. Tensegrity structures may be compounded into and actually originated in fine art (Snelson & Heartney, 2013) (Fig. 18). We can also find them in nature (Fig. 19).

In the mathematical theory of tensegrity, a third kind of element (or “member”) is sometimes allowed that acts in the opposite manner to the cable. This element, called a strut, is straight when compressed and floppy when stretched. In simple mathematical terms, then, the three kinds of elements have the following behaviors:

$$\text{Bar: } t = k(l - l_0)$$

$$\text{Cable: } t = k(l - l_0) \text{ for } l \geq l_0, t = 0 \text{ otherwise}$$

$$\text{Strut: } t = -k(l - l_0) \text{ for } l \leq l_0, t = 0 \text{ otherwise}$$

where t is the internal energy of an element and l its length. The “initial” length of an element is l_0 . Note that when $l = l_0$, $t = 0$, meaning that the element then has zero prestress. The spring constant k and the zero prestress lengths l_0 could be different for each kind of element, or even for each individual element. In one mathematical idealization, k approaches infinity (Fig. 20). Of course, these simple Hookean springs could be generalized to more complicated constitutive relationships (Rimoli, 2016).

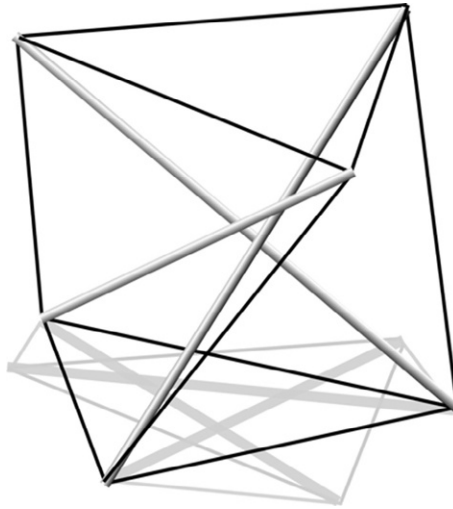
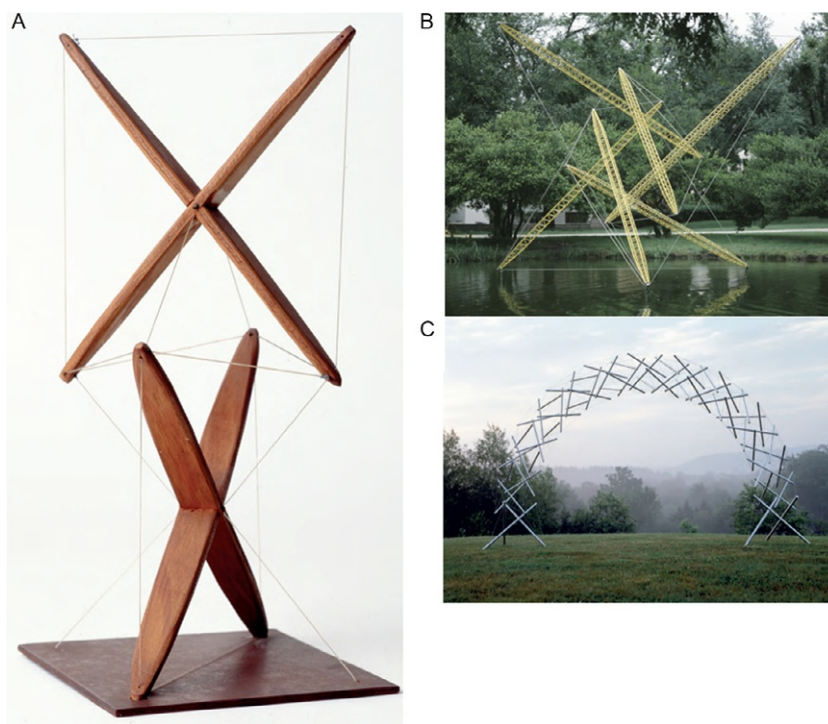


FIG. 17

This is the simplest nontouching rod tensegrity structure consisting of three stiff rods (bars) connected by 9 flexible strings (cables) that are stretched so that they are taut. It has been used as a stool (Passi, 2013).

From Dale, B.F., 2008. An SVG of a physically possible tensegrity structure in 3D, with a shadow. <https://en.wikipedia.org/wiki/File:3-tensegrity.svg>, with permission under a Creative Commons Attribution-Share Alike 3.0 Unported license.

**FIG. 18**

Examples of tensegrity structures as art. (A) Early X-Piece, 1948, wood and nylon, $29 \times 4.5 \times 4.5$ cm. Note that the three rigid parts are not simple rods, which became the archetype later. Also, two of the rigid parts are allowed to touch. The bottom platform could, alternatively, be regarded as a surface to which the elements are “pinned” (Connelly & Guest, 2015), rather than an element on its own. (B) Northwood I, 1969, painted steel and stainless steel, $3.65 \times 3.65 \times 3.65$ m. Collection: Northwood Institute, Dallas, TX. (C) Rainbow Arch, 2001, aluminum and stainless steel, $213.4 \times 386.1 \times 81.3$ cm. Cf. (Snelson, 1990; Snelson & Heartney, 2013).

(C) Reproduced with permission from the late artist Kenneth Snelson.

Snapping between configurations is possible (Gordon, 1999), as between the boat and chair shapes of cyclohexane (Wikipedia, 2016a) (Fig. 21). Sometimes small deviations in the length of elements can result in a large change in the shape of the whole configuration (Connelly & Gortler, 2015) (Fig. 22).

Tensegrity systems have been classified as follows:

A tensegrity [system] that has no contacts between its rigid bodies [bars] is a class 1 tensegrity system, and a tensegrity system with as many as k rigid bodies in contact is a class k tensegrity system (Skelton & de Oliveira, 2009).

In our illustrations, the following are Class 1 tensegrity systems: Figs. 1, 18B and C, 19, 23. Class 2: Fig. 18A. Class 5: Fig. 21. Class 30: Fig. 22. Some systems with $k > 1$ are called “mechanisms” (Connelly & Gortler, 2015).

**FIG. 19**

A three-dimensional spider web made by a tangle-web spider ([Wikipedia, 2016d](#)) in Panacea, Florida. The elastic strands of web in this 3D tensegrity structure are decorated with fog dew drops. The webbing is the elastic component (cables) and the plant is the stiff component (bars).

When we deal with cells or organisms, we are closer to continuum mechanics than these tensegrity models suggest. Contrary to the open spaces in between human and spider-made tensegrity structure elements, in cells we are confronted with what has been called “the crowded cytoplasm” ([Gnutt & Ebbinghaus, 2016](#)). Similarly, the nucleus is crowded ([Nakano et al., 2014](#)), with 2 m of double-stranded DNA ([Greulich, 2005](#)) compacted into a human cell nucleus of 8 μm diameter ([Greeley et al., 1978](#)). Crowding itself has effects on the mechanical properties of cytoskeletal tensegrity structures ([Zhou et al., 2009](#)).

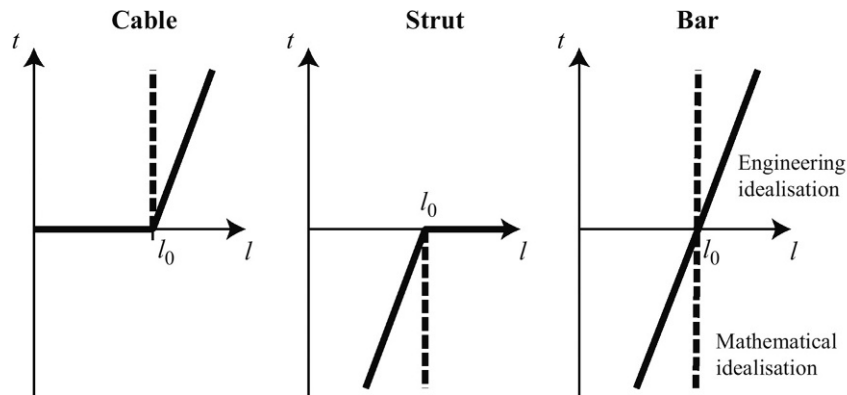


FIG. 20

Constitutive relationships for cables, struts, and bars. The slope of the tilted lines is the Hookean spring constant k . In the mathematical idealization shown by the dashed lines $k = \infty$.

From Connelly, R., Guest, S.D., 2015. *Frameworks, Tensegrities and Symmetry: Understanding Stable Structures*. <http://www.math.cornell.edu/~web7510/framework.pdf>, with kind permission of Robert Connelly and Simon Guest.

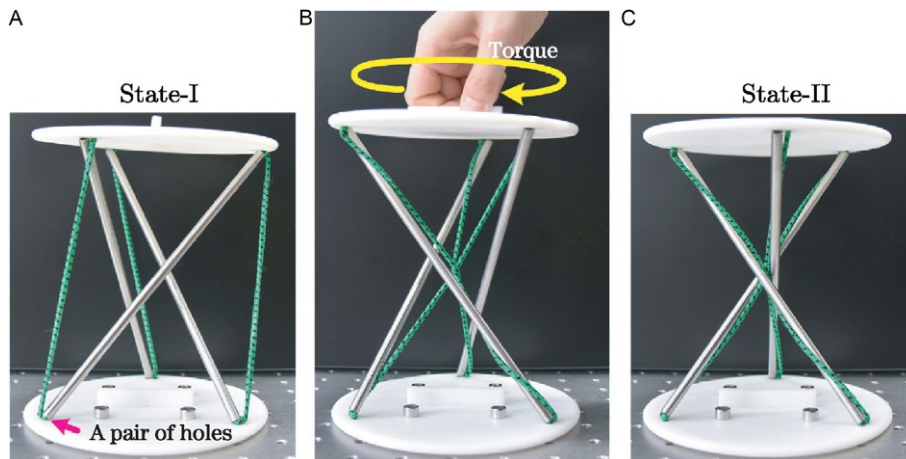
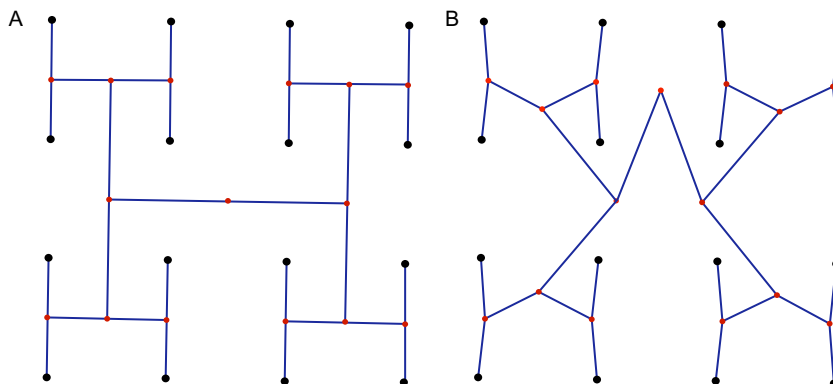


FIG. 21

This tensegrity structure suddenly snaps to a new configuration as a torque is applied on top. State-I is a “nonstandard” tensegrity structure, in that the top and bottom rigid components are not linear, as also in Fig. 20 Left. State-II is nonstandard in that the rigid linear elements are allowed to touch, and the elastic elements also touch the rigid linear elements along their lengths and are no longer single straight lines themselves. They may be regarded as kinked. Thus, these authors have generalized the tensegrity concept, allowing these “exceptions.” “(A) Self-equilibrated and stable state with no interference of elements. (B) Loaded state under applied torque with only side strings intersecting each other. (C) Self-equilibrated and stable state with all bars and side strings intersecting with one another.”

From Zhang, L.Y., Zhang, C., Feng, X.Q., Gao, H.J., 2016. *Snapping instability in prismatic tensegrities under torsion*. *Appl. Math. Mech.* (English Ed.) 37(3), 275–288, with permission of Shanghai University and Springer-Verlag Berlin Heidelberg.

**FIG. 22**

A mathematically rigid structure can sometimes become nonrigid with a small change in parameters. This structure consists only of bars of fixed length. (A) “The large black vertices are pinned to the plane, and the whole framework is universally rigid. . .” (B) “. . .the same framework. . . but with the lengths of the bars increased by $<0.5\%$.” This may be thought of as analogous to buckling: “In practical terms, buckling can be defined as a sudden and dramatic increase in deformations for a relatively small increase in the loads” (Gutiérrez et al., 2017).

From Connelly, R., Gortler, S.J., 2015. *Iterative universal rigidity*. *Discret. Comput. Geom.* 53(4), 847–877, with permission of Springer.

**FIG. 23**

A NASA tensegrity robot named SUPERball. “Each rigid rod is a self-contained robotic system consisting of two smaller intelligent nodes” (Bruce et al., 2014), which can change the lengths of one or more attached cables, which are under tension, causing the structure to roll or climb hills.

From Vytas SunSpiral with his kind permission.

We can look at the Wurfel, for instance, a toddler's toy that we have used as a toy model for changes in gene expression in a cell nucleus (Gordon & Gordon, 2016a; Gordon, 1999), as a space filling tensegrity structure. A Wurfel consists of a set of wooden cubes connected via an elastic band through them that forms a closed loop. The elastic band enters and exits each cube at right angles, pulling them together face to face (Fig. 24). Each pair of connected blocks can be regarded as a strut. There is a discrete set of equivalent energy ground states of a Wurfel (Tromp & Gordon, 2006). However, if we replace the cubes by spheres, we still have a structure of stiff elements held together under tension ("if one imagines hard spherical billiard balls, the centers of any two touching balls form a natural strut" (Connelly & Guest, 2015)), but with a continuum set of ground states (Fig. 25). Cube and sphere-based Wurfels with many ground states have analogies in folded proteins. While most proteins have single, nondegenerate ground states (Khatib et al., 2011), some have many or even a continuum of ground states. The latter are called disordered proteins (Uversky, 2013).

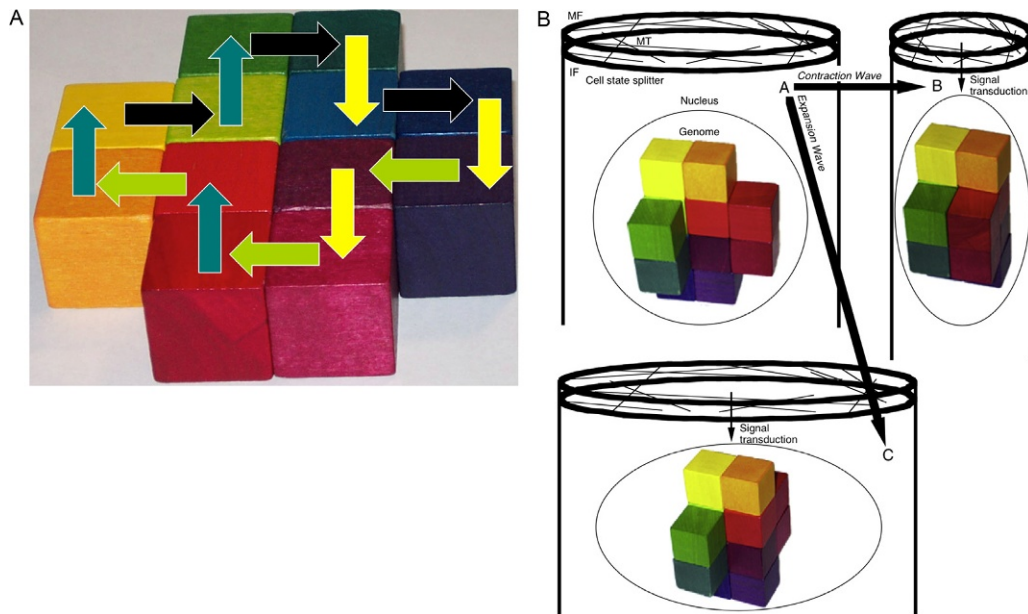


FIG. 24

(A) The Wurfel was invented by Peter Bell of Pappa Geppetto's Toys Victoria Ltd., Victoria, Canada (Flemons, 2016). Arrows show the path of the taut elastic band inside the blocks. The number of rectilinear configurations of a $2n$ -Wurfel ($n=6$ here) increases rapidly (Tromp & Gordon, 2006). Configurations not fitting on a cubic grid are also possible. (B) The same Wurfel in three 3D rectilinear configurations, being used as a toy model for changes in gene expression in a cell nucleus during cell differentiation. Note that the cell state splitter is also a tensegrity structure with the microtubules (MT) being the stiff elements, while the microfilament ring (MF) is in tension. The intermediate filament ring (IF) acts as elastic component. In an epithelium, the top (apical) end of each cell, and thus its cell state splitter, would be polygonal.

(B) From Gordon, N.K., Gordon, R., 2016. *Embryogenesis Explained*. World Scientific Publishing, Singapore, with permission of World Scientific Publishing.

**FIG. 25**

“Baby Beads” are topologically connected just like a Wurfel, but the spheres roll over one another easily. This is then a tensegrity structure with a continuum of equivalent energy (“degenerate”) ground states.

If we allow a set of hard spheres to have attractive forces (nonzero prestress) between all near neighbors, we effectively have a hard sphere model for condensed matter (Camp, 2003) or dispersions when the spheres do not always touch (Gonzalez et al., 2014). This too could be considered a tensegrity structure, albeit a changing one as it flows or its atoms or molecules undergo Brownian motion relative to one another. Thus, any drop of liquid, with its molecules regarded as the stiff elements, is a tensegrity structure. Indeed, tensegrity models for the rigidity of packings of balls have been studied (Connelly, 2008; Connelly et al., 2014), which represent a step towards molecular tensegrity modeling of liquids and solids.

In most liquids, we have to deal only with interactions between near neighbors, to get an accurate picture of the statistics of their structure, such as the radial distribution function (Cockayne, 2008; Gotoh, 2012). Nevertheless, there can be a long-range order imposed by the network of elements under tension, as in packings and crystallization. Alternatively, the structure of long elements, i.e., elements that are far from spherical, can also lead to long-range effects and long-range order. A remarkable example is the case of microtubules, which are so long and thin that one would expect them to buckle like wet spaghetti (Gordon & Gordon, 2016a). However, when supported along their length by attached intermediate filaments, it takes the order of 10^4 times more compressive force to buckle them (Brodland & Gordon, 1990).

While this calculation has been used to justify microtubules as the stiff elements in a tensegrity model for cytoplasm (Ingber et al., 1994), there is some circular reasoning in doing so, since what anchors those particular intermediate filaments at their other ends (cf. pinning in Fig. 18) has not been worked out. Also, the multiple attachments (nodes) along the microtubule make for a structure that differs from standard tensegrity modeling, in which the elements are allowed to rotate freely to any angle about the “joints” or nodes. This is because each long, polymeric structure in the cytoplasm has a stiffness, characterized by a persistence length (Fig. 5.30 in (Gordon & Gordon, 2016a)), so that the amount of bending at each node would be constrained, and any bending would add to the energy (prestress) of the whole structure.

A further step in generalizing tensegrity structures was taken with the invention of tensegrity robots, in which element lengths are manipulated to make a tensegrity structure change shape (Piazza, 2015)

and, for example, move over a rough planetary landscape by shifting the center of gravity of the robot or pushing against terrain (Bruce et al., 2014; SunSpiral, 2015) (Fig. 23). If one combines such force generation by the elements with the change of neighbors in dispersions, we approach a tensegrity model for cytoskeleton dynamically changing via motor molecules, polymerization, and depolymerization, and changing connections (nodes) via bifunctional attachment proteins (Perera et al., 2016). Getting beyond the stick and string tensegrity model for cytoskeleton has just begun (Ingber et al., 2014), for example, by looking at the bistable configurations of the cell state splitter (Gordon & Gordon, 2016a).

However, a tensegrity structure that can make and break connections and grow and dissolve elements is prone to instability and collapse. Indeed, such collapses may be important steps in cell differentiation (Gordon & Gordon, 2016a). A computer simulation framework for investigating such cytoskeletal instability phenomena is under construction based on PushMePullMe (Senatore, 2017).

In zero gravity, the taut strings of a simple tensegrity structure (Fig. 17), for example, would hold the structure together, but need not be under any prestress. If prestressed, the configuration would look much the same, except that the stiff rods would be slightly compressed and the strings slightly stretched or slightly buckled. In the biological literature, the prestress is assumed to be nonzero and essential to the maintenance of the structure (Ingber et al., 2014; Shen & Wolynes, 2005). In the mathematical literature on tensegrity structures, the concept of prestress includes allowing its value to be zero (Connelly & Guest, 2015). Thus, there is a conceptual contradiction here. Of course, mathematically, any small deviation from the equilibrium structure may generate a small prestress, usually driving the structure back towards its equilibrium shape, unless that equilibrium state is metastable, degenerate (Fig. 25), or sensitive to small perturbations (Fig. 22). Nevertheless, the presumption that nonzero prestress is essential to structure maintenance in biology is mathematically incorrect. While nonzero prestress may be present in most biological tensegrity structures, that does not imply the structure would collapse at zero prestress. Thus, the assumption “that the forces required for such a strained assembly in the cell are generated by nonequilibrium polymerizations and movements of motor proteins. . .” may be wrong, when cytoskeletal structure does not require such forces for its stability. For example, while microtubules may undergo frequent elongation and shortening, a process called dynamic instability (Gordon & Gordon, 2016a), they can also be stabilized against such behavior (van der Vaart et al., 2009) and thus act more like simple tensegrity bars. Prestress may be important in building cytoskeletal structures, but sometimes it may not be necessary for maintenance of those structures. These distinctions are important here, because in modeling a tensegrity origin of life, we cannot assume that continuous nonequilibrium, energy requiring processes of nascent cytoskeletal molecules, generating and maintaining prestress, played any role in the abiotic precursors to life.

Most tensegrity modeling ignores the buckling of elements under stress. Buckling can be quite important in cytoskeleton, varying from smooth Eulerian buckling (Brodland & Gordon, 1990) to kinking. Kinking in effect splits an element into two elements with a new node at the kink. However, kinks come in two kinds: stationary and propagating. If a cytoskeletal microtubule or microfilament is bent into a ring (Gordon & Brodland, 1987), so long as the radius of curvature is comparable to its persistence length, we can anticipate that the ring will be circular. Epithelia commonly have microfilament rings, but the cells are generally close-packed in a plane and polygonal in shape. Whether or not individual microfilaments in the bundle forming the polygonal ring end at the corners or are kinked there has apparently not yet been investigated. As the cell state splitter also has an intermediate filament ring

(Gordon & Gordon, 2016a; Martin & Gordon, 1997), the same question arises for its components. An epithelial cell is an example of confinement of a cytoskeletal structure (Gürsoy et al., 2014; Koudehi et al., 2016; Pinot et al., 2009; Soares e Silva et al., 2011; Vetter et al., 2014). Bundles of microfilaments confined to liposomes exhibit kinks and polygonal shapes (Tsai & Koenderink, 2015). Computer simulations have not yet revealed polygonal shapes, perhaps because spherical boundary conditions were imposed (Koudehi et al., 2016).

Details have been worked out for kinking of carbon nanotubes (Iijima et al., 1996; Wang et al., 2016a; Zeng et al., 2004). Analogies have been made between kinking of nanotubes and cytoskeleton (Cohen & Mahadevan, 2003).

Propagating kinks in cytoskeletal rings were discovered by Robert Jarosch (1956, 1957) in cytoplasm squeezed from *Chara foetida* and Kiyoko Kuroda in cytoplasm dripped out of cut *Nitella* cells (Kuroda, 1964) (Fig. 16). Kuroda observed:

... triangles, quadrangles, pentagons, hexagons and other polygons. . . . [Each] consists of a pair of straight lines running in parallel close to each other, their both ends being joined together by tiny circular arcs with a radius of approximately 1 μ . Of various polygons observed, pentagons and hexagons are found most frequently. The distribution of angles, measured in about 300 specimens, shows the sharp peak between 110° and 120° Corners of the polygon propagate as waves along the fibril all in the same direction with the same speed. Since the angle of each corner is also kept constant, the polygon maintains its definite shape while corners propagate successively in one direction. On pulling with two microneedles, the polygon is split into finer fibrils

(Kuroda, 1968).

These dynamic rings were later shown to consist of microfilaments (Higashi-Fujime, 1980), which are presumably the “finer fibrils.” Whether the kink propagates with sliding or kinking of the individual microfilaments has not been investigated. Kink bends can propagate along microtubules (Tuszynski et al., 2005, 2009). It is worth noting that for shaped droplets: “A very large majority of the interior angles of the polygons are seen in experiments to have measures close to 60° or 120° . . .” (Haas et al., 2016). Electron microscopy of triangular Archaea shows unexpected 90° corners, made up by a slight rounding of the edges (Nishiyama et al., 1992, 1995; Takao, 2006) (Fig. 1D). All of these cases suggest specific molecular configurations at corners that warrant investigation and modeling.

This does not exhaust the phenomena we should anticipate in the tensegrity behavior of cytoskeleton and its precursors in protocells. A long molecule such as DNA, when supercoiled, exhibits non-linear phenomena similar to that of a twisted rubber band (Marko & Neukirch, 2012). Supercoiling of microtubules, which are chiral, may alter the binding of motor molecules such as dynein (Gordon & Gordon, 2016a; Gordon, 1999) and perhaps attached bifunctional molecules.

A TOY MODEL FOR THE POLYGONAL SHAPE OF SHAPED DROPLETS

Here we give a physical toy model, based on what happens to a stack of “magnetic buttons” (Horizon Group, 2017b) arranged into a loop (Fig. 26). We can take such magnetic interactions as illustrative stand-ins for the van der Waals forces attracting the linear alkane molecules in the plastic crystal phases making the edges of the polygonal droplets, though their scaling is very different. Suppose there are N buttons arranged in a loop. Because each one is stiff and flat, in order to make a loop, there will be a




Polygon	Energy- Nc	Photo	N
Two lines	$2w(180^\circ)$		$2 \times 26 = 52$
Equilateral triangle	$3w(120^\circ)$		$3 \times 17 = 51$
Square	$4w(90^\circ)$		$4 \times 13 = 52$

FIG. 26

Magnetic buttons of $\frac{3}{4}$ " (1.9 cm) diameter were arranged by hand into polygons. The angle $\theta = \theta_1 - \theta_2$ between magnets at the corners of the triangle, for instance, is 120° . Hexagons were difficult to make, as the groups of 8 magnets kept snapping together. While the two line configuration is unrealistic for a whole shaped droplet, as it encloses zero volume, it may present a model for the filaments that sometimes protrude from the corners of shaped droplets. To create the 12-sided dodecagon, we used thinner, weaker magnets of the same diameter that each has a white adhesive and plastic disc attached. This was about the limit for these weak magnets on this table surface, which provided static friction in all cases.

nonzero angle between certain consecutive buttons. It is clear that the sum of those angles around the loop, so long as a loop topology is retained and the loop resides in a plane, must be 360° . Let the energy of interaction between consecutive buttons be a monotonically decreasing function of the angle between them. Then the total energy of the system is:




Regular pentagon	$5w(72^\circ)$		$5 \times 10 = 50$
Regular hexagon	$6w(60^\circ)$		$6 \times 8 = 48$
Regular dodecagon	$12w(30^\circ)$		

FIG. 26—Cont'd

$$E = \sum_{i=0}^{N-1} w \left(\theta_{\text{mod}(i+1,N)} - \theta_{\text{mod}(i,N)} \right)$$

with the constraint that:

$$\sum_{i=0}^{N-1} \left(\theta_{\text{mod}(i+1,N)} - \theta_{\text{mod}(i,N)} \right) = 360^\circ$$

where “mod” is the modulus function. We are assuming that only nearest neighbor interactions count. For a pair of actual magnets near each other, the angular dependence of their interactions requires integration over each pair of interacting elements and thus on their detailed geometry. If two magnets of magnetic moments m_1, m_2 are far apart, at distance r between their centers, with a relative angle $\theta = \theta_1 - \theta_2$ between them, the approximate mutual potential energy E_p of their point-dipole–point-dipole interaction is (Cullity & Graham, 2011):

$$E_p = \frac{m_1 m_2}{r^3} [\cos(\theta_1 - \theta_2) - 3 \cos \theta_1 \cos \theta_2]$$

This falls to zero when:

$$\theta_1 - \theta_2 = 90^\circ$$

but we find for the magnetic buttons that there is a residual attractive force when they are touching at an edge, at a right angle. We will therefore take as a representative energy of interaction:

$$w(\theta_{\text{mod}(i+1,N)} - \theta_{\text{mod}(i,N)}) = \cos(\theta_{\text{mod}(i+1,N)} - \theta_{\text{mod}(i,N)}) - 3 \cos \theta_{\text{mod}(i+1,N)} \cos \theta_{\text{mod}(i,N)} + c$$

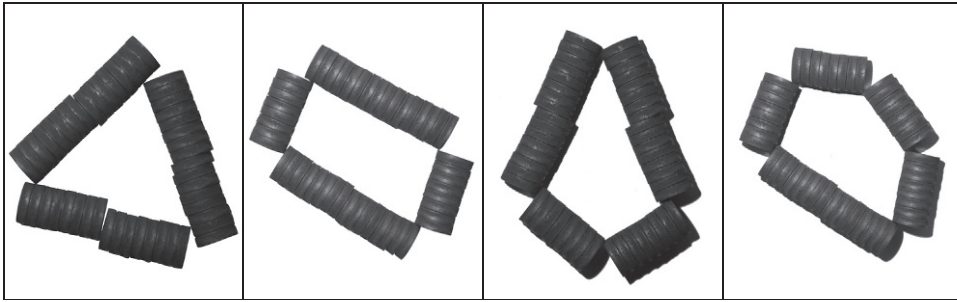
As a rough approximation we take c as a constant, though in principle it is a calculable function. We can now introduce absolute temperature T by the Boltzmann relationship:

$$P(E) = e^{-E/(kT)}$$

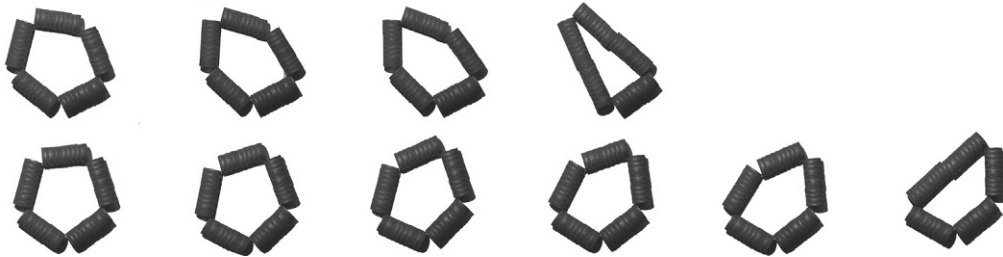
For any set of angles, this then gives the probability P of that configuration as a function of T .

Except for its geometry, this problem is not new. It is merely the one-dimensional lattice with nearest neighbor interactions, continuous state variable, and periodic boundary conditions. While the 1D Ising lattice does not exhibit a sharp phase transition (Brush, 1967; Wikipedia, 2016b) including in the continuous state case (Griffiths, 1969; van Beijeren & Sylvester, 1978) of our toy model, in our problem the global constraint on the sum of the angles makes a sharp phase transition possible, at low enough T . This in turn leads to the stability and metastability of polygonal configurations. Because of thermal fluctuations and/or under the influence of surface tension, transitions between the different polygon states can occur, even in the absence of an analog of plastic crystal edge growth in this toy model. These could be explored via Monte Carlo simulations (Gordon, 1980).

There are many other ways to alter a 1D Ising lattice to produce a phase transition. However, none of them involve the constraint of a finite length looped in 2D. Many of the modified Ising lattices invoke long-range interactions (Cassandro et al., 2014). In a way, a looped system has a long-range interaction: of each unit with itself around the loop. Multiple cycles around the ring may in effect give an infinite range to the interactions. The latter does lead to a phase transition for the 1D Ising lattice (van Beijeren & Sylvester, 1978). This may be the reason that rings exhibit sharp phase transitions. However, unlike any standard Ising systems, in our system the forces generated by neighbor-neighbor

**FIG. 27**

Once hexagons were made, tapping on the table rapidly produced various transitions to lower order polygons. Due to imperfect alignment, most of the original groups of 8 magnets can still be seen.

**FIG. 28**

Top row: a pentagon consisting of 5 groups of 10 magnetic buttons transitions to an isosceles triangle with consecutive hammerings of the surface on which they lie. The metastability was significantly stronger than that of the hexagons. Bottom row: a pentagon transitions to a quadrilateral.

interactions are allowed to alter the positions of the units in space, driving adjacent units towards being parallel to one another.

While setting up the magnetic buttons in various configurations (Fig. 26), it became clear that hexagons were metastable with small thresholds for transitions to lower order polygons. It was hard to achieve these configurations, and tapping on the table caused various transitions (Fig. 27). Pentagons were much more stable than hexagons, but could undergo transitions by hitting the surface nearby with a rubber hammer. Due to friction with the surface, intermediate states could be captured by camera (Fig. 28). Transitions between polygonal dimplings of spherical and cylindrical thin metal shells have been observed by high speed movies (Thompson & Sieber, 2016).

A set of weaker magnets was acquired (Horizon Group, 2017a). In addition to the configurations shown so far, we were able to get up to a 12-sided polygon (Fig. 26), not quite approximating a circular arrangement with many small consecutive angle differences. That would require either weaker magnets or a rougher surface.

The magnetic buttons toy model has a major limitation in that the energies change monotonically with the number of vertices, whereas this function has minima for shaped droplets, for which 60° and

120° appeared “to be the only possible internal angles,” at least when they are not “shape-shifting” (Haas et al., 2017). The toy model does not capture features such as the flexibility of the linear molecules, their multiple layers, and the fact that many molecules (not just two, as with magnets) would be arrayed in specific configurations at each corner, nor three-dimensional effects such as the lenticular shape of the droplets, nor their constant volume.

REFERENCES

- Akca, E., Claus, H., Schultz, N., Karbach, G., Schlott, B., Debaerdemaeker, T., Declercq, J.-P., König, H., 2002. Genes and derived amino acid sequences of S-layer proteins from mesophilic, thermophilic, and extremely thermophilic methanococci. *Extremophiles* 6 (5), 351–358.
- Aktümen, M., Kaçar, A., 2007. Maplets for the area of the unit circle. *J. Online Math. Appl.* 7(May), #1549, http://www.maa.org/external_archive/joma/Volume1547/Aktumen/index.html.
- Alam, M., Claviez, M., Oesterhelt, D., Kessel, M., 1984. Flagella and motility behaviour of square bacteria. *EMBO J.* 3 (12), 2899–2903.
- Albers, S.-V., Meyer, B.H., 2011. The archaeal cell envelope. *Nat. Rev. Microbiol.* 9 (6), 414–426.
- Aliabadi, R., Moradi, M., Varga, S., 2015. Orientational ordering of confined hard rods: the effect of shape anisotropy on surface ordering and capillary nematization. *Phys. Rev. E* 92 (3). #032503.
- Allen, W.V., Ponnampuruma, C., 1967. A possible prebiotic synthesis of monocarboxylic acids. *Curr. Mod. Biol.* 1 (1), 24–28.
- Andrade, K., Logemann, J., Heidelberg, K.B., Emerson, J.B., Comolli, L.R., Hug, L.A., Probst, A.J., Keillor, A., Thomas, B.C., Miller, C.S., Allen, E.E., Moreau, J.W., Brocks, J.J., Banfield, J.F., 2015. Metagenomic and lipid analyses reveal a diel cycle in a hypersaline microbial ecosystem. *ISME J.* 9 (12), 2697–2711.
- Anella, F., Danelon, C., 2014. Reconciling ligase ribozyme activity with fatty acid vesicle stability. *Life (Basel)* 4 (4, Sp. Iss. SI), 929–943.
- Annenkov, V.V., Gordon, R., 2017. Silsim—a program for simulating aggregation of siliceous nanoparticles involved in diatom morphogenesis. In preparation.
- Antón, J., Llobet-Brossa, E., Rodriguez-Valera, F., Amann, R., 1999. Fluorescence *in situ* hybridization analysis of the prokaryotic community inhabiting crystallizer ponds. *Environ. Microbiol.* 1 (6), 517–523.
- Awramik, S.M., Barghoorn, E.S., 1977. The Gunflint microbiota. *Precambrian Res.* 5 (2), 121–142.
- Azadi, A., Grason, G.M., 2016. Neutral versus charged defect patterns in curved crystals. *Phys. Rev. E* 94 (1). #013003.
- Banno, T., Kuroha, R., Miura, S., Toyota, T., 2015. Multiple-division of self-propelled oil droplets through acetal formation. *Soft Matter* 11 (8), 1459–1463.
- Bardavid, R.E., Oren, A., 2008a. Dihydroxyacetone metabolism in *Salinibacter ruber* and in *Haloquadratum walsbyi*. *Extremophiles* 12 (1), 125–131.
- Bardavid, R.E., Oren, A., 2008b. Sensitivity of *Haloquadratum* and *Salinibacter* to antibiotics and other inhibitors: implications for the assessment of the contribution of Archaea and Bacteria to heterotrophic activities in hypersaline environments. *FEMS Microbiol. Ecol.* 63 (3), 309–315.
- Bardavid, R.E., Khristo, P., Oren, A., 2008. Interrelationships between *Dunaliella* and halophilic prokaryotes in saltern crystallizer ponds. *Extremophiles* 12 (1), 5–14.
- Bar-Even, A., Shenhav, B., Kafri, R., Lancet, D., 2004. The lipid world: from catalytic and informational head-groups to micelle replication and evolution without nucleic acids. In: Seckbach, J., ChelaFlores, J., Owen, T., Raulin, F. (Eds.), *Life in the Universe: From the Miller Experiment to the Search for Life on Other Worlds*. Dordrecht, Netherlands, pp. 111–114.

- Bartucci, R., Gambacorta, A., Gliozzi, A., Marsh, D., Sportelli, L., 2005. Bipolar tetraether lipids: chain flexibility and membrane polarity gradients from spin-label electron spin resonance. *Biochemistry* 44 (45), 15017–15023.
- Baxter, B.K., Litchfield, C.D., Sowers, K., Griffith, J.D., Dassarma, P.A., Dassarma, S., 2005. Microbial diversity of Great Salt Lake. In: Gunde-Cimerman, N., Oren, A., Plemenitaš, A. (Eds.), *Adaptation to Life at High Salt Concentrations in Archaea, Bacteria, and Eukarya*. Springer, Dordrecht, The Netherlands, pp. 19–25.
- Bernstein, M.P., Sandford, S.A., Allamandola, L.J., Chang, S., Scharberg, M.A., 1995. Organic compounds produced by photolysis of realistic interstellar and cometary ice analogs containing methanol. *Astrophys. J.* 454 (1), 327–344.
- Berthaud, A., Quemeneur, F., Deforet, M., Bassereau, P., Brochard-Wyart, F., Mangenot, S., 2016. Spreading of porous vesicles subjected to osmotic shocks: the role of aquaporins. *Soft Matter* 12 (5), 1601–1609.
- Bettarel, Y., Bouvier, T., Bouvier, C., Carré, C., Desnues, A., Domaizon, I., Jacquet, S., Robin, A., Sime-Ngando, T., 2011. Ecological traits of planktonic viruses and prokaryotes along a full-salinity gradient. *FEMS Microbiol. Ecol.* 76 (2), 360–372.
- Bivas, I., 2010. Shape fluctuations of nearly spherical lipid vesicles and emulsion droplets. *Phys. Rev. E* 81 (6), #061911.
- Bodaker, I., Sharon, I., Suzuki, M.T., Feingersch, R., Shmoish, M., Andreishcheva, E., Sogin, M.L., Rosenberg, M., Maguire, M.E., Belkin, S., Oren, A., Béjà, O., 2010. Comparative community genomics in the Dead Sea: an increasingly extreme environment. *Isme J.* 4 (3), 399–407.
- Boekema, E.J., Scheffers, D.-J., van Bezouwen, L.S., Bolhuis, H., Folea, I.M., 2013. Focus on membrane differentiation and membrane domains in the prokaryotic cell. *J. Mol. Microbiol. Biotechnol.* 23 (4–5), 345–356.
- Bolhuis, H., 2005. Walsby's square archaeon—it's hip to be square, but even more hip to be culturable. In: Gunde-Cimerman, N., Oren, A., Plemenitaš, A. (Eds.), *Adaptation to life at high salt concentrations in Archaea, Bacteria, and Eukarya*. Springer, Dordrecht, The Netherlands, pp. 185–199.
- Bolhuis, H., te Poele, E.M., Rodriguez-Valera, F., 2004. Isolation and cultivation of Walsby's square archaeon. *Environ. Microbiol.* 6 (12), 1287–1291.
- Bolhuis, H., Palm, P., Wende, A., Falb, M., Rampp, M., Rodriguez-Valera, F., Pfeiffer, F., Oesterhelt, D., 2006. The genome of the square archaeon *Haloquadratum walsbyi*: life at the limits of water activity. *BMC Genomics* 7, #169.
- Boulbitch, A., 2000. Deformation of the envelope of a spherical Gram-negative bacterium during the atomic force measurements. *J. Electron Microsc.* (Tokyo) 49 (3), 459–462.
- Braun, T., Orlova, A., Valegård, K., Lindås, A.C., Schröder, G.F., Egelman, E.H., 2015. Archaeal actin from a hyperthermophile forms a single-stranded filament. *Proc. Natl. Acad. Sci. U. S. A.* 112 (30), 9340–9345.
- Brodland, G.W., Gordon, R., 1990. Intermediate filaments may prevent buckling of compressively-loaded microtubules. *J. Biomech. Eng.* 112 (3), 319–321.
- Bruce, J., Sabelhaus, A., Chen, Y., Lu, D., Morse, K., Milam, S., Caluwaerts, K., Agogino, A., SunSpiral, V., 2014. SUPERball: exploring tensegrities for planetary probes. In: Dupuis, E. (Ed.), *12th International Symposium on Artificial Intelligence, Robotics and Automation in Space (i-SAIRAS)*. i-SAIRAS. http://robotics.estec.esa.int/i-SAIRAS/isairas2014/Data/Session%2205c/ISAIRAS_FinalPaper_0107.pdf.
- Brush, S.G., 1967. History of the Lenz-Ising model. *Rev. Mod. Phys.* 39 (4), 883–893.
- Bukhryakov, K.V., Almahdali, S., Rodionov, V.O., 2015. Amplification of chirality through self-replication of micellar aggregates in water. *Langmuir* 31 (10), 2931–2935.
- Burns, D., Dyall-Smith, M., 2006. Cultivation of haloarchaea. *Methods Microbiol.* 35, 535–552.
- Burns, D.G., Camakaris, H.M., Janssen, P.H., Dyall-Smith, M.L., 2004. Cultivation of Walsby's square haloarchaeon. *FEMS Microbiol. Lett.* 238 (2), 469–473.
- Burns, D.G., Janssen, P.H., Itoh, T., Kamekura, M., Li, Z., Jensen, G., Rodriguez-Valera, F., Bolhuis, H., Dyall-Smith, M.L., 2007. *Haloquadratum walsbyi* gen. nov., sp. nov., the square haloarchaeon of Walsby, isolated from saltern crystallizers in Australia and Spain. *Int. J. Syst. Evol. Microbiol.* 57, 387–392.

- Caluwaerts, K., Despraz, J., Iscen, A., Sabelhaus, A.P., Bruce, J., Schrauwen, B., SunSpiral, V., 2014. Design and control of compliant tensegrity robots through simulation and hardware validation. *J. R. Soc. Interface* 11 (98), #20140520.
- Camp, P.J., 2003. Phase diagrams of hard spheres with algebraic attractive interactions. *Phys. Rev. E* 67 (1).
- Caschera, F., Rasmussen, S., Hanczyc, M.M., 2013. An oil droplet division-fusion cycle. *ChemPlusChem* 78 (1), 52–54.
- Cassandro, M., Merola, I., Picco, P., Rozikov, U., 2014. One-dimensional Ising models with long range interactions: cluster expansion, phase-separating point. *Commun. Math. Phys.* 327 (3), 951–991.
- Castillo, A.M., Gutierrez, M.C., Kamekura, M., Ma, Y., Cowan, D.A., Jones, B.E., Grant, W.D., Ventosa, A., 2006. *Halovivax asiaticus* gen. nov., sp nov., a novel extremely halophilic archaeon isolated from Inner Mongolia, China. *Int. J. Syst. Evol. Microbiol.* 56, 765–770.
- Castillo, A.M., Gutierrez, M.C., Kamekura, M., Xue, Y., Ma, Y., Cowan, D.A., Jones, B.E., Grant, W.D., Ventosa, A., 2007. *Halovivax ruber* sp nov., an extremely halophilic archaeon isolated from Lake Xilinhot, Inner Mongolia, China. *Int. J. Syst. Evol. Microbiol.* 57, 1024–1027.
- Cavalier-Smith, T., 2001. Obcells as proto-organisms: membrane heredity, lithophosphorylation, and the origins of the genetic code, the first cells, and photosynthesis. *J. Mol. Evol.* 53 (4–5), 555–595.
- Chaban, B., Ng, S.Y.M., Jarrell, K.F., 2006. Archaeal habitats—from the extreme to the ordinary. *Can. J. Microbiol.* 52 (2), 73–116.
- Chernykh, N.A., Vasilyeva, L.V., Semenov, A.M., Lysenko, A.M., 1988. DNA homology in prostecobacteria of *Stella* genus. *Izvestiya Akademii Nauk SSSR Seriya Biologicheskaya* (5), 776–779 (Russian).
- Cholakova, D., Denkov, N., Tcholakova, S., Lesov, I., Smoukov, S.K., 2016. Control of drop shape transformations in cooled emulsions. *Adv. Colloid Interface Sci.* 235, 90–107.
- Cholakova, D., Valkova, Z., Tcholakova, S., Denkov, N.D., Smoukov, S.K., 2017. “Self-shaping” of multi-component drops. *Langmuir*. 33 (23), 5696–5706.
- Chong, P.L.G., 2010. Archaeobacterial bipolar tetraether lipids: physico-chemical and membrane properties. *Chem. Phys. Lipids* 163 (3), 253–265.
- Chong, D.T., Liu, X.S., Ma, H.J., Huang, G.Y., Han, Y.L., Cui, X.Y., Yan, J.J., Xu, F., 2015. Advances in fabricating double-emulsion droplets and their biomedical applications. *Microfluid. Nanofluid.* 19 (5), 1071–1090.
- Cockayne, D., 2008. The radial distribution function of amorphous materials. In: Ratinaç, K.R. (Ed.), *50 Great Moments: Celebrating the Golden Jubilee of the University of Sydney’s Electron Microscope Unit*. Sydney University Press, Sydney, Australia, pp. 197–200.
- Cohen, A.E., Mahadevan, L., 2003. Kinks, rings, and rackets in filamentous structures. *Proc. Natl. Acad. Sci. U. S. A.* 100 (21), 12141–12146.
- Connelly, R., 2008. Rigidity of packings. *Eur. J. Comb.* 29 (8), 1862–1871.
- Connelly, R., Gortler, S.J., 2015. Iterative universal rigidity. *Discret. Comput. Geom.* 53 (4), 847–877.
- Connelly, R., Guest, S.D., 2015. Frameworks, Tensegrities and Symmetry: Understanding Stable Structures. <http://www.math.cornell.edu/~web7510/framework.pdf>.
- Connelly, R., Shen, J.D., Smith, A.D., 2014. Ball packings with periodic constraints. *Discret. Comput. Geom.* 52 (4), 754–779.
- Crawford, R.M., 1981. Valve formation in diatoms and the fate of the silicalemma and plasmalemma. *Protoplasma* 106 (1–2), 157–166.
- Cullity, B.D., Graham, C.D., 2011. *Introduction to Magnetic Materials*, second ed. Wiley, Hoboken, New Jersey, USA.
- Damer, B., Deamer, D., 2015. Coupled phases and combinatorial selection in fluctuating hydrothermal pools: a scenario to guide experimental approaches to the origin of cellular life. *Life* 5 (1), 872–887.
- De Rosa, M., Gambacorta, A., Gliozzi, A., 1986. Structure, biosynthesis, and physicochemical properties of archaeobacterial lipids. *Microbiol. Rev.* 50 (1), 70–80.
- Denkova, N., Tcholakova, S., Lesov, I., Cholakova, D., Smoukov, S.K., 2015. Self-shaping of oil droplets via the formation of intermediate rotator phases upon cooling. *Nature* 528 (7582), 392–395.

- Denkov, N., Cholakova, D., Tcholakova, S., Smoukov, S.K., 2016. On the mechanism of drop self-shaping in cooled emulsions. *Langmuir* 32 (31), 7985–7991.
- Diaz Moreno, M., Ma, K., Schoenung, J., Dávila, L.P., 2015. An integrated approach for probing the structure and mechanical properties of diatoms: toward engineered nanotemplates. *Acta Biomater.* 25, 313–324.
- Döbereiner, H.G., Evans, E., Kraus, M., Seifert, U., Wortis, M., 1997. Mapping vesicle shapes into the phase diagram: a comparison of experiment and theory. *Phys. Rev. E* 55 (4), 4458–4474.
- Driessen, A.J.M., Albers, S.V., 2007. Membrane adaptations of (hyper)thermophiles to high temperatures. In: Gerday, C., Glansdorff, N. (Eds.), *Physiology and Biochemistry of Extremophiles*. American Society for Microbiology, Washington, DC, pp. 104–116.
- Dubois, M., Demé, B., Gulik-Krzywicki, T., Dedieu, J.C., Vautrin, C., Désert, S., Perez, E., Zemb, T., 2001. Self-assembly of regular hollow icosahedra in salt-free catanionic solutions. *Nature* 411 (6838), 672–675.
- Duggin, I.G., Aylett, C.H.S., Walsh, J.C., Michie, K.A., Wang, Q., Turnbull, L., Dawson, E.M., Harry, E.J., Whitchurch, C.B., Amos, L.A., Lowe, J., 2015. CetZ tubulin-like proteins control archaeal cell shape. *Nature* 519 (7543), 362–365.
- Dworkin, J.P., Deamer, D.W., Sandford, S.A., Allamandola, L.J., 2001. Self-assembling amphiphilic molecules: synthesis in simulated interstellar/precometary ices. *Proc. Natl. Acad. Sci. U. S. A.* 98 (3), 815–819.
- Dyall-Smith, M.L., Pfeiffer, F., Klee, K., Palm, P., Gross, K., Schuster, S.C., Rampp, M., Oesterheld, D., 2011. *Haloquadratum walsbyi*: limited diversity in a global pond. *PLoS One* 6 (6), e20968, #e20968.
- Elferink, M.G.L., de Wit, J.G., Driessen, A.J.M., Konings, W.N., 1994. Stability and proton permeability of liposomes composed of archaeal tetraether lipids. *BBA-Biomembranes* 1193 (2), 247–254.
- Emerson, D., Chauhan, S., Oriel, P., Breznak, J.A., 1994. *Haloferax* SP D1227, a halophilic archaeon capable of growth on aromatic-compounds. *Arch. Microbiol.* 161 (6), 445–452.
- Engelhardt, H., 2007a. Are S-layers exoskeletons? the basic function of protein surface layers revisited. *J. Struct. Biol.* 160 (2), 115–124.
- Engelhardt, H., 2007b. Mechanism of osmoprotection by archaeal S-layers: a theoretical study. *J. Struct. Biol.* 160 (2), 190–199.
- Engelhardt, H., Peters, J., 1998. Structural research on surface layers: a focus on stability, surface layer homology domains, and surface layer–cell wall interactions. *J. Struct. Biol.* 124 (2), 276–302.
- Engelhardt, H., Gerblrieger, S., Santarius, U., Baumeister, W., 1991. The three-dimensional structure of the regular surface protein of *Comamonas acidovorans* derived from native outer membranes and reconstituted two-dimensional crystals. *Mol. Microbiol.* 5 (7), 1695–1702.
- Ettema, T.J.G., Lindås, A.-C., Bernander, R., 2011. An actin-based cytoskeleton in archaea. *Mol. Microbiol.* 80 (4), 1052–1061.
- Fan, Q., Relini, A., Cassinadri, D., Gambacorta, A., Gliozzi, A., 1995. Stability against temperature and external agents of vesicles composed of archaeal bolaform lipids and egg PC. *BBA-Biomembranes* 1240 (1), 83–88.
- Fiore, M., Strazewski, P., 2016. Prebiotic lipidic amphiphiles and condensing agents on the early Earth. *Life (Basel, Switzerland)* 6 (2), #17.
- Flemons, T., 2016. Undefined tenses, personal communication.
- Forbes, C.C., DiVittorio, K.M., Smith, B.D., 2006. Bolaamphiphiles promote phospholipid translocation across vesicle membranes. *J. Am. Chem. Soc.* 128 (28), 9211–9218.
- Fredrickson, H.L., Rijpsma, W.I.C., Tas, A.C., van der Greef, J., LaVos, G.F., de Leeuw, J.W., 1989. Chemical characterization of benthic microbial assemblages. In: Cohen, Y., Rosenberg, E. (Eds.), *Microbial Mats: Physiological Ecology of Benthic Microbial Communities*. American Society for Microbiology, Washington, DC, pp. 455–468.
- Fritz, I., Strompl, C., Abraham, W.R., 2004. Phylogenetic relationships of the genera *Stella Labrys* and *Angulomicrobium* within the ‘*Alphaproteobacteria*’ and description of *Angulomicrobium amanitifforme* sp. *Int. J. Syst. Evol. Microbiol.* 54, 651–657.
- Fuhrmann, T., Landwehr, S., El Rharbi-Kucki, M., Sumper, M., 2004. Diatoms as living photonic crystals. *Appl. Phys. B Lasers Opt.* 78 (3–4), 257–260.

- Garnett, A., 2015. Basket Bowl. <http://www.alexgarnett.com/product/basket-bowl>.
- Gerakines, P.A., Moore, M.H., Hudson, R.L., 2001. Energetic processing of laboratory ice analogs: UV photolysis versus ion bombardment. *J. Geophys. Res. Planets* 106 (E12), 33381–33385.
- Gerhart, J.C., Kirschner, M.W., 1997. *Cells, Embryos and Evolution: Toward a Cellular and Developmental Understanding of Phenotypic Variation and Evolutionary Adaptability*. Blackwell Science, Malden, MA.
- Gerhart, J., Kirschner, M., 2007. The theory of facilitated variation. *Proc. Natl. Acad. Sci. U. S. A.* 104 (Suppl. 1), 8582–8589.
- Ghai, R., Pašić, L., Beatriz Fernández, A., Martin-Cuadrado, A.-B., Mizuno, C.M., McMahon, K.D., Papke, R.T., Stepanauskas, R., Rodriguez-Brito, B., Rohwer, F., Sánchez-Porro, C., Ventosa, A., Rodríguez-Valera, F., 2011. New abundant microbial groups in aquatic hypersaline environments. *Sci. Rep.* 1. #135.
- Gliozzi, A., Rolandi, R., De Rosa, M., Gambacorta, A., 1983. Monolayer black membranes from bipolar lipids of archaeobacteria and their temperature-induced structural changes. *J. Membr. Biol.* 75 (1), 45–56.
- Gnutt, D., Ebbinghaus, S., 2016. The macromolecular crowding effect—from *in vitro* into the cell. *Biol. Chem.* 397 (1), 37–44.
- Gonzalez, S., Thornton, A.R., Luding, S., 2014. Free cooling phase-diagram of hard-spheres with short- and long-range interactions. *Eur. Phys. J.-Special Topics* 223 (11), 2205–2225.
- Gordon, R., 1980. Monte Carlo methods for cooperative Ising models. In: Karreman, G. (Ed.), *Cooperative Phenomena in Biology*. Pergamon Press, New York, pp. 189–241.
- Gordon, R., 1999. *The Hierarchical Genome and Differentiation Waves: Novel Unification of Development, Genetics and Evolution*. World Scientific & Imperial College Press, Singapore & London.
- Gordon, R., Brodland, G.W., 1987. The cytoskeletal mechanics of brain morphogenesis. *Cell state splitters cause primary neural induction*. *Cell Biophys.* 11 (1), 177–238.
- Gordon, R., Drum, R.W., 1994. The chemical basis of diatom morphogenesis. *Int. Rev. Cytol.* 150 (243–372), 421–422.
- Gordon, N.K., Gordon, R., 2016a. *Embryogenesis Explained*. World Scientific Publishing, Singapore.
- Gordon, N.K., Gordon, R., 2016b. The organelle of differentiation in embryos: the cell state splitter [invited review]. *Theor. Biol. Med. Model.* 13, 11 (Special issue: Biophysical Models of Cell Behavior, Guest Editor: Jack A. Tuszynski).
- Gordon, R., Tiffany, M.A., 2011. Possible buckling phenomena in diatom morphogenesis. In: Seckbach, J., Kociolek, J.P. (Eds.), *The Diatom World*. Springer, Dordrecht, The Netherlands, pp. 245–272.
- Gordon, R., Björklund, N.K., Nieuwkoop, P.D., 1994. Dialogue on embryonic induction and differentiation waves. *Int. Rev. Cytol.* 150, 373–420.
- Gordon, R., Losic, D., Tiffany, M.A., Nagy, S.S., Sterrenburg, F.A.S., 2009. The Glass Menagerie: diatoms for novel applications in nanotechnology. *Trends Biotechnol.* 27 (2), 116–127.
- Gotoh, K., 2012. *Particulate Morphology: Mathematics Applied to Particle Assemblies*. Elsevier Science, Amsterdam, Netherlands.
- Grant, W.D., Larsen, H., 1989. The genus *Haloarcula*. In: Staley, J.T., Bryant, M.P., Pfennig, N., Holt, J.G. (Eds.), *Bergey's Manual of Determinative Bacteriology*, ninth ed. Williams & Wilkins, Baltimore, pp. 2216–2233.
- Grason, G.M., 2016. Perspective: geometrically frustrated assemblies. *J. Chem. Phys.* 145 (11). #110901.
- Greeley, D., Crapo, J.D., Vollmer, R.T., 1978. Estimation of the mean caliper diameter of cell nuclei. 1. serial section reconstruction method and endothelial nuclei from human lung. *J. Microsc.-Oxford* 114, 31–39.
- Greulich, K.O., 2005. Single-molecule studies on DNA and RNA. *ChemPhysChem* 6 (12), 2458–2471.
- Griffiths, R.B., 1969. Rigorous results for Ising ferromagnets of arbitrary spin. *J. Math. Phys.* 10 (9), 1559–1565.
- Gross, R., Fouxon, I., Lancet, D., Markovitch, O., 2014. Quasispecies in population of compositional assemblies. *BMC Evol. Biol.* 14. #265.
- Guixa-Boixereu, N., Calderón-Paz, J.I., Heldal, M., Bratbak, G., Pedrós-Alió, C., 1996. Viral lysis and bacterivory as prokaryotic loss factors along a salinity gradient. *Aquat. Microb. Ecol.* 11 (3), 215–227.

- Gupta, R.S., Naushad, S., Baker, S., 2015. Phylogenomic analyses and molecular signatures for the class *Halobacteria* and its two major clades: a proposal for division of the class *Halobacteria* into an emended order Halobacteriales and two new orders, *Haloferacales* ord. nov and *Natrialbales* ord. nov., containing the novel families *Haloferacaceae* fam. nov and *Natrialbaceae* fam. nov. *Int. J. Syst. Evol. Microbiol.* 65, 1050–1069.
- Gürsoy, G., Xu, Y., Kenter, A.L., Liang, J., 2014. Spatial confinement is a major determinant of the folding landscape of human chromosomes. *Nucleic Acids Res.* 42 (13), 8223–8230.
- Gutiérrez, A., Gordon, R., Dávila, L.P., 2017. Deformation modes and structural response of diatom shells. *J. Mater. Sci. Eng. Adv. Technol.* 15 (2), 105–134.
- Guttman, S., Ocko, B.M., Deutsch, M., Sloutskin, E., 2016a. From faceted vesicles to liquid icoshedra: where topology and crystallography meet. *Curr. Opin. Colloid Interface Sci.* 22, 35–40.
- Guttman, S., Sapir, Z., Schultz, M., Butenko, A.V., Ocko, B.M., Deutsch, M., Sloutskin, E., 2016b. How faceted liquid droplets grow tails. *Proc. Natl. Acad. Sci.* 113 (3), 493–496.
- Haas, P.A., Goldstein, R.E., Smoukov, S.K., Cholakova, D., Denkov, N., 2016. A Theory of Shape-Shifting Droplets. <https://arxiv.org/abs/1609.00584>.
- Haas, P.A., Goldstein, R.E., Smoukov, S.K., Cholakova, D., Denkov, N., 2017. Theory of shape-shifting droplets. *Phys. Rev. Lett.* 118. #088001.
- Hamamoto, T., Takashina, T., Grant, W.D., Horikoshi, K., 1988. Asymmetric cell division of a triangular halophilic archaeobacterium. *FEMS Microbiol. Lett.* 56 (2), 221–224.
- Hanczyc, M.M., 2011. Metabolism and motility in prebiotic structures. *Philos. Trans. R. Soc. B* 366 (1580), 2885–2893.
- Hanczyc, M.M., 2014. Droplets: unconventional protocell model with life-like dynamics and room to grow. *Life-Basel* 4 (4, Sp. Iss. SI), 1038–1049.
- Hanczyc, M.M., Ikegami, T., 2010. Chemical basis for minimal cognition. *Artif. Life* 16 (3), 233–243.
- Hanczyc, M.M., Monnard, P.-A., 2017. Primordial membranes: more than simple container boundaries. *Curr. Opin. Chem. Biol.* 40 (October), 78–86.
- Hazelaar, S., van der Strate, H.J., Gieskes, W.W.C., Vrieling, E.G., 2005. Monitoring rapid valve formation in the pennate diatom *Navicula salinarum* (Bacillariophyceae). *J. Phycol.* 41 (2), 354–358.
- Hemmingsen, B.B., Hemmingsen, E.A., 1980. Rupture of the cell envelope by induced intracellular gas-phase expansion in gas vacuolate bacteria. *J. Bacteriol.* 143 (2), 841–846.
- Henning, T., Salama, F., 1998. Carbon in the Universe. *Science* 282 (5397), 2204–2210.
- Higashi-Fujime, S., 1980. Active movement in vitro of bundle of microfilaments isolated from *Nitella* cell. *J. Cell Biol.* 87 (3), 569–578.
- Hirsch, P., 1974. Budding bacteria. *Annu. Rev. Microbiol.* 28, 391–444.
- Hirsch, P., Schlesner, H., 1981. The genus *Stella*. In: Starr, M.P., Stolp, H., Trüper, H.G., Balows, A., Schlegel, H.G. (Eds.), *The Prokaryotes: A Handbook on Habitats, Isolation, and Identification of Bacteria*. Springer, Heidelberg, pp. 461–465.
- Hirsch, P., Müller, M., Schlesner, N., 1977. New aquatic budding and prosthecate bacterin and their taxonomic position. In: Skinner, F.A., Shewan, J.M. (Eds.), *Aquatic Microbiology*. Academic Press, London, pp. 107–133.
- Holm, N.G., Charlou, J.L., 2001. Initial indications of abiotic formation of hydrocarbons in the Rainbow ultramafic hydrothermal system, Mid-Atlantic Ridge. *Earth Planet. Sci. Lett.* 191 (1-2), 1–8.
- Horibe, N., Hanczyc, M.M., Ikegami, T., 2011. Mode switching and collective behavior in chemical oil droplets. *Entropy* 13 (3), 709–719.
- Horikoshi, K., Aono, R., Nakamura, S., 1993. The triangular halophilic archaeobacterium *Haloarcula japonica* strain TR-1. *Experientia* 49 (6-7), 497–502.
- Horizon Group, 2017a. Adhesive Magnetic Buttons. <http://craftprojectideas.com/products/magnetic-buttons-with-foam-adhesive/>.

- Horizon Group, 2017b. Magnetic Buttons. <http://craftprojectideas.com/products/magnetic-buttons/>.
- Huang, K.C., Mukhopadhyay, R., Wen, B., Gitai, Z., Wingreen, N.S., 2008. Cell shape and cell-wall organization in Gram-negative bacteria. *Proc. Natl. Acad. Sci. U. S. A.* 105 (49), 19282–19287.
- Hunding, A., Kepes, F., Lancet, D., Minsky, A., Norris, V., Raine, D., Sriram, K., Root-Bernstein, R., 2006. Compositional complementarity and prebiotic ecology in the origin of life. *Bioessays* 28 (4), 399–412.
- Iijima, S., Brabec, C., Maiti, A., Bernholc, J., 1996. Structural flexibility of carbon nanotubes. *J. Chem. Phys.* 104 (5), 2089–2092.
- Ingber, D.E., Dike, L., Liley, H., Hansen, L., Karp, S., Maniotis, A.J., McNamee, H., Mooney, D., Plopper, G., Sims, J., Wang, N., 1994. Cellular tensegrity: exploring how mechanical changes in the cytoskeleton regulate cell growth, migration, and tissue pattern during morphogenesis. *Int. Rev. Cytol.* 150, 173–224.
- Ingber, D.E., Wang, N., Stamenović, D., 2014. Tensegrity, cellular biophysics, and the mechanics of living systems. *Rep. Prog. Phys.* 77 (4), #046603.
- Jacquemet, A., Barbeau, J., Lemiègre, L., Benvegnu, T., 2009. Archaeal tetraether bipolar lipids: structures, functions and applications. *Biochimie* 91 (6), 711–717.
- Jain, S., Caforio, A., Driessen, A.J.M., 2014. Biosynthesis of archaeal membrane ether lipids. *Front. Microbiol.* 5, #641.
- Jarosch, R., 1956. Plasmaströmung und Chloroplastenrotation bei Characeen. *Phyton (Argentina)* 6, 87–107.
- Jarosch, R., 1957. Zur Mechanik der Protoplasmafibrillenbewegung. *Biochim. Biophys. Acta* 25 (1), 204–205.
- Javor, B., Requadt, C., Stoeckenius, W., 1982. Box-shaped halophilic bacteria. *J. Bacteriol.* 151 (3), 1532–1542.
- Jicepix, 2015. vieux ballon crevé. <https://eu.fotolia.com/id/33775052>; https://stock.adobe.com/ca/search?k=33775052&filters%5Bcontent_type%3Aphoto%5D=1&filters%5Bcontent_type%3Aillustration%5D=1&filters%5Bcontent_type%3Azip_vector%5D=1&filters%5Bcontent_type%3Avideo%5D=1&filters%5Bcontent_type%3Atemplate%5D=1&filters%5Bcontent_type%3A3d%5D=1&load_type=homepage.
- Jin, L., Takei, A., Hutchinson, J.W., 2015. Mechanics of wrinkle/ridge transitions in thin film/substrate systems. *J. Mech. Phys. Solids* 81, 22–40.
- Kamekura, M., 1998. Diversity of extremely halophilic bacteria. *Extremophiles* 2 (3), 289–295.
- Kates, M., 1992. Archaeobacterial lipids: structure, biosynthesis and function. *Biochem. Soc. Symp.* 58, 51–72.
- Kauffman, S., 2013. What is life, and can we create it? *Bioscience* 63 (8), 609–610.
- Kessel, M., Cohen, Y., 1982. Ultrastructure of square bacteria from a brine pool in Southern Sinai. *J. Bacteriol.* 150 (2), 851–860.
- Khatib, F., DiMaio, F., Cooper, S., Kazmierczyk, M., Gilski, M., Krzywda, S., Zabranska, H., Pichova, I., Thompson, J., Popovic, Z., Jaskolski, M., Baker, D., Foldit Contenders, G., Foldit Void Crushers, G., 2011. Crystal structure of a monomeric retroviral protease solved by protein folding game players. *Nat. Struct. Mol. Biol.* 18 (10), 1175–1177.
- Kim, S.G., Bae, Y.C., 2003. Salt-induced protein precipitation in aqueous solution: single and binary protein systems. *Macromol. Res.* 11 (1), 53–61.
- Kindzelskii, A.L., Xue, W., Todd, R.F., Boxer, L.A., Petty, H.R., 1994. Aberrant capping of membrane proteins on neutrophils from patients with leukocyte adhesion deficiency. *Blood* 83 (6), 1650–1655.
- Kirschner, M., Gerhart, J., 1998. Evolvability. *Proc. Natl. Acad. Sci. U. S. A.* 95 (15), 8420–8427.
- Klibanov, A.M., 2001. Improving enzymes by using them in organic solvents. *Nature* 409 (6817), 241–246.
- Klibanov, A.M., 2003. Asymmetric enzymatic oxidoreductions in organic solvents. *Curr. Opin. Biotechnol.* 14 (4), 427–431.
- Knoche, S., Kierfeld, J., 2011. Buckling of spherical capsules. *Phys. Rev. E* 84 (4), #046608.
- Knoche, S., Kierfeld, J., 2014a. Osmotic buckling of spherical capsules. *Soft Matter* 10 (41), 8358–8369.
- Knoche, S., Kierfeld, J., 2014b. The secondary buckling transition: wrinkling of buckled spherical shells. *Eur. Phys. J. E* 37 (7), #62.
- Knoche, S., Kierfeld, J., 2014c. Secondary polygonal instability of buckled spherical shells. *Epl* 106 (2), #24004.

- König, H., 1994. Analysis of archaeal cell envelopes. In: Goodfellow, M., O'Donnell, A.G. (Eds.), *Chemical Methods in Prokaryotic Systematics*. John Wiley & Sons, Chichester, pp. 85–119.
- Koprowski, G.J., 2013. 'Invisible' airplanes: Chinese, US race for cloaking tech. <http://www.foxnews.com/tech/2013/12/17/invisible-airplanes-chinese-us-scramble-for-cloaking-tech.html>.
- Koudehi, M.A., Tang, H., Vavylonis, D., 2016. Simulation of the effect of confinement in actin ring formation. *Biophys. J.* 110 (3), 126A.
- Krishnamurthy, R.V., Epstein, S., Cronin, J.R., Pizzarello, S., Yuen, G.U., 1992. Isotopic and molecular analyses of hydrocarbons and monocarboxylic acids of the Murchison meteorite. *Geochim. Cosmochim. Acta* 56 (11), 4045–4058.
- Kuhn, D.A., 1981. The genera *Simonsiella* and *Alysiella*. In: Starr, M.P., Stolp, H., Trüper, H.G., Balows, A., Schlegel, H.G. (Eds.), *The Prokaryotes: A Handbook on Habitats, Isolation, and Identification of Bacteria*. Springer-Verlag, Berlin, pp. 390–399.
- Kuroda, K., 1964. Behavior of naked cytoplasmic drops isolated from plant cells. In: Allen, R.D., Kamiya, N. (Eds.), *Primitive Motile Systems in Cell Biology*. Academic Press, New York, pp. 31–41.
- Kuroda, K., 1968. Protoplasmic streaming in a giant plant cell. *Saibō Kagaku Shimpōjiumu* 19, 37–43 (Japanese).
- Kwok, S., 2007. *Physics and Chemistry of the Interstellar Medium*. University Science Books, Sausalito, California, USA.
- Kysela, D.T., Brown, P.J.B., Huang, K.C., Brun, Y.V., 2013. Biological consequences and advantages of asymmetric bacterial growth. *Annu. Rev. Microbiol.* 67, 417–435.
- Laale, H.W., 1984. Polyembryony in teleostean fishes: double monstrosities and triplets. *J. Fish Biol.* 24, 711–719.
- Lafitskaya, T.N., Vasilieva, L.V., 1976. A new triangular bacterium. *Mikrobiologiya* 45 (5), 812–816.
- Lasbury, M., 2013. How Prokaryotes Shape Up. <http://biologicalexceptions.blogspot.ca/2013/08/how-prokaryotes-shape-up.html>.
- Lelkes, P.I., Goldenberg, D., Gliozzi, A., Derosa, M., Gambacorta, A., Miller, I.R., 1983. Vesicles from mixtures of bipolar archaeobacterial lipids with egg phosphatidylcholine. *Biochim. Biophys. Acta* 732 (3), 714–718.
- Leong, T.S.H., Zhou, M.F., Kukan, N., Ashokkumar, M., Martin, G.J.O., 2017. Preparation of water-in-oil-in-water emulsions by low frequency ultrasound using skim milk and sunflower oil. *Food Hydrocoll.* 63, 685–695.
- Levin, S., 2006a. Tensegrity: the new biomechanics. In: Hutson, M., Ellis, R. (Eds.), *Textbook of Musculoskeletal Medicine*. Oxford University Press, Oxford, pp. 69–80.
- Levin, S.M., 2006b. *Biotensegrity & Dynamic Anatomy [DVD]*. Ezekiel Biomechanics Group, McLean, VA.
- Liao, Y., Williams, T.J., Ye, J., Charlesworth, J., Burns, B.P., Poljak, A., Raftery, M.J., Cavicchioli, R., 2016. Morphological and proteomic analysis of biofilms from the Antarctic archaeon, *Halorubrum lacusprofund.* *Sci. Rep.* 6, #37454.
- Lim, H.W.G., Wortis, M., Mukhopadhyay, R., 2002. Stomatocyte–discocyte–echinocyte sequence of the human red blood cell: Evidence for the bilayer–couple hypothesis from membrane mechanics. *Proc. Natl. Acad. Sci.* 99 (26), 16766–16769.
- Liu, J., Kaksonen, M., Drubin, D.G., Oster, G., 2006. Endocytic vesicle scission by lipid phase boundary forces. *Proc. Natl. Acad. Sci. U. S. A.* 103 (27), 10277–10282.
- Liu, H.L., Wu, Z.F., Li, M., Zhang, F., Zheng, H.J., Han, J., Liu, J.F., Zhou, J., Wang, S.Y., Xiang, H., 2011. Complete genome sequence of *Haloarcula hispanica*, a model Haloarchaeon for studying genetics, metabolism, and virus–host interaction. *J. Bacteriol.* 193 (21), 6086–6087.
- Lobasso, S., Lopalco, P., Mascolo, G., Corcelli, A., 2008. Lipids of the ultra-thin square halophilic archaeon *Haloquadratum walsbyi*. *Archaea* 2 (3), 177–183.
- Logan, G.-L., 2015. Deflated Ball. http://www.acclaimimages.com/_gallery/_pages/0017-0309-1921-5000.html.
- Lombard, J., López-García, P., Moreira, D., 2012. The early evolution of lipid membranes and the three domains of life. *Nat. Rev. Microbiol.* 10 (7), 507–515.

- Macleod, G., McKeown, C., Hall, A.J., Russell, M.J., 1994. Hydrothermal and oceanic pH conditions of possible relevance to the origin of life. *Orig. Life Evol. Biosph.* 24 (1), 19–41.
- Malfatti, S., Tindall, B.J., Schneider, S., Fährnich, R., Lapidus, A., LaButti, K., Copeland, A., Del Rio, T.G., Nolan, M., Chen, F., Lucas, S., Tice, H., Cheng, J.-F., Bruce, D., Goodwin, L., Pitluck, S., Anderson, I., Pati, A., Ivanova, N., Mavromatis, K., Chen, A., Palaniappan, K., D'Haeseleer, P., Göker, M., Bristow, J., Eisen, J.A., Markowitz, V., Hugenholtz, P., Kyrpides, N.C., Klenk, H.-P., Chain, P., 2009. Complete genome sequence of *Halogeometricum borinquense* type strain (PR3(T)). *Stand Genomic Sci.* 1 (2), 150–158.
- Mannige, R.V., 2013. Two modes of protein sequence evolution and their compositional dependencies. *Phys. Rev. E* 87 (6), #062714.
- Mannige, R.V., Brooks, C.L., Shakhnovich, E.I., 2012. A universal trend among proteomes indicates an oily last common ancestor. *PLoS Comp. Biol.* 8 (12), e1002839, #e1002839.
- Margolin, W., 2009. Sculpting the bacterial cell. *Curr. Biol.* 19 (17), R812–822.
- Marko, J.F., Neukirch, S., 2012. Competition between curls and plectonemes near the buckling transition of stretched supercoiled DNA. *Phys. Rev. E* 85 (1), #011908.
- Markovitch, O., Lancet, D., 2014. Multispecies population dynamics of prebiotic compositional assemblies. *J. Theor. Biol.* 357, 26–34.
- Marmottant, P., Bouakaz, A., de Jong, N., Quilliet, C., 2011. Buckling resistance of solid shell bubbles under ultrasound. *J. Acoust. Soc. Am.* 129 (3), 1231–1239.
- Marr, A.G., Ingraham, J.L., 1962. Effect of temperature on the composition of fatty acids in *Escherichia coli*. *J. Bacteriol.* 84 (6), 1260.
- Martin, C.C., Gordon, R., 1997. Ultrastructural analysis of the cell state splitter in ectoderm cells differentiating to neural plate and epidermis during gastrulation in embryos of the axolotl *Ambystoma mexicanum*. *Russ. J. Dev. Biol.* 28 (2), 71–80.
- Medlin, L.K., 2016. Evolution of the diatoms: major steps in their evolution and a review of the supporting molecular and morphological evidence. *Phycologia* 55 (1), 79–103.
- Medlin, L.K., Kaczmarek, I., 2004. Evolution of the diatoms: V. Morphological and cytological support for the major clades and a taxonomic revision. *Phys. Chem. Chem. Phys.* 43 (3), 245–270.
- Mehrshad, M., Amoozegar, M.A., Makhdomi, A., Rasooli, M., Asadi, B., Schumann, P., Ventosa, A., 2015. *Halo-varius luteus* gen. nov., sp nov., an extremely halophilic archaeon from a salt lake. *Int. J. Syst. Evol. Microbiol.* 65, 2420–2425.
- Mehrshad, M., Amoozegar, M.A., Makhdomi, A., Fazeli, S.A.S., Farahani, H., Asadi, B., Schumann, P., Ventosa, A., 2016. *Halosiccatus urmianus* gen. nov., sp nov., a haloarchaeon from a salt lake. *Int. J. Syst. Evol. Microbiol.* 66, 725–730.
- Melchior, D.L., 1982. Lipid phase transitions and regulation of membrane fluidity in prokaryotes. *Curr. Top. Membr. Trans.* 17, 263–316.
- Melchior, D.L., Steim, J.M., 1976. Thermotropic transitions in biomembranes. *Annu. Rev. Biophys. Bioeng.* 5, 205–238.
- Mescher, M.F., Strominger, J.L., 1976. Structural (shape-maintaining) role of the cell surface glycoprotein of *Halobacterium salinarum*. *Proc. Natl. Acad. Sci. U. S. A.* 73 (8), 2687–2691.
- Miller, S.L., 1953. A production of amino acids under possible primitive earth conditions. *Science* 117 (3046), 528–529.
- Miller, S.L., Urey, H., 1959. Organic compound synthesis on the primitive earth. *Science* 130 (3370), 245–251.
- Mirghani, Z., Bertoia, D., Gliozzi, A., De Rosa, M., Gambacorta, A., 1990. Monopolar-bipolar lipid interactions in model membrane systems. *Chem. Phys. Lipids* 55 (2), 85–96.
- Mitic, S., 2015. Photo by Sloba Mitic/iStock. <http://www.stthomas.edu/news/failure-youth-sports/>.
- Miyashita, Y., Ohmae, E., Nakasone, K., Katayanagi, K., 2015. Effects of salt on the structure, stability, and function of a halophilic dihydrofolate reductase from a hyperhalophilic archaeon, *Haloarcula japonica* strain TR-1. *Extremophiles* 19 (2), 479–493.

- Mori, K., Nurcahyanto, D.A., Kawasaki, H., Lisdiyanti, P., Yopi Suzuki, K., 2016. *Halobium palmae* gen. nov., sp. nov., an extremely halophilic archaeon isolated from a solar saltern. *Int. J. Syst. Evol. Microbiol.* 66, 3799–3804.
- Mou, Y.Z., Qiu, X.X., Zhao, M.L., Cui, H.L., Oh, D., Dyll-Smith, M.L., 2012. *Halohasta litorea* gen. nov. sp. nov., and *Halohasta litchfieldiae* sp. nov., isolated from the Daliang aquaculture farm, China and from Deep Lake, Antarctica, respectively. *Extremophiles* 16 (6), 895–901.
- Mukhopadhyay, R., Huang, K.C., Wingreen, N.S., 2008. Lipid localization in bacterial cells through curvature-mediated microphase separation. *Biophys. J.* 95, 1034–1049.
- Mullakhanbhai, M.F., Larsen, H., 1975. *Halobacterium volcanii* spec. nov., a Dead Sea halobacterium with a moderate salt requirement. *Arch. Microbiol.* 104 (3), 107–114.
- Murray, J.D., 2012. Why are there no 3-headed monsters? mathematical modeling in biology. *Not. Am. Math. Soc.* 59 (6), 785–795.
- Mushenheim, P.C., Trivedi, R.R., Roy, S.S., Arnold, M.S., Weibel, D.B., Abbott, N.L., 2015. Effects of confinement, surface-induced orientations and strain on dynamical behaviors of bacteria in thin liquid-crystalline films. *Soft Matter* 11 (34), 6821–6831.
- Mutlu, M.B., Guven, K., 2015. Bacterial diversity in Çamalti Saltern, Turkey. *Pol. J. Microbiol.* 64 (1), 37–45.
- Nakano, S.-i., Miyoshi, D., Sugimoto, N., 2014. Effects of molecular crowding on the structures, interactions, and functions of nucleic acids. *Chem. Rev.* 114 (5), 2733–2758.
- Naveh, B., Sipper, M., Lancet, D., Shenhav, B., 2004. Lipidia: An Artificial Chemistry of Self-Replicating Assemblies of Lipid-Like Molecules.
- Newman, S.A., 2014. Physico-genetics of morphogenesis: the hybrid nature of developmental mechanisms. In: Minelli, A., Pradeu, T. (Eds.), *Towards a Theory of Development*. Oxford University Press, Oxford, pp. 95–113.
- Newman, S.A., Comper, W.D., 1990. ‘Generic’ physical mechanisms of morphogenesis and pattern formation. *Development* 110 (1), 1–18.
- Nishiyama, Y., Takashina, T., Grant, W.D., Horikoshi, K., 1992. Ultrastructure of the cell wall of the triangular halophilic archaeobacterium *Haloarcula japonica* strain TR-1. *FEMS Microbiol. Lett.* 99 (1), 43–48.
- Nishiyama, Y., Nakamura, S., Aono, R., Horikoshi, K., 1995. Electron microscopy of halophilic Archaea. In: DasSarma, S., Fleischmann, E.M. (Eds.), *Archaea: A Laboratory Manual*. Halophiles. Cold Spring Harbor Laboratory, Cold Spring Harbor, NY, pp. 29–33.
- Oh, D., Porter, K., Russ, B., Burns, D., Dyll-Smith, M., 2010. Diversity of *Haloquadratum* and other haloarchaea in three, geographically distant, Australian saltern crystallizer ponds. *Extremophiles* 14 (2), 161–169.
- Okubo, M., Minami, H., Morikawa, K., 2001. Production of micron-sized, monodisperse, transformable rugby-ball-like-shaped polymer particles. *Colloid Polym. Sci.* 279 (9), 931–935.
- Oren, A., 1993. Characterization of the halophilic archaeal community in saltern crystallizer ponds by means of polar lipid analysis. *Int. J. Salt Lake Res.* 3, 15–29.
- Oren, A., 1994. The ecology of the extremely halophilic archaea. *FEMS Microbiol. Rev.* 13 (4), 415–439.
- Oren, A., 1999. The enigma of square and triangular halophilic archaea. In: Seckbach, J. (Ed.), *Enigmatic Microorganisms and Life in Extreme Environmental Habitats*. Kluwer Academic Publishers, Dordrecht, pp. 337–355.
- Oren, A., 2005. Microscopic examination of microbial communities along a salinity gradient in saltern evaporation ponds: a ‘halophilic safari’. In: Gunde-Cimerman, N., Oren, A., Plemenitas, A. (Eds.), *Adaptation to Life at High Salt Concentrations in Archaea, Bacteria, and Eukarya*. Springer, Dordrecht, The Netherlands, pp. 41–57.
- Oren, A., Ginzburg, M., Ginzburg, B.Z., Hochstein, L.I., Volcani, B.E., 1990. *Haloarcula marismortui* (Volcani) sp. nov., nom. rev., an extremely halophilic bacterium from the Dead Sea. *Int. J. Syst. Bacteriol.* 40 (2), 209–210.

- Oren, A., Duker, S., Ritter, S., 1996. The polar lipid composition of Walsby's square bacterium. *FEMS Microbiol. Lett.* 138 (2-3), 135–140.
- Oren, A., Ventosa, A., Gutiérrez, M.C., Kamekura, M., 1999. *Haloarcula quadrata* sp nov., a square, motile archaeon isolated from a brine pool in Sinai (Egypt). *Int. J. Syst. Bacteriol.* 49, 1149–1155.
- Otozai, K., Takashina, T., Grant, W.D., 1991. A novel triangular archaeobacterium, *Haloarcula japonica*. In: Horikoshi, K., Grant, W.D. (Eds.), *Superbugs: Microorganisms in Extreme Environments*. Springer-Verlag, Berlin, pp. 61–75.
- Ozawa, K., Yatsunami, R., Nakamura, S., 2000. Cloning and sequencing of *ftsZ* homolog from extremely halophilic archaeon *Haloarcula japonica* strain TR-1. *Nucleic Acids Symp. Ser.* 44, 155–156.
- Ozawa, K., Harashina, T., Yatsunami, R., Nakamura, S., 2005. Gene cloning, expression and partial characterization of cell division protein FtsZ1 from extremely halophilic archaeon *Haloarcula japonica* strain TR-1. *Extremophiles* 9 (4), 281–288.
- Paleos, C.M., 2015. A decisive step toward the origin of life. *Trends Biochem. Sci.* 40 (9), 487–488.
- Paleos, C.M., Tsiourvas, D., Sideratou, Z., 2004. Hydrogen bonding interactions of liposomes simulating cell-cell recognition. a review. *Orig. Life Evol. Biosph.* 34 (1-2), 195–213.
- Parkes, K., Walsby, A.E., 1981. Ultrastructure of a gas-vacuolate square bacterium. *J. Gen. Microbiol.* 126, 503–506.
- Parkinson, J., Brechet, Y., Gordon, R., 1999. Centric diatom morphogenesis: a model based on a DLA algorithm investigating the potential role of microtubules. *Biochim. Biophys. Acta, Mol. Cell Res.* 1452 (1), 89–102.
- Passi, S., 2013. Tensegrity Stool. <https://www.behance.net/gallery/12453419/Tensegrity-Stool>.
- Perera, N., Qiao, J., Blostein, D., Flemons, T., Senatore, G., Gordon, R., 2016. Biotensegrity Simulation at the Full Body and Cytoskeleton Scale. *****.
- Piazza, S., 2015. In-tense robots: Motorized sculptures may represent our best chance for exploring the surfaces of other worlds. *Am. Sci.* 103 (4), 264–267.
- Pickett-Heaps, J., Kowalski, S.E., 1981. Valve morphogenesis and the microtubule center of the diatom *Hantzschia amphioxys*. *Eur. J. Cell Biol.* 25 (1), 150–170.
- Pickett-Heaps, J.D., Tippit, D.H., Andreozzi, J.A., 1979a. Cell division in the pennate diatom *Pinnularia*. III—the valve and associated cytoplasmic organelles. *Biochem. Cell Biol.* 35 (2), 195–198.
- Pickett-Heaps, J.D., Tippit, D.H., Andreozzi, J.A., 1979b. Cell division in the pennate diatom *Pinnularia*. IV—valve morphogenesis. *Biochem. Cell Biol.* 35 (2), 199–203.
- Pinot, M., Chesnel, F., Kubiak, J.Z., Arnal, I., Nedelec, F.J., Gueroui, Z., 2009. Effects of confinement on the self-organization of microtubules and motors. *Curr. Biol.* 19 (11), 954–960.
- Pomp, W., Schakenraad, K.K., van Hoorn, H., Balciğlu, H.E., Danen, E.H.J., Giomi, L., Schmidt, T., 2016. Balance of isotropic and directed forces determines cell shape. *Biophys. J.* 110 (3, Suppl. 1), 305A.
- Powell, R., Mariscal, C., 2015. Convergent evolution as natural experiment: the tape of life reconsidered. *Interface Focus* 5 (6), #20150040.
- Pum, D., Sleytr, U.B., 2014. Reassembly of S-layer proteins. *Nanotechnology* 25 (31), #312001.
- Pum, D., Messner, P., Sleytr, U.B., 1991. Role of the S layer in morphogenesis and cell division of the archaeobacterium *Methanococcus sinense*. *J. Bacteriol.* 173 (21), 6865–6873.
- Quilliet, C., 2012. Numerical deflation of beach balls with various Poisson's ratios: from sphere to bowl's shape. *Eur. Phys. J. E* 35 (6), #48.
- Quilliet, C., Zoldesi, C., Riera, C., van Blaaderen, A., Imhof, A., 2008. Anisotropic colloids through non-trivial buckling [Erratum: 32(4), 419–420]. *Eur. Phys. J. E* 27 (1), 13–20.
- Ram-Mohan, N., Oren, A., Papke, R.T., 2016. Analysis of the bacteriorhodopsin-producing haloarchaea reveals a core community that is stable over time in the salt crystallizers of Eilat, Israel. *Extremophiles* 20 (5), 747–757.
- Reimer, B., Schlesner, H., 1989. Isolation of 11 strains of star-shaped bacteria from aquatic habitats and investigation of their taxonomic position. *Syst. Appl. Microbiol.* 12 (2), 156–158.

- Rimoli, J.J., 2016. On the impact tolerance of tensegrity-based planetary landers. In: 57th AIAA/ASCE/AHS/ASC Structures, Structural Dynamics, and Materials Conference. <https://doi.org/10.2514/2.516.2016-1511>.
- Robledo, A., Rowlinson, J.S., 1986. The distribution of hard rods on a line of finite length. *Mol. Phys.* 58 (4), 711–721.
- Rode, B.M., 1999. Peptides and the origin of life. *Peptides* 20 (6), 773–786.
- Romanenko, V.I., 1981. Square micro colonies in the surface saline water film of the Saxkoye Lake Ukrainian-SSR USSR. *Mikrobiologiya* 50 (3), 571–574 (Russian).
- Rusconi, B., Lienard, J., Aeby, S., Croxatto, A., Bertelli, C., Greub, G., 2013. Crescent and star shapes of members of the Chlamydiales order: impact of fixative methods. *Anton. Leeuw. Int. J. Gen. Mol. Microbiol.* 104 (4), 521–532.
- Sabet, S., Diallo, L., Hays, L., Jung, W., Dillon, J.G., 2009. Characterization of halophiles isolated from solar salt-terns in Baja California, Mexico. *Extremophiles* 13 (4), 643–656.
- Sain, A., Inamdar, M.M., Julicher, F., 2015. Dynamic force balances and cell shape changes during cytokinesis. *Phys. Rev. Lett.* 114 (4), #048102.
- Santos, F., Yarza, P., Parro, V., Meseguer, I., Rosselló-Móra, R., Antón, J., 2012. Culture-independent approaches for studying viruses from hypersaline environments. *Appl. Environ. Microbiol.* 78 (6), 1635–1643.
- Scarr, G., 2014. Biotensegrity: The Architecture of Life. Handspring Publishing, Pencaitland, East Lothian.
- Schmalholz, S.M., Podladchikov, Y., 1999. Buckling versus folding: importance of viscoelasticity. *Geophys. Res. Lett.* 26 (17), 2641–2644.
- Schulte, M., Blake, D., Hoehler, T., McCollom, T., 2006. Serpentinization and its implications for life on the early Earth and Mars. *Astrobiology* 6 (2), 364–376.
- Schulze, E., Kirschner, M.W., 1988. New features of microtubule behaviour observed in vivo. *Nature* 334 (6180), 356–359.
- Schwierz, N., Horinek, D., Sivan, U., Netz, R.R., 2016. Reversed Hofmeister series-the rule rather than the exception. *Curr. Opin. Colloid Interface Sci.* 23, 10–18.
- Scientific Polymer, 2013. Refractive Index of Polymers by Index. <http://scientificpolymer.com/technical-library/refractive-index-of-polymers-by-index>.
- Segré, D., Lancet, D., 2000. Composing life. *EMBO Rep.* 1 (3), 217–222.
- Segré, D., Ben-Eli, D., Deamer, D.W., Lancet, D., 2001. The lipid world. *Orig. Life Evol. Biosph.* 31 (1-2), 119–145.
- Semenov, A.M., Vasilyeva, L.V., 1985. Morphophysiological characteristic of *Labrys monachus* growth—budding prosthecate bacterium with radial cell symmetry under periodical and continuous cultivation. *Izv. Acad. Sci. SSSR Ser. Biol.* [Russian], 288.
- Semenov, A.M., Vasilyeva, L.V., 1987. Stella vacuolata growth upon periodical and continuous cultivation. *Izv. Akad. Nauk SSSR Ser. Biol.* 2, 307–311.
- Semenov, A.M., Hanzliková, A., Jandera, A., 1989. Quantitative estimation of poly-3-hydroxybutyric acid in some oligotrophic polyprosthecate bacteria. *Folia Microbiol.* 34 (3), 267–270.
- Senatore, G., 2017. PUSHMEPULLME 3D. <http://expeditionworkshed.org/workshed/push-me-pull-me-3d/>.
- Sharov, A.A., 2016. Coenzyme world model of the origin of life. *BioSystems* 144, 8–17.
- Sharov, A.A., 2017. Coenzyme world model of the origin of life. In: Gordon, R., Sharov, A.A. (Eds.), *Habitability of the Universe Before Earth*. In: Rampelott, P.H., Seckbach, J., Gordon, R. (Series Eds.), *Astrobiology: Exploring Life on Earth and Beyond*. Elsevier B.V., Amsterdam, pp. 407–426 (Chapter 17).
- Sharov, A.A., Gordon, R., 2017. Life before Earth. In: Gordon, R., Sharov, A.A. (Eds.), *Habitability of the Universe Before Earth*. In: Rampelott, P.H., Seckbach, J., Gordon, R. (Series Eds.), *Astrobiology: Exploring Life on Earth and Beyond*. Elsevier B.V., Amsterdam, pp. 265–296 (Chapter 11).
- Shen, T.Y., Wolynes, P.G., 2005. Nonequilibrium statistical mechanical models for cytoskeletal assembly: Towards understanding tensegrity in cells. *Phys. Rev. E* 72 (4), #041927.

- Shenhav, B., Kafri, R., Lancet, D., 2004. Graded artificial chemistry in restricted boundaries. In: Pollack, J., Bedau, M., Husbands, P., Ikegami, T., Watson, R.A. (Eds.), *Artificial Life IX: 9th International Conference on the Simulation and Synthesis of Artificial Life (ALIFE9)*, Boston, MA, September 12–15, pp. 501–506.
- Shenhav, B., Bar-Even, A., Kafri, R., Lancet, D., 2005. Polymer GARD: computer simulation of covalent bond formation in reproducing molecular assemblies. *Orig. Life Evol. Biosph.* 35 (2), 111–133.
- Sherwood Lollar, B., Westgate, T.D., Ward, J.A., Slater, G.F., Lacrampe-Couloume, G., 2002. Abiogenic formation of alkanes in the Earth's crust as a minor source for global hydrocarbon reservoirs. *Nature* 416 (6880), 522–524.
- Shimane, Y., Minegishi, H., Echigo, A., Kamekura, M., Itoh, T., Ohkuma, M., Tsubouchi, T., Usui, K., Maruyama, T., Usami, R., Hatada, Y., 2015. *Halarchaeum grantii* sp nov., a moderately acidophilic haloarchaeon isolated from a commercial salt sample. *Int. J. Syst. Evol. Microbiol.* 65, 3830–3835.
- ShopAdvisor, 2015. Spalding Deflated TF-1000 Classic Basketball—Size 7. <https://www.shopadvisor.com/p/ERUKRHAD2MJHMMLE0VDJVJN9WKWZ/deflated-tf-1000-classic-basketball-size-7-29-5-spalding>.
- Simon, J., Kühner, M., Ringsdorf, H., Sackmann, E., 1995. Polymer-induced shape changes and capping in giant liposomes. *Chem. Phys. Lipids* 76, 241–258.
- Simoneit, B.R.T., 1995. Evidence for organic-synthesis in high temperature aqueous media—facts and prognosis. *Orig. Life Evol. Biosph.* 25 (1–3), 119–140.
- Sims, J.R., Karp, S., Ingber, D.E., 1992. Altering the cellular mechanical force balance results in integrated changes in cell, cytoskeletal and nuclear shape. *J. Cell Sci.* 103 (Pt 4), 1215–1222.
- Sirota, E.B., King, H.E., Singer, D.M., Shao, H.H., 1993. Rotator phases of the normal alkanes: an x-ray-scattering study. *J. Chem. Phys.* 98 (7), 5809–5824.
- Skelton, R.E., de Oliveira, M.C., 2009. *Tensegrity Systems*. Springer, Dordrecht, Netherlands.
- Sleep, N., Meibom, A., Fridriksson, T., Coleman, R., Bird, D., 2004. H₂-rich fluids from serpentinization: geochemical and biotic implications. *Proc. Natl. Acad. Sci. U. S. A.* 101 (35), 12818–12823.
- Sleytr, U.B., Messner, P., 1983. Crystalline surface layers on bacteria. *Annu. Rev. Microbiol.* 37, 311–339.
- Sleytr, U.B., Messner, P., Sara, M., Pum, D., 1986. Crystalline envelope layers in archaebacteria. *Syst. Appl. Microbiol.* 7 (2–3), 310–313.
- Smith, W.P.J., Davit, Y., Osborne, J.M., Kim, W., Foster, K.R., Pitt-Francis, J.M., 2017. Cell morphology drives spatial patterning in microbial communities. *Proc. Natl. Acad. Sci. U. S. A.* 114 (3), E280–E286.
- Snelson, K., 1990. Letter from Kenneth Snelson to R. Motro. *Int. J. Space Struct.* 7, N2.
- Snelson, K., Heartney, E., 2013. Kenneth Snelson; Art and Ideas. Marlborough Gallery, New York, NY.
- Soares e Silva, M., Alvarado, J., Nguyen, J., Georgoulia, N., Mulder, B.M., Koenderink, G.H., 2011. Self-organized patterns of actin filaments in cell-sized confinement. *Soft Matter* 7 (22), 10631–10641.
- Staley, J.T., 1968. Prosthecomicrobium and Ancalomicrobium: new prosthecate freshwater bacteria. *J. Bacteriol.* 95 (5), 1921–1942.
- Sterrenburg, F.A.S., Gordon, R., Tiffany, M.A., Nagy, S.S., 2007. Diatoms: living in a constructal environment. In: Seckbach, J. (Ed.), *Algae and Cyanobacteria in Extreme Environments. Cellular Origin, Life in Extreme Habitats and Astrobiology*, vol. 11. Springer, Dordrecht, The Netherlands, pp. 141–172.
- Stetter, K.O., 1982. Ultrathin mycelia-forming organisms from submarine volcanic areas having an optimum growth temperature of 105°C. *Nature* 300 (5889), 258–260.
- Stoeckenius, W., 1981. Walsby's square bacterium: fine structure of an orthogonal procaryote. *J. Bacteriol.* 148 (1), 352–360.
- Stolarow, J., Heinzelmann, M., Yeremchuk, W., Syladt, C., Hausmann, R., 2015. Immobilization of trypsin in organic and aqueous media for enzymatic peptide synthesis and hydrolysis reactions. *BMC Biotechnol.* 15 (1), #77.
- Sumper, M., 1993. S-layer glycoproteins from moderately and extremely halophilic archaebacteria. In: Beveridge, T.J., Koval, S.F. (Eds.), *Advances in Bacterial Paracrystalline Surface Layers*. Plenum Press, New York, pp. 109–117.

- SunSpiral, V., 2015. NASA ARC—Super Ball Bot—Structures for Planetary Landing and Exploration (@ 33:03 into the video). <http://livestream.com/viewnow/NIAC2015/videos/75238510>.
- Szathmáry, E., 2006. The origin of replicators and reproducers. *Philos. Trans. R. Soc., B* 361 (1474), 1761–1776.
- Szathmáry, E., Santos, M., Fernando, C., 2005. Evolutionary potential and requirements for minimal protocells. In: Walde, P. (Ed.), *Prebiotic Chemistry: From Simple Amphiphiles to Protocell Models*. Springer, Berlin, pp. 167–211.
- Takao, 2006. *Haloarcula Japonica* TR-1 T (= NBRC 101032 T). <http://www.nite.go.jp/nbrc/genome/project/annotation/ongoing/hj1.html>.
- Takashina, T., Hamamoto, T., Otozai, K., Grant, W.D., Horikoshi, K., 1990. *Haloarcula japonica* sp. nov., a new triangular halophilic archaeobacterium. *Syst. Appl. Microbiol.* 13 (2), 177–181.
- Takei, A., Jin, L., Hutchinson, J.W., Fujita, H., 2014. Ridge localizations and networks in thin films compressed by the incremental release of a large equi-biaxial pre-stretch in the substrate. *Adv. Mater.* 26 (24), 4061–4067.
- Taylor, P., 1998. Ostwald ripening in emulsions. *Adv. Colloid Interface Sci.* 75 (2), 107–163.
- Tcholakova, S., Mitrinova, Z., Golemanov, K., Denkov, N.D., Vethamuthu, M., Ananthapadmanabhan, K.P., 2011. Control of Ostwald ripening by using surfactants with high surface modulus. *Langmuir* 27 (24), 14807–14819.
- Tcholakova, S., Valkova, Z., Cholakova, D., Vinarov, Z., Lesov, I., Denkov, N., Smoukov, S.K., 2017. Efficient self-emulsification via cooling-heating cycles. *Nat. Commun.* 8. #15012.
- Thompson, J.M.T., Sieber, J., 2016. Shock-sensitivity in shell-like structures: with simulations of spherical shell buckling. *Int. J. Bifurcation Chaos* 26 (2). #1630003.
- Thompson, D.H., Wong, K.F., Humphrybaker, R., Wheeler, J.J., Kim, J.M., Rananavare, S.B., 1992. Tetraether bolaform amphiphiles as models of archaeobacterial membrane lipids: Raman spectroscopy, ³¹P NMR, x-ray scattering, and electron microscopy. *J. Am. Chem. Soc.* 114 (23), 9035–9042.
- Torrella, F., 1986. Isolation and adaptive strategies of haloarculae to extreme hypersaline habitats. In: *Abstracts of the Fourth International Symposium on Microbial Ecology*. Slovene Society for Microbiology, Ljubljana, Slovenia. p. 59.
- Tromp, J.T., Gordon, R., 2006. The Number of 3D Configurations of a Labeled Size 2*n “Wurfel” [A117613: The On-Line Encyclopedia of Integer Sequences]. <http://oeis.org/A117613>.
- Tsai, F.-C., Koenderink, G.H., 2015. Shape control of lipid bilayer membranes by confined actin bundles. *Soft Matter* 11 (45), 8834–8847.
- Tully, B.J., Emerson, J.B., Andrade, K., Brocks, J.J., Allen, E.E., Banfield, J.F., Heidelberg, K.B., 2015. De novo sequences of *Haloquadratum walsbyi* from Lake Tyrrell, Australia, reveal a variable genomic landscape. *Archaea*. #875784.
- Turk-MacLeod, R., Nghe, P., Woronoff, G., Schnettler, D., Szathmáry, E., Griffiths, A.D., 2015. Compartmentalization of the formose reaction to test metabolism-first theories on the origin of life. In: *Doran, P. (Ed.), Astrobiology Science Conference 2015, Habitability, Habitable Worlds, and Life*, June 15–19, Chicago, Illinois. Lunar and Planetary Institute, Houston. p. #7162.
- Tuszynski, J., Portet, S., Dixon, J., 2005. Nonlinear assembly kinetics and mechanical properties of biopolymers. *Nonlinear Anal. Theory Methods Appl.* 63 (5-7), 915–925.
- Tuszynski, J.A., Portet, S., Dixon, J.M., Nishino, M., Yu-Lee, L.Y., 2009. Propagation of localized bending deformations in microtubules. *J. Comput. Theor. Nanosci.* 6 (3), 525–532.
- Uversky, V.N., 2013. Unusual biophysics of intrinsically disordered proteins. *Biochim. Biophys. Acta* 1834 (5), 932–951.
- van Beijeren, H., Sylvester, G.S., 1978. Phase transitions for continuous-spin Ising ferromagnets. *J. Funct. Anal.* 28 (2), 145–167.
- van der Vaart, B., Akhmanova, A., Straube, A., 2009. Regulation of microtubule dynamic instability. *Biochem. Soc. Trans.* 37 (Pt 5), 1007–1013.

- van Roij, R., Dijkstra, M., Evans, R., 2000. Orientational wetting and capillary nematization of hard-rod fluids. *Europhys. Lett.* 49 (3), 350–356.
- Vasilyeva, L.V., 1970. A star-shaped soil microorganism. *Izv. Akad. Nauk SSSR Ser. Biol.* 2 (1), 308–310 (Russian).
- Vasilyeva, L.V., 1985. *Stella*, a new genus of soil prosthecobacteria, with proposals for *Stella humosa* sp. nov. and *Stella vacuolata* sp. nov. *Int. J. Syst. Bacteriol.* 35 (4), 518–521.
- Vasilyeva, L.V., Semenov, A.M., 1984. New budding prosthecate bacterium *Labrys monahos* with radial cell symmetry. *Microbiology (English translation of Mikrobiologiya)* 53, 68–75.
- Vasilyeva, L.V., Semenov, A.M., 1985. *Labrys monachus* sp. nov. in: validation of the publication of new names and new combinations previously effectively published outside the IJSB, List no. 18. *Int. J. Syst. Bacteriol.* 35, 375–376.
- Vasilyeva, L.V., Semenova, A.M., 1986. Prosthecobacteria of *Stella* genus and description of a new *Stella inoculata* species. *Izv. Akad. Nauk SSSR Ser. Biol.* 4, 534–540.
- Vasilyeva, L.V., Lafitskaya, T.N., Aleksandrushkina, N.L., Krasilnikova, E.N., 1974. Physiological-biochemical peculiarities of the prosthecobacteria *Stella humosa* and *Prosthecomicrobium* sp. *Izv. Akad. Nauk SSSR Ser. Biol.* 5, 699–714.
- Vetter, R., Wittel, F.K., Herrmann, H.J., 2014. Morphogenesis of filaments growing in flexible confinements. *Nat. Commun.* 5, (#4437). #4437.
- Vliegenthart, G.A., Gompper, G., 2011. Compression, crumpling and collapse of spherical shells and capsules. *New J. Phys.* 13 (24). #045020.
- Wächtershauser, G., 2003. From pre-cells to Eukarya: a tale of two lipids. *Mol. Microbiol.* 47 (1), 13–22.
- Wakai, H., Nakamura, S., Kawasaki, H., Takada, K., Mizutani, S., Aono, R., Horikoshi, K., 1997. Cloning and sequencing of the gene encoding the cell surface glycoprotein of *Haloarcula japonica* strain TR-1. *Extremophiles* 1 (1), 29–35.
- Walsby, A.E., 1980. A square bacterium. *Nature* 283, 69–71.
- Walsby, A.E., 1994. Gas vesicles. *Microbiol. Rev.* 58 (1), 94–144.
- Walsby, A.E., 2005. Archaea with square cells. *Trends Microbiol.* 13 (5), 193–195.
- Wang, C.G., Liu, Y.P., Al-Ghalith, J., Dumitrica, T., Wade, M.K., Tan, H.F., 2016a. Buckling behavior of carbon nanotubes under bending: from ripple to kink. *Carbon* 102, 224–235.
- Wang, Z., Xu, J.Q., Xu, W.M., Li, Y., Zhou, Y., Luu, Z.Z., Hou, J., Zhu, L., Cui, H.L., 2016b. *Salinigranum salinum* sp nov., isolated from a marine solar saltern. *Int. J. Syst. Evol. Microbiol.* 66, 3017–3021.
- Wanger, G., Onstott, T.C., Southam, G., 2008. Stars of the terrestrial deep subsurface: a novel ‘star-shaped’ bacterial morphotype from a South African platinum mine (Corrigendum: (6), 421). *Geobiology* 6 (3), 325–330.
- Weiss, M.C., Sousa, F.L., Mrnjavac, N., Neukirchen, S., Roettger, M., Nelson-Sathi, S., Martin, W.F., 2016. The physiology and habitat of the last universal common ancestor. *Nat. Microbiol.* 1. #16116.
- Whang, K., Hattori, T., 1990. A square bacterium from forest soil. *Bull. Jpn. Soc. Microb. Ecol.* 5 (1), 9–11.
- Wieczorek, R., 2012. On prebiotic ecology, supramolecular selection and autopoiesis. *Orig. Life Evol. Biosph.* 42 (5), 445–450.
- Wikipedia, 2016a. Cyclohexane conformation. https://en.wikipedia.org/wiki/Cyclohexane_conformation-Boat_conformation.
- Wikipedia, 2016b. Ising Model. https://en.wikipedia.org/wiki/Ising_model.
- Wikipedia, 2016c. List of Sequenced Archaeal Genomes. https://en.wikipedia.org/wiki/List_of_sequenced_archaeal_genomes.
- Wikipedia, 2016d. Theridiidae. <https://en.wikipedia.org/wiki/Theridiidae>.
- Wu, M., Higgs, P.G., 2008. Compositional inheritance: comparison of self-assembly and catalysis. *Orig. Life Evol. Biosph.* 38 (5), 399–418.

- Wu, M.L., van Teeseling, M.C.F., Willems, M.J.R., van Donselaar, E.G., Klingl, A., Rachel, R., Geerts, W.J.C., Jetten, M.S.M., Strous, M., van Niftrik, L., 2012. Ultrastructure of the denitrifying methanotroph “*Candidatus Methyloirabilis oxyfera*,” a novel polygon-shaped bacterium. *J. Bacteriol.* 194 (2), 284–291.
- Xu, W.M., Xu, J.Q., Zhou, Y., Li, Y., Lü, Z.Z., Hou, J., Zhu, L., Cui, H.L., 2016. *Halomarina salina* sp nov., isolated from a marine solar saltern. *Anton. Leeuw. Int. J. Gen. Mol. Microbiol.* 109 (8), 1121–1126.
- Yang, Y., Cui, H.-L., Zhou, P.-J., Liu, S.-J., 2007. *Haloarcula amylolytica* sp nov., an extremely halophilic archaeon isolated from Albi salt lake in Xin-Jiang, China. *Int. J. Syst. Evol. Microbiol.* 57, 103–106.
- Yang, D.C., Blair, K.M., Salama, N.R., 2016. Staying in shape: the impact of cell shape on bacterial survival in diverse environments. *Microbiol. Mol. Biol. Rev.* 80 (1), 187–203.
- Yatsunami, R., Ando, A., Yang, Y., Takaichi, S., Kohno, M., Matsumura, Y., Ikeda, H., Fukui, T., Nakasone, K., Fujita, N., Sekine, M., Takashina, T., Nakamura, S., 2014. Identification of carotenoids from the extremely halophilic archaeon *Haloarcula japonica*. *Front. Microbiol.* 5, #100.
- Yenjerla, M., Lopus, M., Wilson, L., Oroudjev, E., 2010. Analysis of dynamic instability of steady-state microtubules in vitro by video-enhanced differential interference contrast microscopy. *Methods Cell Biol.* 95, 189–206.
- Yin, S., Wang, Z., Xu, J.Q., Xu, W.M., Yuan, P.P., Cui, H.L., 2015. *Halorubrum rutilum* sp nov isolated from a marine solar saltern. *Arch. Microbiol.* 197 (10), 1159–1164.
- Yokoi, T., Isobe, K., Yoshimura, T., Hemmi, H., 2012. Archaeal phospholipid biosynthetic pathway reconstructed in *Escherichia coli*. *Archaea*. #438931.
- Young, K.D., 2006. The selective value of bacterial shape. *Microbiol. Mol. Biol. Rev.* 70 (3), 660–703.
- Young, K.D., 2007. Bacterial morphology: why have different shapes? *Curr. Opin. Microbiol.* 10 (6), 596–600.
- Young, K.D., 2010. Bacterial shape: two-dimensional questions and possibilities. *Annu. Rev. Microbiol.* 64, 223–240.
- Yuen, G.U., Lawless, J.G., Edelson, E.H., 1981. Quantification of monocarboxylic acids from a spark discharge synthesis. *J. Mol. Evol.* 17 (1), 43–47.
- Yuen, G., Blair, N., Des Marais, D.J., Chang, S., 1984. Carbon isotope composition of low molecular weight hydrocarbons and monocarboxylic acids from Murchison meteorite. *Nature* 307 (5948), 252–254.
- Zaks, A., Klibanov, A.M., 1985. Enzyme-catalyzed processes in organic solvents. *Proc. Natl. Acad. Sci. U. S. A.* 82 (10), 3192–3196.
- Zeng, M.Y., Wu, C.X., Sun, G.Y., 2004. Kink angle of multiwall carbon nanotubes due to interlayer interaction as viewed by elastic theory. *Phys. Rev. B* 70 (13). #132409.
- Zenke, R., von Gronau, S., Bolhuis, H., Gruska, M., Pfeiffer, F., Oesterheld, D., 2015. Fluorescence microscopy visualization of halomucin, a secreted 927 kDa protein surrounding *Haloquadratum walsbyi* cells. *Front. Microbiol.* 30 (6), 249.
- Zhou, E.H., Trepatt, X., Park, C.Y., Lenormand, G., Oliver, M.N., Mijailovich, S.M., Hardin, C., Weitz, D.A., Butler, J.P., Fredberg, J.J., 2009. Universal behavior of the osmotically compressed cell and its analogy to the colloidal glass transition. *Proc. Natl. Acad. Sci. U. S. A.* 106 (26), 10632–10637.

FURTHER READING

- Brau, F., Damman, P., Diamant, H., Witten, T.A., 2013. Wrinkle to fold transition: influence of the substrate response. *Soft Matter* 9 (34), 8177–8186.
- Comolli, L.R., Duarte, R., Baum, D., Luef, B., Downing, K.H., Larson, D.M., Csencsits, R., Banfield, J.F., 2012. A portable cryo-plunger for on-site intact cryogenic microscopy sample preparation in natural environments. *Microsc. Res. Tech.* 75 (6), 829–836.

- Dale, B.F., 2008. An SVG of a Physically Possible Tensegrity Structure in 3D, With a Shadow. <https://en.wikipedia.org/wiki/File:3-tensegrity.svg>.
- Gambacorta, A., Gliozzi, A., Derosa, M., 1995. Archaeal lipids and their biotechnological applications. *World J. Microbiol. Biotechnol.* 11 (1), 115–131.
- König, E., Schlesner, H., Hirsch, P., 1984. Cell wall studies on budding bacteria of the *Planctomyces/Pasteuria* group and on a *Prosthecomicrobium* sp. *Arch. Microbiol.* 138 (3), 200–205.
- Mikhailov, A., 2014. File:*Triceratium morlandii* var. *morlandii*.jpg. https://commons.wikimedia.org/wiki/File:Triceratium_morlandii_var._morlandii.jpg.
- Stidolph, S.R., Sterrenburg, F.A.S., Smith, K.E.L., Kraberg, A., 2012. Stuart R. Stidolph Diatom Atlas: U.S. Geological Survey Open-File Report 2012–1163. <http://pubs.usgs.gov/of/2012/1163>.
- Wikipedia, 2008. File:Haloquadratum walsbyi00.jpg. https://commons.wikimedia.org/wiki/File:Haloquadratum_walsbyi00.jpg.
- Zhang, L.Y., Zhang, C., Feng, X.Q., Gao, H.J., 2016. Snapping instability in prismatic tensegrities under torsion. *Appl. Math. Mech. (English Ed.)* 37 (3), 275–288.